Åbo Akademi University

Carl-Mikael Tåg

Liquid Transportation and Distribution during (Re)Wetting: Impact on Coated Papers in Printing

Carl-Mikael Tåg

Born 1979

Masters degree in Åbo Akademi 2005

PhD dissertation defence in Åbo Akademi 2013

Åbo Akademi University Press
Tavastgatan 13, FI-20500 Åbo, Finland
Tel. +358 (0)2 215 3478
E-mail: forlaget@abo.fi

Sales and distribution:
Åbo Akademi University Library
Domkyrkogatan 2–4, FI-20500 Åbo, Finland
Tel. +358 (0)2 -215 4190
E-mail: publikationer@abo.fi

Liquid Transportation and Distribution during (Re)Wetting:

Impact on Coated Papers in Printing

Carl-Mikael Tåg

Åbo 2013

Doctoral Thesis

Supervised by

Professor Dr. Jarl B. Rosenholm
Department of Chemical Engineering
Laboratory of Physical Chemistry
Åbo Akademi University, Åbo, Finland

and

Professor Dr. Patrick A.C. Gane
School of Chemical Technology
Department of Forest Products Technology
Aalto University, Aalto, Finland

Reviewed by

Professor Dr. Patrice J. Mangin
Département de Génie Chimique
Centre de recherche sur les matériaux lignocellulosiques
Université du Québec à Trois-Rivières
Québec, Canada

and

Dr. Janet Preston
Senior scientist
Imerys Minerals Ltd.
Cornwall, England

and

Dr. (Tech.) Sanna Rousu
Team Leader
VTT Printed Intelligence
Oulu, Finland

Dissertation opponent

Professor Dr. Patrice J. Mangin

Dissertation kustos

Professor Dr. Jouko Peltonen

ISBN 978-952-12-2830-8
Painosalama Oy – Turku, Finland 2013

To my family

Table of contents

Foreword and acknowledgements

This doctoral thesis includes most of the contents of the listed publications and summarises the most important results and findings and inter-link them based on the knowledge gained throughout the research period. Existing public research has extensively been digested and used as a base for the different topics. The idea behind the field of research has arisen from personal experiences and inspirations taken from real-life.

Many important decisions have been made inside humid chambers, “Saunas”, including the idea, the brainstorming and the realization of this doctoral work. Another mind/result-processing process has taken place during the long and even ultra-long running distances in various climates. Thus, the role played by liquid/moisture, both from an absorptive and evaporative viewpoint, has been vital all the way from the early stages of this project to the very end of printing this thesis. Obviously, this work was not done by only one person. I wish to acknowledge especially the following persons, having acted as supervisors/advisors, and having provided much valued camaraderie whilst giving their input to this work.

I want to express my gratitude to Professor Jarl Rosenholm for taking me to his team in the Department of Physical Chemistry. Nalle, I think I have never met a person like you, in a very positive manner, spreading your humour around you and in the next second being a very critical and demanding supervisor. I´m grateful to you for giving me the opportunity to walk my own path, supporting and encouraging me all the way until this day. Logically after this, I want to thank the whole department for many nice times together as well as the time at the Graduate School of Materials Research and the Center for Functional Materials. Thanks also for the financial support from Tekniikan Edistämissäätiö, Alfred Kordelinin säätiö and Magnus Ehrnrooth´s stiftelse. And last but not least, Professor Jouko Peltonen, who helped me, crossing the finish line.

The years at Forest Pilot Center were memorable and the things I got in my bag from that time, has enabled new networks, new knowledge and especially opened the eyes to better understand the link between laboratory and production scale. I will be ever thankful to Päivi Miettinen, for her support and for her encouragement to work on my thesis. Thanks for giving me the opportunity to play with the bigger machines whenever I wanted. Without your help, the quality of this work would have suffered. Thanks also to the whole FPC crew and especially to Kimmo, Teemu and Annica. Not every engagement story has a happy ending, unfortunately, but

it is not a bad qualification when I say that I was the one performing the last trial on the coater and the both offset printing machines at FPC.

During the years, I have had the chance to meet many people, some of them becoming very close to my heart. Four years ago, I had the luck to meet one person during one evening in Helsinki. After a nice dinner, a few beers and ending the night by emptying the mini bar at his hotel, and in the morning doing the first measurements together, this research idea was born. Thanks to you Mikko Juuti, I´m standing here today. Hopefully you have enjoyed this time as much as myself. We created a "Dream team" which has achieved a lot. We wouldn´t have made it without Maunu Toiviainen, who has given a lot of guidance and expertise in the field of NIR, in the measurements and in the analysis of results. Thanks Maunu for having had patience with me and my questions during the years. The way of working has always been open and we have kept up the momentum from day one. I´m confident, that our cooperation will continue in the future, too. Thanks also to Kaj Backfolk, for helping me during this process. The cooperation with you has given me a lot, especially in the sense of setting up trial plans and looking in a critical way on obtained results. Your feedback has sometimes pushed me to the limits, forcing me to find explanations to your questions. I have also had the luck to work with a stubborn Finn, nowadays living in Stockholm. I want to thank you, Jan-Erik "Vandalen" Nordström, for giving me so much during the last years. I appreciate our discussions and your direct opinions about everything. I want to cheer for Cathy Ridgway, who has always been so kind and helpful and always being so nice to talk to. I also want to thank Mr "Lars Peukku" alias Jarkko Saarinen for helping me with the layout of this work.

Dear Professor Patrick Gane. I take this opportunity to express my profound gratitude and warmest regards to you. Although, most of our discussions have taken place over emails, with many iterations, the guidance has been exemplary and our cooperation has been seamless. This story would never have seen this day without you. I admire you as a person, your diplomatic way to work and handle, sometimes quite lost, students. Your sense of humour, your effective way to bring things forward and your extraordinary talents in research, makes you simply the best. It is very easy to work with you. I just can´t understand how you can deal with everything and being able to respond in such a short notice…..always. It has been my privilege, and I will never forget this time with you. I´m sure our timeline doesn´t end here, this was just a milestone.

During the years at Åbo Akademi, I have met a lot of new friends. The support from my "second family" has been something totally fantastic. Although we don´t meet that regularly at the moment, friends will always be friends.

Lastly, I thank almighty, My family: You have given me the chance to work hard to reach this aim. Mamma Pirjo and pappa Calle, Tack för allt ert stöd under åren! Not to forget my little sister Pia, who will always be my little sister. The time in Germany with you and Alex is like a beer, every minute of it is enjoyable. Päivi, the love of my life. With my hand on my heart, your support has been my victory. It has been a journey for you also. Let´s enjoy life together with our sunshines, Max and Neela. I admit that it took time, but Rome wasn´t either built in a day. Now when thinking back, it was worth every second. Maybe a re-start……NO!

I am obliged to Stora Enso and especially to Research Centre Mönchengladbach, who has given me the opportunity to continue my research career and supporting my activities in Germany. I´m really looking forward to the future with you.

I have to quote a very good expression from one Swedish European Song Contest contestant who sang "*I was aiming for the sky, ended up flat on the ground. But once again the sun is rising: I'd better keep on walking" (Salem Al Fakir)*. These words really describe the mixture of feelings I have had during this process, but highlight the motto, not to give up. Every story has an end, and luckily this had a happy end! Fortunately the future is still unwritten. Hopefully this takes me forward in the long journey of life on which I am about to embark.

Carl-Mikael Tåg, November 2012, Korschenbroich, Germany

Publications

Paper I: Tåg, C.-M., Juuti, M., Koivunen, K., Gane, P.A.C., Dynamic Water Transport in a Pigmented Porous Coating Medium: Novel Study of Droplet Absorption and Evaporation by Near-Infrared Spectroscopy, Industrial Engineering and Chemistry Research, 49, 9, 4181–4189, 2010.

Paper II: Tåg, C.-M., Toiviainen, M., Juuti, M., Gane, P.A.C., Dynamic analysis of temporal moisture profiles in heatset printing studied with near-infrared spectroscopy, Measurement Science and Technology, 21, 105602, 1-11, 2010.

Paper III: Tåg, C.-M., Toiviainen, M., Juuti, M., Ridgway, C., Gane, P.A.C., Online Detection of Moisture in Heatset Printing: the role of substrate structure during liquid transfer, Industrial Engineering and Chemistry Research, 50, 8, 4446–4457, 2011.

Paper IV: Tåg, C.-M., Toiviainen, M., Juuti, M., Rosenholm, J.B., Backfolk, K., Gane, P.A.C., The effect of isopropyl alcohol and non-ionic surfactant mixtures on the wetting of porous coated paper, Journal of Transport in Porous Media, 94, 1, 225-242, 2012.

Paper V: Tåg, C.-M., Toiviainen, M., Juuti, M., Gane, P.A.C., Online Detection of Moisture in Heatset Printing: liquid transfer to printed and non-image areas, Nordic Pulp and Paper Research Journal, 27, 1, 112-121, 2012.

Contribution of the author

The author is responsible for the planning of the measurements and trials, performing the tests and data analysis as well as writing the first draft of each manuscript, with the following exceptions:

Paper I: The model pigment coating structures were prepared by Dr. Kimmo Koivunen. The NIR measurements were carried out together with Dr. Mikko Juuti.

Paper II: The NIR measurements were carried out together with MSc. Maunu Toiviainen. The operators at Forest Pilot Center ran the printing machine.

Paper III: The NIR measurements were carried out together with MSc. Maunu Toiviainen. The substrate analysis was carried out under guidance of Dr. Cathy Ridgway. The operators at Forest Pilot Center ran the printing machine.

Paper IV: The hyperspectral measurements were carried together with MSc. Maunu Toiviainen.

Paper V: The NIR measurements were carried out together with MSc. Maunu Toiviainen. The operators at Forest Pilot Center ran the printing machine.

Supporting publications

1. Järn, M., Tåg, C.-M., Järnström, J., Granqvist, B., Rosenholm, J.B., Alternative models for determining the surface energy components in offset printing, Journal of Colloid and Interface Science, 301, 2, 668–676, 2006.

2. Granqvist, B., Järnström, J., Tåg, C.-M., Järn, M., Rosenholm, J.B., Acid–base properties of polymer-coated paper, Adhesion Science and Technology, 21, 5–6, 465–485, 2007.

3. Järnström, J., Granqvist, B., Järn, M., Tåg, C.-M., Rosenholm, J.B., Alternative methods to evaluate the surface energy components of ink-jet paper, Colloids and Surfaces A: Physicochemical and Engineering Aspects, 294, 1-3, 46–55, 2007.

4. Tåg, C.-M., Järn, M., Granqvist, B., Järnström, J., Peltonen, J., Rosenholm, J.B., Influence of surface structure on wetting of coated offset papers, Holzforschung, 61, 5, 516–522, 2007.

5. Tåg, C.-M., Juuti, M., Peiponen, K.-E., Rosenholm, J.B., Print mottling: Solid–liquid adhesion related to optical appearance, Colloids and Surfaces A: Physicochemical and Engineering Aspects, 317, 1-3, 658–665, 2008.

6. Tåg, C.-M., Pykönen, M., Rosenholm, J.B., Backfolk, K., Wettability of model fountain solutions: The influence on topo-chemical and -physical properties of offset paper, Colloid and Interface Science, 330, 428–436, 2009.

7. Järn, M., Tåg, C.-M., Järnström, J., Rosenholm, J.B., Dynamic Spreading of Polar Liquids on Offset Papers, Adhesion Science and Technology, 24, 3, 567–581, 2010.

8. Tåg, C.-M., Järn, M., Rosenholm, J.B., Radial Spreading of Inks and Model Liquids on Heterogeneous Polar Surfaces, Adhesion Science and Technology, 24, 3, 539–565, 2010.

9. Tåg, C.-M., Karesoja, M., Rosenholm, J.B., Backfolk, K., The Influence of Isopropyl Alcohol and Non-ionic Surfactant Solutions on the Mechanical Properties of Offset Paper, Adhesion Science and Technology, 25, 13, 1561–1579, 2011.

10. Järnström, J., Järn, M., Tåg, C.-M., Peltonen, J., Rosenholm, J.B., Liquid Spreading on Ink-Jet Paper Evaluated by the Hydrodynamic and Molecular-Kinetic Models, Adhesion Science and Technology, 25, 6-7, 761–779, 2011.

11. Oksman, A., Kuivalainen, K., Tåg, C.-M., Juuti, M., Mattila, R., Hietala, E., Gane, P.A.C., Peiponen, K.-E., Diffractive optical element–based glossmeter for the on-line measurement of normal reflectance on a printed porous coated paper, Optical Engineering, 50, 4, 043606-1-9, 2011.

12. Gane, P.A.C., Silfsten, P., Tåg, C.-M., Pääkkönen, P., Hiltunen, J., Kuivalainen, K., Oksman, A., Peiponen, K.-E., Isolating contributions to gloss from surface mechanical and optical roughness, thin layer refractive index and wavelength filtering as a function of illumination, and geometry of incidence, Journal of Print and Media Technology Research, 1, 2, 77-91, 2012.

13. Tåg, C.-M., Rajala, P., Toiviainen, M., Juuti, M., Gane, P.A.C., Combining simulation and on-line measurements to determine moisture transport dynamics throughout the heatset offset printing process, Applied Thermal Engineering 50, 1021-1028, 2013.

14. Silfsten, P., Dutta, R., Pääkkönen, P., Tåg, C.-M., Gane, P.A.C., Peiponen, K.-E., Surface roughness and gloss study of prints: application of specular reflection at near infrared, Measurement Science and Technology, 23, 2012, 125202 (8pp), 2012.

15. Tåg, C.-M., Rosenholm, J. B., Backfolk, K., Wetting of model fountain solutions in offset printing: The influence of additive concentration and surface roughness on wetting kinetics, The 6th International Conference on Imaging Science and Hardcopy, ICISH'2008, January 2008, Zhanjiang, China, 264-268, 2008.

16. Tåg, C.-M., Pykönen, M., Rosenholm, J. B., Backfolk, K., Wettability of various fountain solutions and their influence on paper properties, 60th Annual Technical Conference of the Technical Association of the Graphic Arts, TAGA, Session 5, March 16–19, 2008, San Francisco, California, United States, 2008.

17. Tåg, C.-M., Toiviainen, M., Juuti, M., Gane, P.A.C., Dynamic analysis of temporal moisture profiles in heatset printing studied with near-infrared spectroscopy, 37th International Research Conference of IARIGAI, Montreal, Canada, 12-15 September 2010. Advances in Printing Media Technology Vol. XXXVII, Ed. Nils Enlund and Mladen Lovreček, 243-252, 2010.

18. Tåg, C.-M., Juuti, M., Koivunen, K., Gane, P.A.C., Liquid absorption and evaporation in porous coating structures studied by near-infrared spectroscopy, TAPPI Advanced Coating Fundamentals Symposium, 11-13 October 2010, Munich, Germany, 89-107, 2010.

19. Tåg, C.-M., Toiviainen, M., Juuti, M., Ridgway, C., Gane, P.A.C., The role of substrate structure on liquid transfer in heatset offset printing, 38th International Research Conference of IARIGAI, Budapest, Hungary, 11-14 September 2011, Advances in Printing Media Technology Vol. XXXVIII, November 2011, Ed. Nils Enlund and Mladen Lovreček, 123-132, 2011.

20. Rosenholm, J.B., Tåg, C.-M., Chemical Interaction and Transport Processes During Printing, in Network of Competence in Formation of Surface Properties: Molecular Understanding of Printability, J.B. Rosenholm and C.-M. Tåg (Eds.), Åbo Akademi University Turku, Finland, 2007.

Abbreviations and symbols

A.U.	Absorbance Units
AFM	Atomic Force Microcopy
dH	deutsche Härte
nf/bf–GCC	narrow fine/broad fine–Ground Calcium Carbonate
H_2O	Water
HSWO	Heatset Web Offset
IPA	Isopropyl alcohol
IR	Infrared
LOD	Limit of Detection
LOQ	Limit of Quantification
LWC	Lightweight coated
MCT	Mercury Cadmium Telluride
NIR	Near-infrared
PDL	Process Detection Limit
PQL	Process Quantification Limit
RH	Relative humidity
RMS	Root Mean Square
SC	Supercalendered
SD	Standard Deviation
SNR	Signal to Noise Ratio
SNV	Standard Normal Variant
SWIR	Short Wave Infrared
ToF-SIMS	Time of Flight Secondary Ion Mass Spectrometry
ViWa	Visual Waviness
VOC	Volatile Organic Compound
wt	weight percentage
γ	Liquid surface tension
SV	Solid–Vapour
LV	Liquid–Vapour
SL	Solid–Liquid
Θ	Contact angle
θ	Angle
r	Ratio between actual surface and geometric surface
r_{cap}	Capillary radius
R_{pore}	Equivalent cylindrical capillary pore radius
R	Reflectance
η	Viscosity
x	Penetration depth
t	Time
T	Transmission
ρ	Density
Q	Volume flow rate
L	Length
k	Darcy permeability coefficient
P	Pressure
A	Absorbance
A_{cross}	Cross-sectional area
υ	velocity of light
n	Refractive index
α	Absorption coefficient
ℓ	Path length

I_0	Power of incident light
I	Power of transmitted light
I_{sample}	Sample raw signal
$I_{white\ ref.}$	White reference raw signal
λ	Wavelength
D	Dark current
W	White reference
m	Mass
a, e, y	Vectors
b	Bias slope coefficient

Abstract

The key factors discussed in this thesis are highlighted in the abstract with bold italics.

In many industrial applications, such as the printing and coatings industry, wetting of porous materials by liquids includes not only ***imbibition and permeation into the bulk*** but also ***surface spreading and evaporation***. By understanding these phenomena, valuable information can be obtained for improved process control, runnability and printability, in which liquid penetration and subsequent drying play important quality and economic roles. Knowledge of the position of the wetting front and the ***distribution/degree of pore filling*** within the structure is crucial in describing the transport phenomena involved. Although exemplifying ***paper as a porous medium*** in this work, the generalisation to ***dynamic liquid transfer*** onto a surface, including ***permeation and imbibition into porous media***, is of importance to many industrial and naturally occurring environmental processes. This thesis explains the phenomena in the field of ***heatset web offset printing*** but the content and the analyses are applicable in many other printing methods and also other technologies where water/moisture monitoring is crucial in order to have a stable process and achieve high quality end products.

The use of ***near-infrared technology*** to study the water and moisture response of porous pigmented structures is presented. The use of sensitive ***surface chemical and structural analysis***, as well as the ***internal structure investigation of a porous structure***, to inspect liquid wetting and distribution, complements the information obtained by spectroscopic techniques. Strong emphasis has been put on the scale of measurement, to filter irrelevant information and to understand the relationship between interactions involved. The near-infrared spectroscopic technique, presented here, samples directly the changes in signal absorbance and its variation in the process at multiple locations in a print production line. The ***in-line non-contact measurements*** are facilitated by using several diffuse reflectance probes, giving the ***absolute water/moisture content*** from a defined position in the dynamic process in real-time. The near-infrared measurement data illustrate the changes in moisture content as the paper is passing through the printing nips and dryer, respectively, and the analysis of the mechanisms involved ***highlight the roles of the contacting surfaces and the relative liquid carrier properties of both non-image and printed image areas***.

The thesis includes laboratory studies on wetting of porous media in the form of ***coated paper*** and ***compressed pigment tablets*** by mono-, dual-, and multi-component liquids, and paper

water/moisture content analysis in both ***offline*** and ***online*** conditions, thus also enabling direct sampling of temporal water/moisture profiles from multiple locations.

One main focus in this thesis was to establish a measurement system which is able to monitor rapid changes in moisture content of paper. The study suggests that near-infrared diffuse reflectance spectroscopy can be used as a moisture sensitive system and to provide accurate online qualitative indicators, but, also, when accurately calibrated, can provide quantification of water/moisture levels, its distribution and dynamic liquid transfer. Due to the high sensitivity, samples can be measured with excellent reproducibility and good signal to noise ratio. Another focus of this thesis was on the evolution of the moisture content, i.e. changes in moisture content referred to (re)wetting, and liquid distribution during printing of coated paper.

The study confirmed different ***wetting phases*** together with the factors affecting each phase both for a ***single droplet*** and a ***liquid film*** applied on a porous substrate. For a single droplet, initial capillary driven imbibition is followed by equilibrium pore filling and liquid retreat by evaporation. In the case of a liquid film applied on paper, the controlling factors defining the transportation were concluded to be the applied liquid volume in relation to surface roughness, capillarity and permeability of the coating giving the liquid uptake capacity. The printing trials confirmed moisture gradients in the printed sheet depending on process parameters such as speed, fountain solution dosage and drying conditions as well as the printed layout itself. Uneven moisture distribution in the printed sheet was identified to be one of the sources for waving appearance and the magnitude of waving was influenced by the drying conditions.

Definitions

The thesis, as such, focuses on wetting phenomena occurring when liquids are brought into contact with the nano- and micro-porous coated paper. Wetting is the general term describing the interaction. Wetting, however, needs to be further fragmented, whether it is wetting on the surface, inside the porous matrix, free non-impact wetting or forced wetting under pressure. The goal is to use one single term for each separate phenomenon so that they are not mixed, and the relations between them are more easily understood. In order to clarify the different key wetting terms and to ease the reading, they are hereby separated and described:

Wetting: wetting is the ability of a liquid to be in intimate contact with a solid surface. Intermolecular interactions keep the two together in the form of adhesion, which is the interaction energy between two phases.

Static and dynamic wetting: static wetting is used when, for example, a contact angle value is studied at equilibrium at a specific time, while dynamic wetting refers to the evolution of wetting with time. The dynamic wetting can further be separated into dynamic surface and bulk wetting.

Rewetting: rewetting refers here to the phenomenon when a paper is wetted by liquid(s) multiple times.

Wettability: wettability is the degree of wetting through a force balance between surface energy difference of solid and liquid phase in contact with the vapour (solid-liquid) and cohesive (liquid-liquid) forces.

Spreading: liquid movement along a surface plane under wetting conditions.

Absorption: in order not to confuse, the term used here for liquid absorption into the substrate is named **imbibition,** which is the displacement of air by liquid via spontaneous capillary-driven suction into porous media. The term absorption, in the contest of this thesis work, is only used for **light absorption**.

Permeation: here used to describe liquid penetration under pressure (**pressure permeation**), and the rate of permeation in a saturated porous medium is related to the constant of permeability.

Moisture: moisture is referred to as water vapour or condensate in trace amounts in the material. The moisture contents presented here are absolute values obtained from calibration curves for

total H_2O content irrespective of phase, i.e. including both liquid in larger imbibed and/or permeated volumes plus vapour. It is very difficult to state whether the water is in a liquid (volume) or vapour (adsorbed or free) state, or the ratio between them. Thus, for simplicity, the word “moisture” is used hereafter generically to mean total H_2O content.

Evaporation: evaporation is the phase transition from liquid phase to gas phase that occurs only on the surface of a liquid. However, here the term is also used for evaporation from the inside of a material since it is contrasted to boiling occurring in the entire mass of the liquid.

Unprinted paper refers to a plain paper not processed through the step of printing, while areas of the **printed paper** are separated by **image** (printed with ink) and **non-image** (contacted with fountain solution only) areas.

As separated in the definitions list, moisture and wetting by liquid are two different things. By using near-infrared spectroscopy, both can be identified. Here, the moisture is the initial moisture content and wetting is the liquid application in comparison to the initial moisture. The study is based on changes in total H_2O content during wetting, which in non-rigorous papermaking parlance is termed total moisture. The liquid wetting mechanisms are not directly monitored on-line, whereas the water/moisture content is, which in turn reflects these mechanisms as they are the liquid delivery controlling factors.

1 Introduction

Paper is one of the greatest culturally advancing inventions ever to have been developed. In the very beginning, paper was used as a medium to write on and transfer information through various signs, symbols and images. Nowadays this versatile product is used as material for newspapers, high quality magazines and packages. Paper and fibres are also used as replacing material such as for plastics, and this area has gained much interest in the field of research. Paper as a functional material sets many challenges for material construction, but due to its good recyclability, and above all sustainability, it is considered as an alternative for flexible printed electronics and sensor technology. The surface properties of the paper can be enhanced with different types of coatings, including particles of wide ranging size distributions and shapes. By tailoring the surface, optimized printability, desired optical effects, mechanical effects, and electronic effects can be reached.

Paper is a natural product, the properties of which change with temperature and moisture content affecting the dimensional stability of the sheet. Moisture is stored in paper in capillaries and pores in the form of liquid (free water) and vapour, as well as in the form of physically bound water between the cellulose fibres exhibiting the potential for hydrogen bonding. It is not always obvious that this is the case but paper contains some 5 wt% water depending on the paper grade. Some of the water is a remnant from the manufacturing process but paper also takes up moisture from air (humidity) during transport, storage and processing. Control of moisture is a vital part of the manufacturing of the product but is also a cost factor when needed to be dried. Moisture plays an important role in the final quality and also affects the stability of the process. There are two main aspects of concern in moisture control in paper: allowing too much moisture or too little of it, while the operating window is in the end quite narrow. Too low moisture content in the paper makes it more brittle (induces cracks and web breaks) and is bad from an energy viewpoint during manufacture (unnecessary over-drying). Too high moisture content and excess of fountain solution tends to make the paper too elastic inducing creases and register problems in printing, as well as affecting the drying time of the inks or disrupting the adhesion of the inks and their resulting tendency to adhere to contact rollers [Donigian *et al.,* 2004].

As mentioned, in addition to the existing moisture, paper is also exposed to moisture/liquid during converting and in the latter stages during printing. In offset printing, the capillary forces provide for penetration of the ink solvent and the applied external pressure in the printing nips leads to fountain solution being permeated into the pore network of paper, where capillary forces

continue the action of imbibition. The rate and the amount of imbibition/penetration are determined by the surface characteristics, both chemical and structural, together with their spatial heterogeneity, as well as the capillarity and permeability properties of the paper. All these factors define the capacity of the paper to take up liquid in relation to the delivered applied liquid volume. The interactions between liquids and solids are crucial for achieving optimal processing performance and quality. However, like in many other industrial applications, wetting of porous materials by liquids includes not only the bulk liquid imbibition but also its evaporation and surface spreading. Knowledge of the position of the wetting front and the distribution/degree of pore filling within the structure is crucial in describing the transport phenomena involved.

Many technological processes require control of liquid spreading over solid surfaces, for example in printing. To obtain optimal wetting by the water-based fountain solution in the offset printing process, for example, the surface tension of the liquid has to be reduced. This is done by various additives, such as isopropyl alcohol and surfactants. These additive components either directly modify the surface tension of the fountain solution (alcohol) or are adsorbed onto the liquid-vapour, solid-liquid, and solid-vapour interfaces, and so subsequently modify the wetting behaviour at the three-point contact between them. In order to achieve good print quality, the wetting characteristics have to be optimised for a certain liquid-solid combination.

The strengths in being able to monitor moisture differences over a surface, for example in inked and non-inked areas, allow new possibilities in material construction, machine runnability, optimization and quality control. Although exemplifying paper as a porous medium in this work, the generalisation to dynamic liquid transfer onto the surface, including permeation and imbibition into porous media, is of importance to many industrial and naturally occurring environmental processes. Accurate measurement of predominantly water-containing fountain solution picked up by the ink and the paper has been a missing link in the evaluation of the behaviour of paper on the printing press, and is required for understanding the mechanism of the interaction between fountain solution, ink and paper. Both online and offline applications have previously been published, but, so far, real-time analyses from multiple locations from both non-image and printed areas of the printed sheet have not been reported.

As seen in many publications, the different areas on the paper are identified as printed and unprinted, as well as gradations of print density or tone related to a sum of microscopic printed dots and unprinted space around them. It is obvious that the processed unprinted areas also have

run through the printing machine with application of fountain solution, i.e. “printed with non-imaging” fountain solution. Thus, for clarification, hereafter, these respective areas are defined as image and non-image areas. When the term unprinted is used in this thesis, it describes an unprinted paper not being further processed after manufacturing.

2 Background

2.1 Papermaking

Paper is a thin, flexible, fibrous web consisting of cellulose fibres deposited upon each other, randomly deposited and oriented to varied degrees, depending on manufacture, in either one (complete alignment) or two dimensions (no directionality) of the plane of the paper to create a fibre matrix [Paulapuro, 1999]. The fibres are bonded by proposed hydrogen bonds, which form during drying, in association with the water or moisture menisci remaining after drying [Niskanen, 1998].

The first stage in the paper making process is the production of the fibres from wood (pulp) to constitute the sheet. The pulping process separates the individual fibres allowing them to enter into a new random configuration within the paper material. The pulping process is either performed by grinding wood to pulp or cooking of wood with chemicals, or both [Paulapuro, 1999]. The pulping process is followed by the paper formation stage in the paper machine wet end as the dilute fibre suspension (stock) is laid on a drainage wire to dewater.

It is important to know and to highlight already at this stage that the moisture related issues appearing in the printing process originate all the way from the making of the base paper sheet and the subsequent coating and calendering. It is the focus of this work to consider the impact of rewetting in respect to this built-in behaviour resulting from the moisture history of the paper.

2.2 Pigment coating

In the pigment coating process, the surface of the base paper is applied with a layer or multi-layers of pigment coating to give it certain qualities, including weight, strength, gloss, smoothness, but also properties to control ink pigment and varnish penetration [Paltakari, 2009]. The base paper can be pre-coated and top-coated with the same or different formulations depending on the quality targets. Depending on the solids content of the coating dispersion, it contains a certain amount of water and that means addition of moisture to the base paper during the coating process.

Through the coating process, the surface pore structure characteristics of the paper will be determined. The final paper contains pores of various size ranges and has a surface structure with nano, micro and macro-scale features [Gane, 2001]. The liquid evaporation during coating

drying can be accelerated by producing a more permeable structured paper (increased porosity and pore connectivity) but this obviously also affects the surface characteristics of the paper. Controlling dewatering rate is important in the coating application, minimizing the penetration of water into the base paper, which is important for subsequent printing [Zou, 2007].

2.3 Calendering

Calendering by the application of pressure between roller nips compresses the coating structure, aligns particles of high aspect ratio (shape factor) and thus increases paper smoothness and gloss [Lepoutre, 1989]. The major compressive action is transmitted to the base paper. Depending on calendering conditions, paper passes through nips of steel and/or softer cotton/polymer rolls, which can be heated, and moisture is used to control the deformability of the underlying base paper [Rautiainen, 2010]. When the paper is calendered, its density will be increased and the pore volume reduced [Lepoutre, 1989]. Calendering also affects the light scattering properties of the paper [Hiorns, *et al.,* 1998].

Uneven calendering may lead to uneven imbibition/permeation of liquids in the printing process. Some authors have pointed out that calendering can cause areas on the paper having almost closed surfaces, especially due to incompressibility of a rough base paper [Whalen-Shaw and Eby, 1991; Allem, 1998].

2.4 Printing – history and future trends

The history of printing started around 3 000 BC when images were impressed on clay tablets to form beautiful artwork. The first efficient printing press was built by Johannes Gutenberg in the fifteenth century, which is one of the milestone developments in printing history [Meggs, 1998]. Nowadays, printing is understood to be the process where the paper is applied with ink, and thereby text and high quality images are reproduced [Oittinen and Saarelma, 2009]. The printing process gives the paper added-value and is an essential part of publishing and transaction printing.

During the last decade, printed media technology have shown a change of direction towards digital printing, mainly due to its flexibility in terms of variable data printing, contributing to personalization in so-called direct mail etc. Digital printing technologies have taken, and continue to take, an increasing market share from offset printed products. There are, however, still great challenges with digital printing to reach the same high image quality, high speed,

broad web printing and cost-effectiveness as has traditionally been the case in high volume print jobs [Kipphan, 2001]. These are the main reasons why offset printing still is a competitive printing method and today has a share of about 50 % of all printed products [Smyth, 2009]. The heatset web offset share is roughly 16 %. Despite the tough markets, there is still room for improvement in the offset print technology, and this is a trend that is both driving and shaping the market. Four trends which are important in webfed offset printing are that the machines must be fast, productive, environmentally-friendly and economic [Botel, 2010], and, above all, cheaper in terms of what is printed. Strong focus is also put on the make-ready times and in setting targets to produce less waste. The combination of conventional and digital printing allows new unforeseen possibilities for hybrid printing. The availability of narrow web machines additionally allows possibilities for short-run print jobs.

2.5 Heatset web offset printing process (HSWO)

Offset is an indirect lithographic printing process since the ink is not directly applied from the image plate onto the paper (Figure 1). The printed and non-image areas are created by a flat image carrier on which the image to be printed takes up ink from ink rollers, while the areas without ink accepts a water-based film, called fountain solution, which keeps the non-image areas free of ink [Kipphan, 2001]. Hence, the different surface chemistries of the printing plate are based on the attraction of oil and water, respectively, and this prevents the ink from spreading to the non-image areas. Offset printing is a method which applies the process colours wet-on-wet. This is achieved by “setting off” the surface contents of the image plate onto a printing blanket. This printing blanket thus enables the transfer to the paper. The paper is thus also wetted with water in the printing process by a film of fountain solution applied from the printing plate via the rubber blanket to the paper [Aspler, 2006]. In the HSWO process, water/ink is applied simultaneously on both sides and printing layouts are usually very different on the different sides. This has also an impact on the implications described in this work. However, to avoid this complication and to allow a tractable analysis only one sided was studied. In contrast to both sheetfed and coldset offset, heatset offset uses heat to dry the applied ink film.

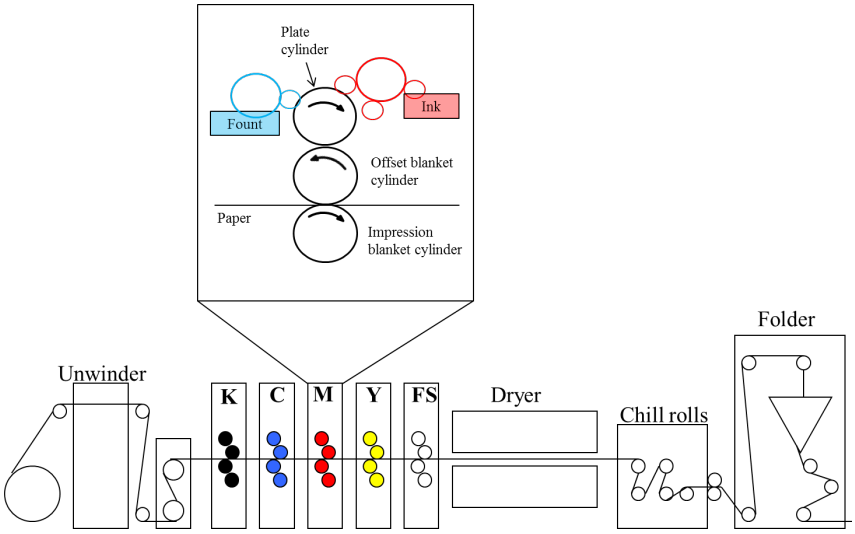

Figure 1. Simplified schematic of a heatset printing press and printing units.

The paper to be printed passes through several printing nips, usually four or more, creating a complete image. The paper takes up moisture partly from the surroundings and partly from the printing machine. The water-based fountain solution is applied from the printing units as a liquid film, affecting the moisture content of the paper. After the printing units, the paper web goes into the dryer, which normally is composed of 2–4 hot air sections. In the dryer, parts of the solvent in the ink (30- 40 wt% mineral oil in heatset ink) are evaporated. Drying can be seen as being comprised of two different mechanisms, namely surface evaporation and internal moisture transfer [Gerstner *et al.,* 2012; Songok *et al.,* 2012]. Drying, or solvent removal from a coating, is a critical step in producing high quality prints. Heatset dryers blow hot air at temperatures of up to 300 °C which may result in web temperatures of 150 ºC in order to remove the high boiling point oil-based solvents [Kipphan, 2001]. Drying air velocity, temperature and solvent concentration are important operating conditions for drying efficiency, and can be chosen to produce printed paper that meets the required quality specifications [Kipphan, 2001]. Improper drying can lead to high residual solvent content, blisters and waving and also smearing in the post-print operations. After drying, the printed paper is rapidly cooled down in the chill roller section after which the silicone emulsion is applied on the paper to improve runnability in the folding station by reducing smearing on rollers, reducing static electricity build-up and reduce friction [Kipphan, 2001].

The heatset offset process sets certain requirements on paper, such as smoothness, gloss, brightness, adequate stiffness and surface strength. The coating needs to be well bound because considerable tack forces in the *z*-direction, i.e. perpendicular to the plane of the paper, are exerted by the highly viscous paste-like inks. At the same time, the coating must be sufficiently porous to permit fast, but controlled and balanced penetration of the printing ink solvent without reducing the print gloss, whilst having high water penetration resistance but sufficiently fast penetration of the fountain solution to prevent adhesion failure of subsequently applied ink layers. A very thorough review on the main variables in offset printing, including effects on print quality, measurement and control has been published by Dalphond [1999].

The most common paper grades printed in heatset offset are light-weight-coated papers (LWC) and uncoated highly pigment-filled supercalendered papers (SC). A few of the typical products printed with heatset offset include newspapers, magazines, brochures, stationery and books.

2.6 Printability – Runnability – Print quality

In this section, printability and runnability issues, being influenced by the liquid/moisture in or applied on the paper, are discussed.

Printability and runnability on the printing press are two terms which are very widely discussed when a product is developed or improved. Runnability mainly refers to problem-free running of the paper in the process and is both mechanical and substrate dependent. Printability refers to the ability to achieve proper interactions between machine-paper-ink etc. in terms of ink transfer, setting and drying as well as the overall printing conditions. Substrate structural, mechanical and chemical properties define the printability in respect to a given ink. By optimizing printability and runnability, a good print quality is achieved. A good print quality is the perceived high quality of the image and value defined by the end-user, i.e. optical/perceptual properties and the aesthetics of the printed paper. Moisture is a key factor controlling the printability, but also the process stability and runnability.

It is well known that moisture differences between the printed and non-image areas cause tension gradients resulting in dimensional instabilities in the printed paper [Kipphan, 2001]. The effect of the ratio of the moisture content in the image area, namely that ink-water emulsion transported together with the ink film, to the non-image area is very important, especially when the image area is dominant and unbalanced in respect to area distribution on the overall printed

sheet [MacPhee, 2000; Simmons *et al.,* 2001]. Concerning moisture, the rapid and uneven changes in moisture distribution of coated and highly filled paper, and the total vaporisation of water bound to paper fibres, cause blistering, fibre puffing, dimensional instabilities, such as waviness, deposit build-ups on blankets and plates and breaks in subsequent folding, as well as adverse effects on printability. Moisture loss can also cause registration problems. All these effects are closely related to an uneven moisture profile in the paper and/or the combinations of draw tension and drying, respectively [MacPhee, 2000]. The waving defect has been widely studied and one of the reasons behind the occurrence is the exposure to high heat creating a differential moisture loss/retention across the web between image and non-image areas [Strong, 1984; Hirabayashi, 1998]. One suggested solution to reduce waving presented in the literature is to use excessively high dryer temperatures, which obviously is not an energy efficient solution to the problem. Waviness results from stretching of the material in one direction while being prevented from shrinking in the perpendicular direction [MacPhee *et al.,* 2000]. Air permeability variation has been indicated as being related to the key factor affecting waving/fluting tendency, with inelastic deformations promoted by high drying temperatures preserving waving [Kulachenko, 2006]. Kulachenko showed in his study that when the humidity was increased, the amplitude of the created waves increased. Land [2004] again claimed that a high tension resulted in shorter wavelengths and that higher moisture uptake resulted in a greater waviness.

Both ink transfer and ink refusal in lithographic offset printing can be described by the weak boundary film splitting mechanism, meaning that the position of the splitting will shift if an even weaker boundary is present [Tian *et al.,* 2009]. Tests have shown that fast ink setting papers result in rapid tack build-up which can lead to ink fracture and piling problems [Kirmeier, 2007]. Piling is a problem related mainly to coated papers in offset printing. Pigment particles that are weakly bonded or are washed out as the coating reacts with fountain solution can result in the development of accumulation on the printing blanket, i.e. piling. A study by Chami Khazraji *et al.* [2009] showed that depending e.g. on the pH of the fountain solution, calcium ions present in the magenta ink pigment promote a risk of contamination of printing blankets. Passoja *et al*., [2007] have studied the piling arising from a previously applied ink at a prior print station by monitoring the accumulation build-up on the blanket at a subsequent station of that same ink in the current colour non-image area using online microscopic imaging. However, a high water feed reduces the risk of ink being deposited in the non-image areas. Depending on the fountain solution formulation, the presence of surfactants on the non-image areas may lead to a pick up of

loosely bonded particles by the blanket and the plate (dependent on the surfactant concentration). Under the influence of nip pressure, the piling may wander to the trailing edges of print areas due to the action of the printing nip displacing fountain solution from the surface of the ink layer to the tail edge of the image. Especially during long production runs, piling can thus lead to a lower print (colour) density.

Moisture pick up by the paper also interferes with image formation, and this applies not only to offset printing. These general effects will depend also on the moisture uniformity resulting in the *xy* plane in respect to potential mottling, i.e. apparent unevenness of print density and/or print gloss [Arai *et al.,* 1988; Ström and Karathanasis, 2008]. Mottling induced by water occurs frequently from poor water-absorbing characteristics of the base paper [Ström, 2005], or as has been more recently shown by excessive hygroscopy of surface components [Kamal Alm *et al.,* 2010a; Kamal Alm, 2010b].

The dimensional changes, and the resultant poor print quality, are dependent on the amount of transferred water, its distribution in the sheet, the time in and between the printing units, the nip pressure, the rubber blanket (surface properties), printing layout and the paper grade [Kipphan, 2001]. The paper can be exposed to water either by surrounding water vapour (changes in the relative humidity) or by contact with an aqueous film, as studied here. The offset printing performance, itself, depends strongly on the content of surface water [Lie *et al.,* 1992].

When the printing ink is dried, the main part of the internal moisture of the paper is evaporated. The liquid evaporating from the paper might break the structure of the paper, thus causing fibre roughening. The roughening process involves fibre swelling, bond breaking and release of internal stresses due to the molecular diffusion of water into fibre walls. Enomae and Lepoutre [1997] have discussed the role of moisture diffusion into the bulk and its effect on swelling behaviour of coated paper.

As reviewed, the fountain solution is prone to induce several print quality defects and machine runnability problems. Waterless offset printing is an alternative, avoiding the disturbances originating from the fountain solution [Nordström, 2003]. However, fountain solution also acts as a cleaning or washing agent, as well as a coolant for the press. Waterless offset brings its own challenges, therefore, in terms of press cooling and the likely build-up of paper derived contamination. The advantages and disadvantages between conventional heatset offset and waterless offset printing have been extensively reported by Nordström [Nordström,

2003]. Heatset offset and waterless offset processes have previously been compared to determine the role of fountain solution on the roughening of the printed paper [Sederholm and Nieminen, 1998]. It was concluded that fountain solution contributed to roughening. However, the amount of fountain solution did not appear to affect the degree of roughening, suggesting that it is principally a vapour effect. The amount of coat weight also reduced the roughening tendency, since a higher coat weight reduces the fountain solution penetration into the underlying fibre structure and the heat transfer in the drying process. The authors also showed that a paper with lower moisture content, exhibited less roughening, however increasing the risk for cracking at the fold.

2.7 Heatset offset printing inks, the printing unit and ink-water balance

Offset inks are based on pigments, resins, vegetable and mineral oils, as well as additives. Normally, only synthetic organic pigments are used and they define the shades and fastness (colour resistance to fading under influence of light) properties of the ink [Frank, 2006]. The inks used in the heatset offset printing process consist mainly of 30-50 wt% binder, 30-50 wt% solvent, 20-30 wt% pigment and some 0-10 wt% of additives, for example to control rheology. Heatset offset inks need a high proportion of mineral oils with defined evaporation behaviour. The four-colour ink set is usually applied respectively from each of four printing units in a determined order. More units may be present to provide for the printing of spot colours, usually to support trademarks etc., and optically active speciality inks, such as metallic reflectance finishes and varnishes. The ISO 12647-2:2004 standardizes the chromatic ink sequence to cyan (C), magenta (M) and yellow (Y). The standard defines black as either first or last, and both are considered acceptable. The use of the letter K for black ink stands for key.

The heatset offset inking unit consists of several rollers, forming the so-called ink train, giving the required thin, uniform and smooth distribution characteristics for the printed image [Oittinen and Saarelma, 2009]. The ink is transported from roller to roller via ink film splitting. The aim of the splitting transport is to get ever decreasing ink film thickness. However, once on the printing blanket, the transport (trapping) from rubber to paper should be maximized. The ink layer thickness applied to the paper is around 0.25-1.5 μm [Blayo and Pineaux, 2005]. Ink and fountain solution are inevitably mixed in the offset printing process, and this is a characteristic that is quite pronounced for heatset offset printing.

The stability of droplets of fountain solution in the ink are influenced by the shear stresses experienced by the ink and fountain solution, the temperature, the emulsification time and the supply of fountain solution to the ink [Massolt and Hohtari, 2002]. The degree of emulsification affects the process runnability/stability and print quality. Ink can carry a certain amount of liquid water (30-50 wt%) within itself [Olejniczak *et al.,* 2004; Aspler, 2006]. The ink-water balance is critical in order to have a stable process. If the fountain solution feed volume is too low in the printing process, ink is transferred to the non-image areas (toning) and if the fountain solution feed is too high, the print density drops, halftone dots become ragged and fountain solution partly stays on the ink surface as surface water and interferes with ink transfer (water marking) [Kipphan, 2001]. The aim for the printer is to adjust the fountain solution feed level to just above the lower volume limit where inking of the non-image areas begins to occur, known as the toning limit. Pickup of fountain solution in ink, despite the best control of fountain solution volume delivery, leads to an undesirable excessive fountain solution emulsification and problems such as changes in the rheological properties of the ink, toning and ink pigment flocculation can occur. Research has shown that the degree of emulsification of ink and fountain solution results in different penetration depths into uncoated paper, and higher emulsification resulting in deeper penetration due to lower viscosity of the emulsion [Liu *et al.,* 2006]. Another study showed that emulsified inks had a faster gloss development than pure inks, probably due to the change in viscosity for emulsified inks [Xiang and Bousfield, 2002]. Research on ink-fountain solution balance, shows that the most important effect of emulsified fountain solution on ink-fountain solution-paper interactions following offset printing is the decrease of ink cohesion [Fröberg *et al.,* 2000]. Hence, this effect is primarily due to the introduction of defects in the ink film, which lowers the cohesive force due to the generation of free surface within the ink film.

The trends seen in heatset offset inks are mainly related to the use of lower/moderate boiling point mineral oils to minimize the effect of waviness and fold cracking by reducing the drying intensity required in the press. This also allows lower drying temperatures in the heatset dryer. Ink development is being driven to meet the needs of larger and faster printing presses [Frank, 2006].

2.8 Heatset offset fountain solutions and fountain solution transportation

Together with the printing ink, fountain solution is the main component in order to be able to run the heatset offset printing machine. The fountain solution is expected to keep the ink off the non-image areas of the printing plate via the formation of an oleophobic liquid film, thus

maintaining the hydrophilic nature of the non-image areas, to promote fast spreading over the plate, to lubricate the plate and the rubber blanket, and to control the emulsification of ink and water [Kipphan, 2001].

The fountain solution in heatset offset printing is a water based mixture of many components. All ingredients play their role to finally form the solution and give it its distinct properties. The fountain solution units deliver a thin layer of solution of about 0.3-1 μm to the non-image areas of the plate. The dosage of fountain solution, as discussed in the previous section, is adjusted so that the printing plate does not run dry (no toning, i.e. no ink on non-image areas). Much of the fountain solution is evaporated during the printing process, some is emulsified within the ink and some is transported all the way to the paper substrate. The proportions between these phenomena are crucial in order to understand the problems in runnability and printability caused by applied liquid/moisture. A comparison of changes in moisture content suggests that in a properly operated lithographic press most of the fountain solution is lost through evaporation in the inker, and not transferred to the paper [MacPhee and Thompson, 1999].

The fountain solution properties are highly dependent on the local tap water quality, it being over 80 % of the solution. Many printing houses overcome the issue with fluctuating tap water quality by using reverse osmosis systems. The water quality and especially the hardness of the water affect the properties of the fountain solution. The water hardness is determined by the sum of all dissolved metal ions in water arising from the dissolved minerals from the ground. The most common metals are calcium, magnesium, sodium and iron. Calcium is the most sensitive ion having potential to disturb the chemical balance in the printing process [Kiuru *et al.,* 2010]. The slightly acidic fountain solution may dissolve $CaCO_3$ from paper until the equilibrium [Ca^{2+}] concentration is reached. Iron may cause problems with corrosion while magnesium and sodium practically are non-disturbing metal ions. The problems induced by the metal ion are mainly seen as pH and conductivity changes affecting the ink-fountain solution interactions. Harder water requires a stronger acid buffer system than soft water [Stephens, 1993]. The water hardness scale is classified according to degrees of ºdH (deutsche Härte), where 1 ºdH corresponds to 10 mg calcium oxide per litre. Both very soft (0-4 ºdH) and very hard (above 20 ºdH) water can cause difficulties during printing, and especially during long runs. The general recommendation for proper runnability/quality is that the hardness should be around 10 ºdH [Pineaux *et al.,* 1997].

Apart from the water, the main component/components in a heatset offset fountain solution is/are isopropyl alcohol (IPA) and/or an IPA replacing agent, a surfactant. The surfactant used as a substitute for IPA is usually a non-ionic one, since they create less foam [Dougherty, 1989], which otherwise disturbs the process. The foaming problem can also be solved by using a defoamer. The surfactant is typically also glycol based [Medina, 1997; Musselman and Chander, 2002]. The trend in the replacement of IPA is observed globally, but heatset web offset presses in Europe still commonly use some IPA, but the concentration is much lower than before. The reason for this is the health issue concerning volatile organic compounds (VOC). IPA is used mainly to lower the surface tension and hence to promote wettability of the plate and the blanket by the fountain solution. IPA makes the water phase more non-polar which promotes better contact with the offset plate and creates a lower interfacial tension [Lee, 1998]. A fountain system containing IPA is usually cooled to +10 ºC to diminish excessive evaporation. The use of IPA also prevents microbiological activity (fungus, biofilm build-ups etc.). The role of the surfactant is similar, however much smaller quantities are required to reach the same functionality [Aurenty *et al.,* 1999]. Like IPA, the surfactant also reduces the surface tension of the solution and affects the ink-in-water and water-in-ink emulsification. Importantly, surfactants additionally alter the wetting properties when in contact with the various surfaces, including the printed paper. The wetting involves the adsorption of the surfactant(s) at the liquid-vapour interface and at the solid-liquid interface and influences the spreading at the perimeter of the three-phase contact line (air-solid-liquid). The wetting kinetics, therefore, are no longer dependent on the surface tension of the liquid alone, as was the case for IPA, but on the interfacial tension between liquid and solid. The dynamic adsorption efficiency of the surfactants during the precursor film formation is critical in order for new wettable surfaces to be created sufficiently rapidly.

The trend for fountain solutions in heatset offset printing is to run at higher pH levels, with decreased amount of, or zero, VOCs, increased buffer capacity and more stringent cost control. Issues challenging the paper industry in respect to reaction to wetting involve reaching ever lower basis weights, increasing use of ground (GCC) and precipitated (PCC) calcium carbonate, and hence alkalinity, LWC paper grade usage moving to cheaper SC grades, and permeable narrow particle size distribution for optically bright, high light scattering coatings providing less protection from liquid permeation into the base sheet [Gerson and Lewis, 2008].

Adjustment of the fountain solution circulation rate, flow rate and composition for various paper grades/surfaces, and the concentration adjustment during a press run, are all steered by the fountain solution picked up by the ink and the paper, and equilibrium is established by controlling the print quality and press runnability. It is important that the fountain solution rapidly penetrates into the paper structure, or is otherwise removed from the surface of the paper, in order not to interfere with the ink from the subsequent colour units, known as ink repellence [Kipphan, 2001]. The fountain solution is transferred to the paper in the printing nip and the resulting penetration is highly dependent on paper properties, such as surface chemistry, surface roughness and pore structure. Tuominen *et al.,* [2003] have concluded that the coating structure has more influence on the amount of fountain solution transferred than the fountain solution composition.

There have been several attempts to study the transfer of fountain solution to paper by using, for example, tracing elements such as lithium or caesium salts mixed in water [Reinius *et al.,* 2003; Lipponen *et al.,* 2004; Preston *et al.,* 2008]. The location of the ion species has afterwards been analysed with surface sensitive image analysis of the sample surface or cross-section with, for example, time-of-flight secondary ion mass spectroscopy (ToF-SIMS). Some obstacles may, however, arise when using this kind of indirect determination of the amount of liquid inside a material. For example, it has been discussed in the literature whether some kaolin species may chemically exchange Cs^+ cations from the solution [Tamura, 1961]. Additionally, when imbibing any Group I cation (element periodic table) from its soluble salt, via the fountain solution into a coating structure, an unknown proportion of the cation will become adsorbed onto the pigment surface via dispersing agent, e.g. polyacrylate, and may even partially solubilise the dispersant in the case of calcium carbonate coatings. Concerning image analysis it is thus very important to take into account the amount of free Group I ions in the substrate but also the salt bound ions. Lithium is a good tracing element due to the higher sensitivity compared to caesium, and in addition, e.g. the $C_{10}H_{13}$, C_9H_9O, $C_6H_{13}O_3$, $C_4H_{13}OSi_2$, $C_3H_9O_2Si_2$ peaks, disturb (overlap) the Cs peak in the mass spectra. These peaks can originate from mineral oil and e.g. polystyrene. However, lithium and its compounds are used in many industrial applications and thus are present in many materials.

2.9 Paper moisture content

The relative humidity (RH) of paper is defined as the proportion of water vapour present in paper in comparison with what the air could contain at the same given temperature. At various

relative humidity, paper holds different percentages of water and will absorb/adsorb or give up water until it comes to equilibrium under the existing room temperature. The moisture content of paper is not only dependent on the surrounding humidity, but is also affected by the temperature, grammage, hygroscopic properties, and, of course, the equilibrium time in a given environment [Niskanen, 1998]. The paper moisture content varies a lot throughout the manufacturing process. According to previous research, the region from 7-30 wt% moisture is the region where the *z*-directional moisture gradients are the highest [Paltakari, 2000; Timofeev *et al.,* 2002]. The paper coming from the paper machine usually contains 3-7 wt% moisture depending on the paper grade. The moisture content of paper and its variation is critical both in the manufacturing and the later finishing and converting of the paper.

The moisture content has been shown to have clear effects on the calendering response, print quality, friction and structural dimensions of paper [Whalen-Shaw and Eby, 1991, Allem, 1998; Hiorns, 1998; Dimmic and Huhtala, 2005; Dimmic, 2007]. The moisture is lost from paper during drying, creating an uneven moisture profile in the structure [Ferderer, 2002]. The moisture content, as well as having a great influence on the dimensional stability of paper, strongly impacts on the physical and mechanical properties of printed substrates during their manufacture [McCormick-Goodhart, 1996]. Since variations in paper moisture content, especially during printing, also induce severe problems in both quality and runnability, there have been several attempts to re-moisten the paper uniformly by using liquid application systems. Re-moistening levels out the variations in the cross web moisture profile.

The internal liquid and vapour contents of paper are eventually rapidly changed during the drying process in several printing technologies, such as heatset web offset (studied here), thermal drying of inkjet etc., which can lead further to distortion due to mechanical stresses, which disrupt the internal or surface structure and ultimately may even break the paper. The paper quality, and thus the composite structure, is obviously critical when considering the rate of liquid and vapour removal during print drying in relation to the prior storage of, and retained, moisture inside the reel. The storage environment of the reels, in respect to the subsequent surrounding conditions of the printing house, plays a dominant role. In the case of coated paper, the interrelation between liquid and vapour transmission within the porous coating, thus defining the transport of moisture to and from the underlying base paper by permeation, capillarity and diffusion, becomes the major controlling factor in respect to paper stability.

2.10 Wetting and liquid penetration in porous media

Liquid wetting of a porous medium is related to lateral spreading in the surface cavities/grooves, in the just sub-surface pores, as well as to a penetration by capillary driven imbibition into the coating structure and the underlying fibre matrix of the paper substrate. The main factor controlling wetting of a non-porous surface is the outermost surface properties (surface chemical and physical properties of the surface), or, more precisely, the relative surface volume per unit planar area manifesting these properties. The initial surface wetting starts as soon as the liquid comes into contact with the substrate, and it has been shown, that the spreading volume is dependent on the roughness of a non-absorbent substrate [Salminen, 1988]. Many studies have been published regarding the rapid initial droplet imbibition, observing the change in contact angles with a high-speed camera [Elftonson and Ström, 1995; Swerin *et al.,* 2007; Ström *et al.,* 2008]. The wetting on a longer time scale is controlled by diffusion of additive molecules to the liquid-vapour and the solid-liquid interface. When a wetting liquid penetrates by capillary imbibition into the coating layer, the pore size and accessible surface area as well as the permeability, surface chemistry and structure of the coating layer are important. The competing capillarity of the coating pores between the packed pigments and binder, and the pores between and within the fibres in the base paper, plays a crucial role. The link between the pore size distribution and the behaviour of the contact point wetting has qualitatively been demonstrated by Schoelkopf *et al*. [2000] with the finding that pores < 0.1 μm define the short timescale local capillary imbibition, acting prior to the onset of viscous drag within the structure. This regime is proposed to repeat throughout the structure wherever fine connecting pores link the remaining structure to a larger reservoir pore [Schoelkopf *et al.,* 2000]. Since the surface chemistry plays an important role in offset printing, many studies of the surface chemical properties of substrates used in offset have been carried out [Krishnan and Klein, 1991; Lyne and Huang, 1993; Ström, 1993; Al-Turaif *et al.,* 1995].

Porous pigmented structures and the imbibition rate and volume dependency of porous network structures have previously been used to determine the penetration rate of liquids [Gane *et al.,* 2004]. It has been found that the imbibition rate of low viscosity fluids can be correlated to short timescale inertia-controlled imbibition into the porous network structure of the coating layer. The interplay between preferential plug flow-like filling of the finest pores and the inertially retarded filling of larger pores defines the imbibition dynamic on the nanosecond timescale. Both simulated and experimental studies have been subsequently published

[Schoelkopf *et al.,* 2000]. Further longer time uptake into the bulk structure continues this nano-scale interplay at each and every geometrical connective feature within the structure, whilst simultaneously superposing the viscous drag of the permeable network. This was demonstrated by Ridgway and Gane [2002] adopting an algorithm based on the Bosanquet equation [Bosanquet, 1923] applied to a model porous network, concluding that pores up to a given diameter in a porous network fill rapidly while bigger features remain by-passed and tend to remain unfilled under conditions of limited supply volumes of fluid. This confirmed the observations made by Schoelkopf *et al*., [2000] studying liquid uptake from an applied droplet into tablet structures of porous pigmented coating. The short time scale wetting was also confirmed in a standard fine capillary by observation using a high-speed camera, showing the inertial plug flow to viscous laminar flow transition aspects of the Bosanquet behaviour [Quéré, 1997].

The coating pore structure also influences the imbibed amount of fountain solution and the final setting rate of the ink [Ström *et al., 2003*]. Preston *et al*. [2002] highlighted that to gain access to internal pores, an adequate surface pore density is required, and manipulated the deviation from square root pore size and time behaviour by introducing a surface pore density distribution and applying an arbitrary root time scaling [Preston *et al.,* 2002]. Rousu *et al*. [2000] showed that the coating structure can be optimized to control fluid phase kinetics.

In the case of a printing nip, the action of pressure also needs to be considered. Pressure will lead to two additional phenomena: forced wetting of the surface and permeation of the porous structure in the case of low viscosity liquid, e.g. fountain solution. Zang and Aspler [1995] have published simulations on the free fluid penetration after the ink penetration into uncoated paper in the printing nip.

In literature, there is a broad interpretation of how much water is transferred to paper in a printing process. Despite its large impact, the amount of fountain solution picked up by paper is a very small quantity in absolute terms, though significant in reference to the mass, pore volume and thickness of paper. Gravimetric methods, therefore, cannot be expected to provide the accuracy which is required, especially since fountain solution is lost in the delivery system and in roller trains through spillage and evaporation. It has been pointed out in previous studies that in some cases more fountain solution is transferred to the printed areas of the paper by the water-ink emulsion than in the non-image areas [Lim *et al.*, 1996]. The fact that ink carries most of the

solution has been established [Lindquist *et al.,* 1981; MacPhee, 1985; Aspler 2006] but quantitative information on the amount of the solution carried by the ink and the paper has not been firmly reported so far. Non-intrusive techniques have been discussed in the literature to provide information about liquid and moisture uptake. For example, terahertz imaging has been recently used to observe the development of drying of paper in laboratory scale [Banerjee *et al.,* 2009]. This complex measurement technology has, however, not yet been used for online and multipoint analyses. A number of measurement principles to quantify water content can be adapted to on-press applications, based on, for example, infrared [Rosenberg, 1985; Thormählen, 1988] and trace element detection [Säynevirta and Karttunen, 1973]. However, knowledge of the emulsified state and how much is transferred with the ink to the printed and non-image areas is lacking.

2.11 Infrared spectroscopy (IR)

Infrared spectroscopy is a widely used technique to verify, follow-up and evaluate, the chemical nature of materials by studying specific components. Infrared radiation is part of the broad electromagnetic energy spectrum at wavelengths longer than the visible but shorter than microwave radiation (Figure 2).

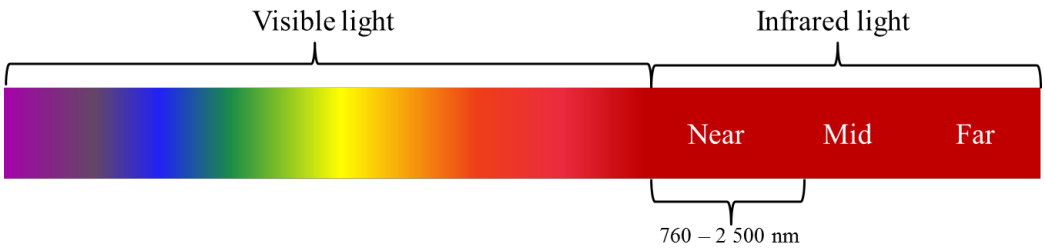

Figure 2. Spectral wavelength range for near-infrared in comparison to the whole infrared and visible light.

It corresponds to the wide range of energies associated with molecular vibrations. The infrared wavelength range is divided into three regions: near-infrared (NIR) (780 nm – 2 500 nm), mid-infrared (MIR) (2 500 nm - 4 000 nm) and far-infrared (FIR) (4 000 – 10 000 nm). IR absorption by a material is generally presented in the form of an absorbance spectrum as a function of wavelength (nm), or more often related to interaction reciprocal space as wavenumber (cm^{-1}), displayed as the *x*-axis and absorption intensity as the *y*-axis. Different

functional groups in chemical compounds on exposure absorb characteristic frequencies of the IR radiation.

The most popular way of obtaining IR spectra is to pass an IR beam directly through the sample. Transmission spectra for water detection are good for thin samples (< 20 μm), but since, in this study, the focus is set on the analysis of penetration and drying of water-based liquids where the total thickness is between 50 - 200 μm, diffuse reflectance measurements are more useful both in terms of sensitivity (measurement of surface layers) and accuracy. The diffuse scattered radiation can be collected in a wide spatial angle.

2.12 Near-infrared spectroscopy (NIR)

For a medium containing, for example, water molecules, portions of the electromagnetic spectrum are absorbed by the water molecules during the transmission of electromagnetic radiation. This NIR absorption occurs preferentially at certain characteristic wavelengths. NIR is concerned with a specific region of the IR, adjacent to the red end of the visible spectrum. Most materials absorb NIR light at specific wavelengths depending on the composition of the material, but water is one of the best-known examples of an NIR absorber. Strong absorbance by water vapour occurs at wavelengths around 2 900, 1 950 and 1 450 nm, (1 950 and 1 450 nm being within the NIR range) with weaker absorption around 1 200 and 970 nm (Figure 3). Water vapour also exhibits three additional sets of absorption lines near 930, 820, and 730 nm [Jacquemoud and Ustin, 2003].

The results presented in this thesis focus on water absorption bands located at 1 450 nm and 1 950 nm, to avoid overlap with other absorption bands associated with the compositional components of the sheet, and thus the other bands are excluded hereafter from the discussion.

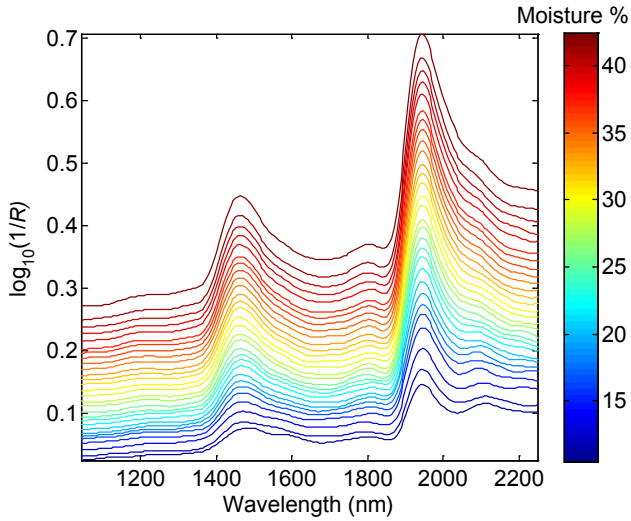

Figure 3. The influence of water content on the NIR absorbance spectrum of paper. The baseline is raised and the water absorption bands at 1 450 nm and 1 940 nm appear when the moisture content increase.

NIR spectroscopy has previously been used to determine the moisture content [Pugh, 1980] and *z*-directional moisture profiles of paper coatings [Paaso *et al.,* 2006; Keränen *et al.,* 2008]. Since the IR absorption bands of water are easily determined in the near-infrared spectral region, the measuring of moisture contents of various samples has gained much interest in the field [Paaso, 2007]. By application of NIR analysis it has been found that the choice of drying strategy during coating clearly influences the water penetration and the immobilisation of the coating [Paaso *et al.,* 2006]. The moisture content of paper can of course also be measured with other techniques, like gravimetry [Anderson, 1992] or NMR (Nuclear magnetic resonance) [Wessman *et al.,* 2000], but the advantages with the NIR technique are that it can measure the whole spectrum of a sample very rapidly, and so it can, in principle, be used for online process evaluation. Although the NIR reflection wavelength has a limited penetration depth into the sample, a dual sided measurement is also possible in the case of paper samples [Lehtonen, 2005]. As well, online NIR measurements have been used to monitor thickness of printed layers [Mirschel *et al.,* 2012]. One advantage of NIR applications compared to mid-infrared radiation, for example, is that NIR can typically penetrate much farther into a sample, albeit limited, due to the lower selective absorbance and higher energy. In addition, NIR sensors are accurate, fast, non-destructive and this enables non-contact measurements, which offers great possibilities also in online measurements [Workman, 1999].

3 Objectives

A lot of research has been done to understand the role, control and optimization of liquid/moisture during paper processing, but this unstable and ever changing feature has set many challenges, not least its reliable real time determination.

The heatset offset printing method was chosen for the process analysis in this thesis, since the long run-lengths used, affecting both quality and runnability, emphasize the relevance of the findings established in this thesis. The focus of the thesis is on the evolution of the moisture content, with particular attention given to an on-line measurement procedure for total H_2O content, i.e. changes in moisture content in respect to wetting and liquid distribution during printing of coated paper. This has been carried out with a multipoint approach in order to understand and control the whole process in real-time on a printing press.

The factors underlying the problems arising in the printing process are specifically related to an uneven moisture profile of the paper web between printed and non-image areas, but the full understanding of the mechanisms underlying these problems is, however, still lacking. This thesis sets out to develop further insight into these mechanisms, and, ultimately, through monitoring them on-line, to provide the opportunity to establish solutions to commonly observed problems. The hypotheses set for the study, therefore, relate to the liquid transport behaviour, the liquid transport profile, and the mechanisms of liquid uptake as a function of liquid volume in relation to the substrate surface and bulk, namely:

- *Hypothesis I* – surface roughness determines the amount of transferred fountain solution depending on the relationship between volume of liquid in the printing nip and the surface void volume.
- *Hypothesis II*– the permeability of paper coating controls the liquid transport under pressure at surface liquid saturation.
- *Hypothesis III* – it is possible to consider spectroscopic methods based on near-infrared (NIR) to determine the amount of applied water in respect to moisture increase in paper as a function of the number of wetting events.
- *Hypothesis IV* – the unevenness of moisture distribution between image and non-image areas can be monitored and related to the waving/fluting tendency of paper.

4 Theoretical section

4.1 Surface wetting – spreading on rough surfaces

The investigation of liquid spreading on solid surfaces is usually restricted to nearly ideal, smooth surfaces. Due to their complexity, less attention has been directed towards rough, porous and chemically heterogeneous surfaces. However, many surfaces are rough to some degree. A surface may involve highly ordered roughness with defined structure, or a surface may be disordered, each including a nano-, micro- and macro-rough structure [Beland and Mangin, 1995]. Paper belongs to this category. An important requirement for paper to achieve proper wetting, is a uniform distribution of the imbibition and penetration controlling parameters over the surface and in the bulk. As mentioned previously, one of the most important phenomena related to wetting interactions between paper fibres and water is swelling of the fibre matrix. When swelling occurs, intermolecular bonds within fibres are broken by internal stress. This reduces the degree of order within the fibres and their surface area is increased. It is this swelling of paper which causes dimensional changes and these instabilities are linked to many end-use problems including the characteristic increase in roughness.

The surface roughness of coated paper affects the extension of liquid wetting and spreading. Roughness enhances wetting and broadens the three-phase-contact line [Wenzel, 1936]. In most cases, for wetting purposes, it is not sufficient to define the surface structure with one parameter alone. In order to model the surface on a molecular level, it is necessary to characterize the nature of the surface sites by using, for example, height asymmetry, surface porosity and the number, size and form of local minima and maxima, as well as roughness related to depth of pores and curvature of surface pores [Yan and Aspler, 2003]. Thus, the understanding of the role of surface properties on surface wetting can be considerably enhanced. Peltonen *et al*. [2004] have published a set of parameters which are needed to relate the wetting behaviour to the structural nature of a surface and these regimes can then be related to the observed contact angle representing the affinity of the liquid for the solid surface.

4.2 Wetting and contact angles

To initiate wetting, a liquid is brought into contact with a solid surface, i.e. two molecular species are brought together by intermolecular interactions. The wetting and substrate wettability is usually illustrated with a small liquid droplet resting on a flat horizontal solid surface, from

which the angle at the three phases (solid-liquid-air) in contact can be determined (Figure 4). The shape of the droplet is determined by the Young's relation (Eq. 4.1), which is satisfied at equilibrium,

$$\cos\Theta = \frac{\gamma_{SV} - \gamma_{SL}}{\gamma_{LV}}, \qquad (4.1)$$

where the subscripts relate to : sv = solid-vapour, lv = liquid-vapour, sl = solid-liquid.

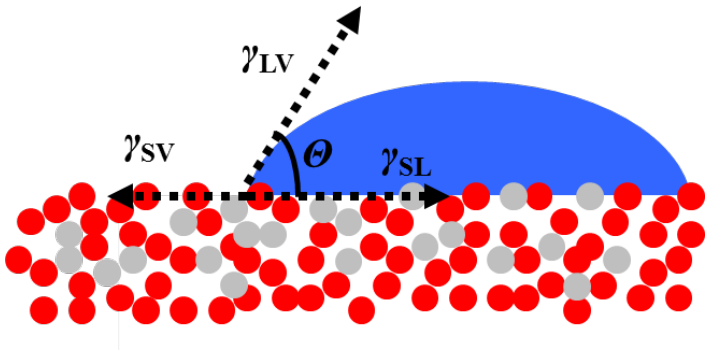

Figure 4. Contact angle and the three-phase-contact line.

The initial wetting as the droplet falls to the surface takes place in a non-diffusive regime, controlled by inertia, gravity and capillarity. The wetting on longer timescales is controlled by the diffusion of additive molecules to the liquid-vapour and solid-liquid interfaces. Adhesion forces between a liquid and a solid causes spreading across the surface and further inside the porous structure. Cohesive forces within the liquid cause an opposing retraction.

The mechanism of wetting is described for the droplet case in terms of the liquid droplet spreading (I) proceeding by a liquid precursor film (II) and vapour molecules (III) [Bascom *et al.,* 1964; de Gennes, 1985; Ausserré *et al.,* 1986]. The contribution of the adsorbed vapour layer to the solid surface is considerable. This precursor film formed from the condensed vapour, having a thickness of less than a micrometre, advances ahead of the motion of the droplet [Rosenholm, 2007]. This is illustrated in Figure 5. The contact area between the drop and the surface is in the mm^2 range, of course depending on the droplet volume and size applied, the condensing liquid being controlled by hydrodynamic forces once connecting to the wetting line

is in the nm-µm range, while the gaseous mobile molecular layer is in the sub-nanometre size range.

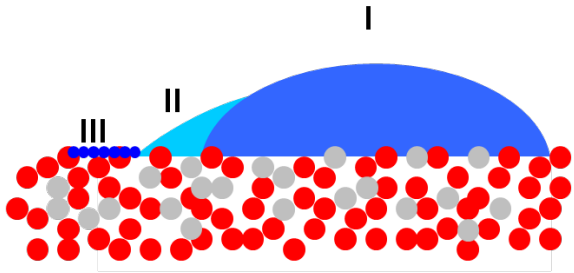

Figure 5. Liquid droplet wetting a chemically and structurally heterogeneous surface. This figure represent wetting on a nano-second timescale.

Since porous coated paper surfaces are both chemically and physically heterogeneous, this must be considered and corrected for when evaluating the wetting of such a substrate by liquids [Oliver and Mason, 1976]. The influence of surface roughness and texture on the wetting behaviour has been reported in several publications [Wenzel 1936; Shibuichi *et al.,* 1996; Bico *et al.,* 1999; Taniguchi *et al.,* 2002].

Related to the root mean square (RMS) roughness description of a typical surface, the most frequently used correction procedure was developed by Wenzel, who reported the interdependence of wettability and surface roughness for polar surfaces [Wenzel, 1936]. The Wenzel model (Eq. 4.2) for non-porous rough materials, on which the surface micro-roughness is filled by the wetting liquid, is defined by the following equation for the dependence of the apparent contact angle

$$\cos\Theta^{*} = r\cos\Theta\,. \qquad (4.2)$$

The roughness factor, r, is defined as the ratio between the actual surface and the geometric surface. The equation describes how surface roughness affects an otherwise chemically homogeneous surface. Θ is the Young contact angle as defined for an ideal, flat surface. The liquid spreads spontaneously also over a rough surface, while r is always greater than one, the apparent contact angle Θ^{*} is always smaller than the idealised Young contact angle for wetting surfaces.

If we consider the pore structures exemplified in this thesis, and the liquid volumes applied, the scales of pore size and droplet volume are very different. Furthermore, Wenzel refers only to a surface roughness, and not a progressively filling underlying network structure, which can direct liquid via that network ahead of the external wetting front, thus reducing the apparent contact angle as liquid contacts liquid rather than material surface. Such a reduction in contact angle is counter-intuitive to the Wenzel model which caters for roughness only. However, the comparison can be made with the volume ratio of < 0.1 μm pores – the size limit of the fastest acting imbibing pores upon contact according to the Bosanquet analysis of Gane e*t al*. [2000] and Schoelkopf e*t al.* [2000], - compared to the actual wetting line, namely the contact angle in the three-phase-contact point. Thus, the contact angles discussed in this thesis are defined as apparent contact angles. The contact angles can be used to study liquids on surfaces, their wetting evolution, their relative differences and how they behave in relation to liquid or solid surface/bulk properties. The wetting can be discussed in terms of a liquid behaviour on a substrate, and inside a porous structure, but there is always the evaporation factor (background evaporation), especially in the case of water-based liquids, which also needs to be included.

In printing, the liquid application is via a pressure pulse and film split as the printing blanket contacts the coated paper surface. This is a very rapid process and is critical for offset printing process conditions. Although it differs greatly from the idealised droplet, it still contains the essential elements of being approximately non-diffusive in the printing nip, exhibits inertia as mass transport occurs under the nip flow and film splitting with surface energy playing its role in peripheral wetting, though the thinness of the film precludes gravity. Capillarity acts instantaneously, involving also inertial wetting, together with the action of the pressure pulse in respect to initiating permeation through the outermost permeable coating structure. The important observation is that the apparent contact angle is not a direct measure of surface energy, but a convolution of surface energy and the lateral sub-surface pore capillarity in combination with the discontinuity of surface posed by the pores present. In reality, the liquid behaviour/wetting is influenced by surface chemistry, surface chemical evenness and surface roughness as an average property but also influenced locally by single roughness features such as craters or holes. The possible dissolution of chemical species, surface contamination, liquid adsorption and particle orientation play also crucial roles.

4.3 Liquid imbibition

The approach in many previous studies investigating liquid bulk wetting has been the porosity and pore size distribution determined by using mercury intrusion porosimetry [Larrondo *et al.,* 1995; Abrams *et al.,* 1996]. The method is reliant on the use of a non-wetting liquid, namely, mercury, which requires the application of an external pressure to force the liquid to intrude into the pores.

The use of mercury intrusion porosimetry requires very high pressures to sample the finest pores, and this expresses the physical compressibility of the skeletal structure of the porous medium. To obtain reliable data for the finest pores, therefore, this predominantly elastic compression effect has to be compensated for, as well as the thermal expansion of mercury and the penetrometer vessel under pressure and temperature [Gane *et al.,* 1996]. Schoelkopf *et al*., [2000] have demonstrated a 3D pore network model consisting of cubic pores and cylindrical connecting throats (PoreCor) derived from a fit to the compression-corrected cumulative mercury intrusion data (PoreCor is a software package of the Environmental and Fluid Modelling Group, University of Plymouth, UK.). The advantage of resorting to a 3D network model is that the pore shielding effect can be explicitly introduced into the structure. It has to be stressed, therefore, that the porosity itself does not give the required information about liquid imbibition behaviour, but rather the surface energy and the adhesion of the liquid to the porous substrate at static equilibrium only. The influence of pore volume as well as surface chemistry on liquid sorption has been reported by Rennes and Eklund [1989] and modelled by Bousfield [2000].

The liquid penetration into the coating structure under the printing nip depends on the surface void volume, which is a dimensionless parameter equivalent to the surface porosity, in relation to the volume of the liquid film. The subsequent liquid imbibition is traditionally explained in terms of capillarity describing the ability of a liquid to be drawn into a porous material due to inter-molecular interactions between the liquid and the surrounding pore structure. The Lucas-Washburn equation (4.3) is derived by considering fully developed laminar flow in a cylindrical pore under capillary pressure giving the rate of penetration [Washburn, 1921],

$$\frac{\mathrm{d}x}{\mathrm{d}t} = \frac{R_{pore}\gamma\cos\Theta}{4\eta x}, \qquad (4.3)$$

where x is the penetration depth, t is time, R_{pore} is the equivalent cylindrical capillary pore radius, γ is the liquid surface tension, Θ is the contact angle, η is the fluid viscosity. Some authors have claimed an interpretation of the amount of fluid entering a porous substrate by using the Lucas-Washburn equation [Aspler *et al.,* 1997; Desjumaux *et al.,* 1998], but, due to the false assumption that equilibrium laminar flow is dominating, these are likely to be deviating from reality, as was shown by Schoelkopf *et al*. [2002]. The equation is derived in the absence of a gravitational field, though in the case of the small volumes of liquid and the many orientations of the substrate this is not an issue in printing.

External pressure increases the rate of liquid penetration and increases the relative influence of the coating structure permeability compared to coating surface chemistry. Sandås and Salminen [1987] have shown that in a pressurized system, the penetration in coatings is dependent on the pore size, and in particular the permeability of the structure defined by pore size and connectivity and thus reducing the role of surface chemistry on wetting.

The Washburn equation can, therefore, not be used alone to explain the mechanism of liquid penetration due to the factors surrounding non-equilibrium laminar flow, which is manifest in the penetration differentiation between small and big pores for applied thin liquid films, and the presence of an external pressure pulse. The pore differentiating mechanism is taken into account, e.g. by including inertial wetting terms, provided by the Bosanquet equation [Bosanquet, 1923], or by considering pore entry energy loss [Szekely *et al.,* 1971] or by direct calculation from Gibbs surface free energy gradient [Ma *et al.,* 2007]. Without direct knowledge of the pore entry geometry or the surface area characteristics and formulation content of the coating, the Bosanquet analysis based on inertia provides the most convenient analytical method for determining the liquid front position, x, in a pore network structure [Ridgway *et al.,* 2002].

The Bosanquet equation (Eq. 4.4) (not to be confused with the Bosanquet diffusion formula) concludes that there exists an optimum for flow in a single capillary as a function of time coupled with the capillary radius [Schoelkopf *et al.,* 2000]. The Bosanquet equation is applicable in both capillaries and complex void structures. Bosanquet considered the inertial and viscous forces which act as the liquid enters the capillary tube from an infinite reservoir, providing a short timescale solution for liquid travel proportional to linear time, t, before relaxing to the Lucas-Washburn condition proportional to $\sqrt{t}$ for longer time capillarity under Poiseuille flow including external pressure-driven flow, if present [Schoelkopf *et al.,* 2000],

$$\frac{\mathrm{d}}{\mathrm{d}t}\left(\pi {r_{cap}}^2 \rho x \frac{\mathrm{d}x}{\mathrm{d}t}\right) + 8\pi\eta x \frac{\mathrm{d}x}{\mathrm{d}t} = P_\mathrm{e}\pi {r_{cap}}^2 + 2\pi r_{cap}\gamma_{\mathrm{SL}}\cos\Theta \qquad (4.4)$$

where r_{cap} represents the local capillary radius, ρ the liquid density contributing to inertia (the first term in the equation, acting over the shortest timescales in a given network feature), η the liquid viscosity (in the Poiseuille second term in the equation, acting over longer timescales after laminar flow is established in the averaged single hydraulic pore-equivalent structure), these both being balanced by the terms on the right hand side forming the driving forces, P_e the external nip pressure, and the wetting force via γ_{SL}, the solid-liquid interfacial tension, and Θ, the liquid-solid contact angle.

Inertial forces are relevant whenever the liquid is undergoing a rapid change in acceleration, i.e. at the initial imbibition phase or within the structure as the liquid front reaches points of rapidly changing geometry, such as the junction of a large pore with a fine pore [Schoelkopf *et al.,* 2000]. Small pores lead to faster liquid penetration in this very short timescale over which the momentum change is occurring. The retardation experience by the mass transfer into large pores, and the plug flow viscosity-independent imbibition into the nano-pores results in a preferential pathway throughout the structure.

Darcy's Law (Eq. 4.5) is a phenomenologically derived constitutive equation that describes the flow of a fluid under pressure through a porous medium [Darcy, 1856]. Darcy flow assumes laminar pipe flow in each stage, resulting in a volume flow rate, Q (= dV/dt) of a liquid of viscosity, η, across cross-sectional area, A_{cross}, of a saturated sample of length, L, under a negative pressure difference $-(P_\mathrm{b} - P_\mathrm{a})$.

$$Q = \frac{-kA_{cross}}{\eta}\frac{P_\mathrm{b} - P_\mathrm{a}}{L} \qquad (4.5)$$

The Darcy permeability coefficient, k, will give the relation of flow volume rate to external pressure at a given viscosity and equivalent path length through the structure.

The equivalent capillary imbibition distance of a porous material can be described approximately by the Darcy length, which is the distance of travel of the wetting front assuming all the available porosity is filled with the known absorbed volume of liquid. It is defined at a given time as the volume absorbed divided by the porosity. It is, however, a false representation in our porous media, while the whole porosity is not filled due to pore size and connectivity

differentiation mechanisms, as mentioned above in respect to the inertial mechanism of pore size differentiation. The liquid penetration under vanishingly small timescale within the space of the geometrical changes in the structure is via plug flow into the finest pores prior to the establishment of viscous drag. The model thus defines the preferential imbibition on a nano-scale into the smallest pores before saturation of the larger voids is reached. In support of this mechanism, it has been shown that imbibition of liquids initially occurs with an uneven wetting front, leaving some pores unsaturated [Dubé *et al.,* 2005]. Dubé *et al.* [2005] developed a numerical model for liquid flow through paper and demonstrated that the interface is fractal, with a well-defined roughness exponent. They examined the interface of penetration, which is rougher for spontaneous imbibition, and smoother for permeation under pressure. At longer wetting times, the wetting front becomes more evenly distributed due to saturation, and at this point, the Darcy permeability controls the resistive factor acting against the pore wall wetting forces, i.e. the point at which the square root of time relationship becomes established.

4.4 Optical characteristics of paper

Physically, light can be described as small energetic massless particles, photons, or as electromagnetic waves. The speed of light, c (=299 792 458 ms^{-1}) describes the maximum speed of massless particles in a universal free space frame of reference. The rate at which the waves oscillate per second is termed the frequency, f, and the wavelength, λ, is the length of one wave, high frequency radiation having shorter wavelengths and vice versa, where $c = f\lambda$ in vacuum. The wavelengths discussed in this thesis are within the near-infrared and presented in nanometres (nm). It should also be highlighted that the term absorption, in the contest of this thesis work, is only used for light absorption.

The speed of light changes as it enters a material. The ratio between the speed inside the material and in vacuum is called refractive index. In optics, the refractive index, n, of a substance is a number that describes how light, or any other electromagnetic radiation, propagates through that medium.

Snell's law (Eq. 4.6) describes the relationship between the angles of incidence and refraction, when referring to light passing through a boundary between two different isotropic media (Figure 6). Snell's law states that the ratio of the sines of the angles of incidence and refraction is equivalent to the ratio of phase velocities in the two media, or inversely equivalent to the ratio of the indices of refraction:

$$\frac{\sin\theta_1}{\sin\theta_2} = \frac{\upsilon_1}{\upsilon_2} = \frac{n_2}{n_1} \tag{4.6}$$

with each θ as the angle measured from the normal, υ as the velocity of light in the respective medium (SI units are metres per second, ms^{-1}) and n once again as the refractive index (dimensionless) of the respective medium. θ_1 and θ_2 are the angles of incidence and refraction, respectively, of a ray crossing the interface between two media with refractive indices n_1 and n_2.

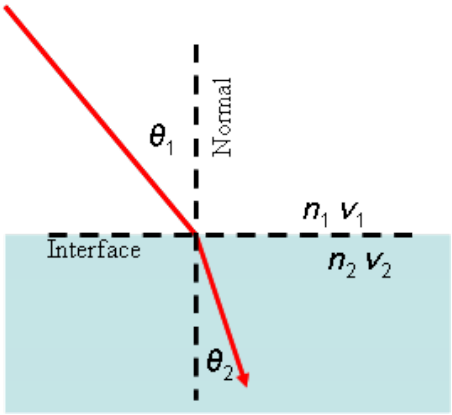

Figure 6. Light refraction at the interface between two media.

It is the change in speed that leads to a change in the direction of light as seen in Figure 6. The refractive index also determines how much of the illuminated light will be reflected. Typical values of the refractive index are: 1 for air (T=0 °C, p=1 atm, λ=589 nm), 1.33 for water (T=20 °C, λ=589 nm), 1.46 for mineral oil, 1.5 for calcite (which acts birefringently), 1.55 for cellulose and 1.66 for latex [Elton and Preston, 2006].

During wetting, the internal porosity characteristic of the paper, i.e. the void volume, is replaced by the liquid whose refractive index is higher than that of air. The refractive indices for process inks used in the heatset offset printing process have been determined by Granberg [2002] and Niskanen e*t al*. [2007]. The refractive index for inks is wavelength dependent, each having dominating wavelengths, and the estimates presented in the literature have been measured in the visible wavelength range. As well, the refractive index increases during ink setting because of the increase in its density [Preston *et al.,* 2003; Niskanen *et al.,* 2007]. In this respect, optical measurements on paper are not only dependent on roughness but also the refractive index

differential between different layers [Gate and Leaity, 1991; Elton, 2009]. The isolation of the wavelength contributions to gloss has been reported by Gane *et al.,* [2012] taking into account both roughness and the geometry of incidence.

In a paper substrate, light scattering occurs due to its heterogeneous inter-surface structure (Figure 7). The two components of surface reflection distribution are the specular reflection (θ_i=θ_r) and diffuse scattering, respectively. In the case of a porous material, like coated paper, some proportion of light is also transmitted or forward-scattered into/through (depending on thickness) the substrate. Otherwise the light becomes absorbed or backscattered at only a short distance into the sample. The mechanisms of diffuse reflection include surface scattering from roughness and sub-surface scattering from internal interfaces and optical contrast irregularities.

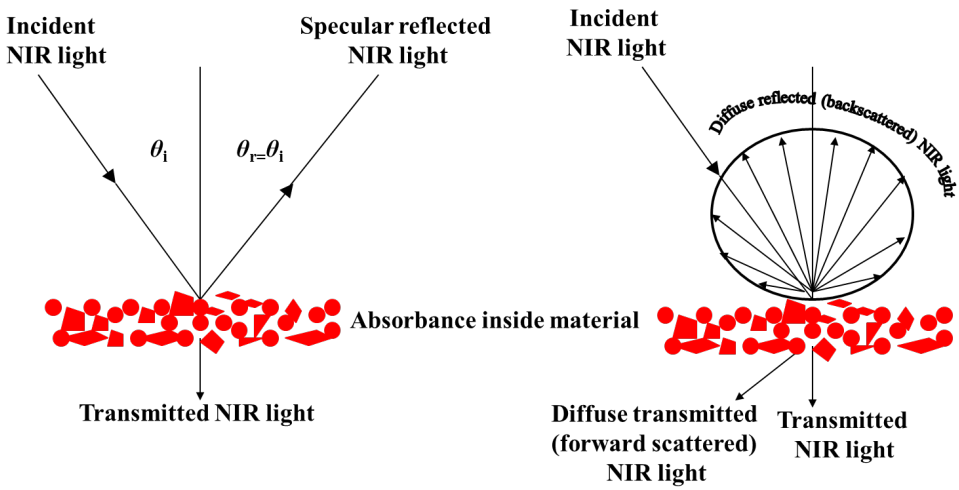

Figure 7. Surface reflection distributions. θ_i stands for incident and θ_r for reflected, respectively.

The penetration depth depends on the wavelength of light, the incident angle, the refractive index of the medium and the light absorption coefficient of the medium. The refractive index of the medium behind the interface also has an influence on the absorption depth, as a higher refractive index increases the evanescent wave (internal boundary reflected) absorption depth. In optics, the Lambert–Beer law (Eq. 4.7) relates the absorption of light to the properties of the material through which the light is travelling and is the basis for quantitative analysis of

absorption spectrometry. The law basically states that the intensities of absorption bands are linearly proportional to the concentration of each component in the equivalent homogeneous mixture. The law states that there is a logarithmic dependence between the transmission, T, of light through a substance and the product of the absorption coefficient of the substance, α, and the distance the light travels through the material (i.e. the path length), ℓ.

$$T = \frac{I}{I_0} = \exp(-\alpha\ell) \tag{4.7}$$

where I_0 and I are the intensity (or power) of the incident light and the transmitted light, respectively.

The light absorbance, A, is expressed in terms of the logarithm of the inverse of transmission, which, for liquids, is defined conveniently as (Eq. 4.8),

$$A = -\log_{10}\left(\frac{I}{I_0}\right) = \log_{10}\left(\frac{I_0}{I}\right) \tag{4.8}$$

The absorbance (A) is thus the logarithm to the base 10 of the ratio of radiant power incident (I_0) to the power transmitted (I).

5 Experimental section

5.1 Materials and methods

The experimental section gives a comparison of substrates and characterization methods used in the study. Since a more detailed description of the substrates is presented in the specific publications, the details of those will not be reviewed here. Additionally, many of the analysis methods are well described in the literature and in the publications building up this thesis, and thus only the key methodology information is presented.

The studied papers have thoroughly been characterized with a broad range of highly sensitive techniques. The characterization has focused on both the surface and the bulk of the substrates analysing both structural features and chemical properties. Moreover, the distribution of chemical species, i.e. tracer ions in the context of the work considered here, have been detected.

As previously mentioned, offset paper is both structurally and chemically heterogeneous. There are numerous techniques nowadays to study different structural and chemical paper characteristics [Wygant *et al.,* 1995; Vyörykkä *et al.,* 2006]. The different characterization methods are today very accurate. The main challenge is, however, to define the right measurement area of interest, the geometry and the amount of repetitive measurements. Important is to compare different length scales and several measurement spots along the paper sheet/web in order to be able to get the right interpretation of the results.

5.2 Substrates

The well-defined porous coatings, with selective particle size distributions containing calcium carbonate pigments, were prepared from a dispersed pigment slurry. Tablets were formed by dewatering the slurry mix in a cylindrical steel die, following the method of Ridgway *et al*. [2004]. After forming, the tablets were oven dried overnight. Any other components, such as thickening agents, were excluded in order to avoid unnecessary liquid-induced and dispersion component interactions.

Some of the paper substrates used in the study was manufactured by coating at a pilot coater (the erstwhile Forest Pilot Center Oy, Raisio, Finland). These trial points, containing coatings of calcium carbonate having different particle size distributions, were kept uncalendered in order to

achieve as porous a structure as possible, with the highest achievable permeability for each pigment packing characteristic. In one of the published papers, the uncalendered paper surface, calendered to different levels, functioned for monitoring better the transition from surface void filling to pressure-driven permeation in the heatset offset printing process [Paper III]. Styrene acrylic latex binders were preferred because of their known minimal interaction with ink and water components [Rousu *et al.,* 2005]. In addition, mill papers were used in the trials as references.

5.2.1 Inks

The Premoking series of inks used in the printing trials were supplied by Flint Group. The inks comply with ISO 2846-1 colour standard for four colour printing.

5.2.2 Fountain solutions

Model, laboratory-made and commercial fountain solutions have been used throughout the study. The model fountain solutions were primarily formulated for comparison by varying the main components, i.e. IPA and surfactant. Fountain solutions with a series of IPA concentrations and surfactant concentrations were studied by investigating the influence of the individual components and their concentration on wetting. For some of the pilot scale test printings, tailor-made fountain solutions were prepared in the laboratory.

5.3 Analytical instruments

5.3.1 Atomic force microscopy (AFM)

Atomic force microscopy belongs to the scanning probe microscopy family, i.e. the measurement scans the surface of a sample with a probe at scales down to nano-size features [Howland and Benatar, 2005]. The measurement principle defines a sharp tip scanning over the sample with piezoelectric scanners. As the tip comes into close contact with the surface, interaction forces cause a bending and torque of the cantilever [Niemi *et al.,* 2002]. The position of the scanning tip is determined with a segmented photodiode. The AFM measurements used in this study were carried out with a Nanoscope IIIa microscope (Veeco Instruments Inc., Santa Barbara, USA). All images were measured in the tapping mode in ambient air using standard Si_3N_4 cantilevers. Due to the surface rough nature of paper, AFM might restrict the desired scan area [Di Risio and Yan, 2006]. Nonetheless, topographical images of different areal portions of the sample were captured, and the number of repetitive measurements was defined at 10 to

generate statistical relevance. The raw data were analysed using the Scanning Probe Image Processor (SPIP, Image Metrology, Denmark) software.

5.3.2 Time of Flight Secondary Ion Mass Spectroscopy (ToF-SIMS)

Mapping of elemental and molecular species present on the surface and in the bulk was studied with the ToF-SIMS technique. The ToF-SIMS instrument used was a PHI Trift II spectrometer. The samples were coated with platinum before imaging. The homogeneity and the distribution of Li^+ ions were acquired from a 100 × 100 μm^2 area. The samples were scanned from five spots. The distribution and amount of the Li^+ ions were then traced from the surface and the cross-sections prepared. It should be highlighted that the instrument is not able to differentiate the state of the Li^+ ion, i.e. both the free Li^+ cations and the salt bound ions are detected the same way. The distribution of lithium was followed with imaging using its isotope at 7 u (isotopic mass). Note that the ToF-SIMS technique is highly surface sensitive with an analysis depth of less than 2 nm. The detection limit is in the ppm - ppb range. The lateral resolution is 1 μm.

5.3.3 Mercury intrusion porosimetry

The mercury intrusion porosimetry measurements were performed on a Micromeritics Autopore IV (Norcross, GA, USA) porosimeter using the technique described by Ridgway and Gane [Ridgway and Gane, 2003]. In the data analysis, the obtained intrusion values were corrected using a spreadsheet-based program Pore-Comp (Environmental and Fluid Modelling Group, University of Plymouth, UK) to correct for mercury compressibility and penetrometer expansion effects [Gane *et al.,* 1996].

5.3.4 Contact angle measurements

The contact angle measurements, defining the three phase contact between solid, liquid and vapour at the lateral wetting front of a sessile droplet, were performed with a high-speed camera (KSV Instruments Ltd., Helsinki, Finland). In the measurements, a droplet is put on the substrate sample surface and the spreading takes place without any external pressure. A saturation of the surface pores in the coating layer obviously takes place with such a liquid droplet volume. This saturated condition strongly affects the relation between spreading on the surface, pore filling and, thus, the contact angle, since, the spreading of the liquid happens partly on the liquid itself, having reached via sample internal network capillarity to beyond the surface wetting front. Thus, the apparent contact angle evolution as a function of time was monitored in the knowledge of the

limitations arising from the reality of these practical conditions. The apparent contact angle data derived are used to describe the behaviour of the specific liquids on the studied substrates.

5.3.5 Liquid permeability measurements

A stack of paper samples was prepared in a resin surrounded tablet form. The open area of the porous sample, i.e. that free from resin, is evaluated so that the permeable planar cross-sectional area can be established. Permeability is measured by pre-saturating the compacted paper layered sample and applying an external pressure to a liquid head, measuring the resultant flow rate through the sample. To avoid liquid-solid interactions which would lead to changes in the structure (e.g. swelling or diffusive interpolymer absorption), or chemistry of the substrate, and to minimise evaporation, the liquid chosen was a non-polar alkane, hexadecane. More details of the measurement setup can be found in Ridgway *et al*. [Ridgway *et al.,* 2003].

5.3.6 Prüfbau laboratory printing trials

The Prüfbau (Prüfbau Dr.-Ing. H. Dürner GmbH, Dr.-Herbert-Dürner-Platz, Peissenberg, Germany) printability tester is used to simulate commercial offset printing. The Prüfbau printer was used in this study to transfer fountain solution and ink in different layer combinations (e.g. fountain solution + ink and ink + fountain solution) to the studied paper substrate. An exact dosage (50 µl) of fountain solution was placed into a sealed, water vapour tight application box. The fountain solution was distributed on the application rollers having defined surface areas, and therefore defined water carriage capacity. The liquid film was applied with one revolution of the applicator roller on the paper over a 20 mm wide strip via a rubber blanket. After each measurement, the application box was opened to allow any residual liquid to evaporate in order not to influence the following measurement.

5.3.7 ViWa – Visual Waviness (ViWa)

The Visual Waviness measurement device was used in one study to interpret the waving tendency of printed papers. A laser scanning method was used to create a three dimensional surface topographic image of the printed sheet [Gerstner, *et al.,* 2010]. A laser scanned the paper samples by moving along in the machine direction (MD) and transferred the data to an acquisition system. The measurement is done on a 10 cm × 10 cm green printed area (C100, Y100) in the printed layout. From the topography data, the amplitude in the 0–15 mm and 15–30 mm wavelength interval was used to characterize waving. The camera records the surface height deviations with an in-plane resolution of ca. 100 μm^{-1} and an out of plane resolution of 50 μm^{-1}.

5.3.8 Moisture determination with near-infrared (NIR) spectroscopy

In the conducted NIR measurements, the sample was illuminated with light in the near-infrared wavelength region. At a specific wavelength the illuminated light is absorbed, e.g. by water, and the reflected response is measured. In this case, the more water the sample contains, the more NIR energy is absorbed (less is reflected), i.e. the amount of reflected light is inversely proportional to the moisture content.

The multipoint NIR instrument utilized in this work was designed to perform diffuse reflectance measurements over the full NIR wavelength range simultaneously at multiple locations (Figure 8). It consists of a halogen lamp as light source and an NIR spectral camera (SWIR (short wave infrared) Spectral Camera, Specim Ltd., Oulu, Finland) as spectrometer. The light source contains a high power (~50 W) halogen lamp, from which the radiation is collected into multiple illumination output fibres. The measurement probes include mirror-optics which project the illuminating light from the source fibre onto the sample and, conversely, collect the back-scattered light into the detection fibre. Both the incident and the reflected angle were 15.5 ° from the normal of the paper surface and the collection angular width was 3.1 °. To permit a true non-contact measurement, the sample-to-probe distance was optimized to be 165 mm, although the variation of ± 5 mm was permitted which makes the instrument robust against the vibrations of the paper web in the *z*-direction in the current application. The illumination spot has an elliptical shape of the size 4 mm x 7 mm (minor and major axis) on the sample surface, and the elliptical detection spot of the size 1 mm x 3 mm resides within the larger illumination spot. Using a spectrograph, the polychromatic light from a single detection fibre is dispersed into a full spectrum in the wavelength range 1 000–2 500 nm onto a column of the 256 × 320-pixel MCT (Mercury Cadmium Telluride) detector matrix. Due to the low transmission of the utilized quartz optical fibres at long wavelengths, the effective wavelength range was limited to 1 000–2 100 nm.

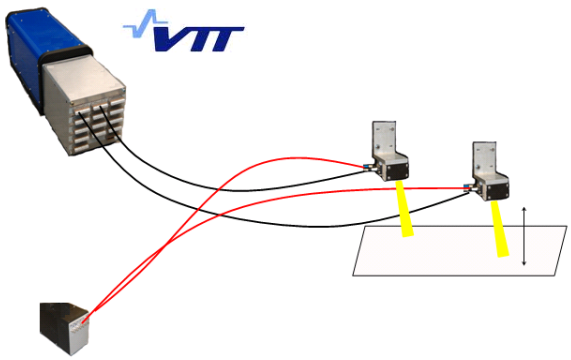

Figure 8. Near-infrared measurement device.

The experiments involved the collection of data at both static and dynamic printing process conditions. The single moisture levels of the static trial points were obtained by averaging all spectra of the corresponding measurement and subsequently calculating the moisture level with a constructed calibration model.

5.4 Spectral references and their analysis

Conventionally, the linearity of measured spectral data is enhanced by subjecting them to the log(1/*R*) transform, where the reflectance, *R*, at the wavelength λ is given by Eq. 5.1,

$$R(\lambda) = \frac{I(\lambda) - D(\lambda)}{W(\lambda) - D(\lambda)}, \qquad (5.1)$$

and this transform was utilized in this study, as well [Papers II, III and V]. The numerator in Eq. (5.1) consists of the raw signal $I(\lambda)$ corrected for the instrumental dark current $D(\lambda)$, whereas the denominator contains the instrumental response, i.e. the white reference $W(\lambda)$ after dark-correction. The white reference is usually measured with a non-absorbing material, such as optical Teflon (Spectralon, which is powdered Teflon® (DuPont) and has high reflectivity to IR light), which scatters light strongly and has no absorption bands in the NIR wavelengths. In this study, the instrumental response was measured using a white reflectance standard (1.5 mm thick optical diffuse material, Gigahertz-Optik, Germany). The integration time of the detector was set to 7 ms and the frame rate to 100 Hz. The amount of data was reduced and signal quality was improved by averaging 100 consecutive spectra to obtain one spectrum per second. It should be highlighted that the corrections made on each spectrum were only for physical factors and no

signal processing was used, e.g. baseline differences are inherent to log(1/*R*) spectra and they are often corrected, e.g. by averaging each spectrum and projection about a zero mean line. The baseline differences are caused by varying probe-sample distance, variations in illumination between probes and variations in the light scattering properties of the sample. In the online measurements, the variations between the measurement probe signals, caused by, manufacturing or differences in illumination and detection optical fibres were evaluated as well as the noise level of the running printing machine by running plain paper through the printing machine with all printing nips open. The probes were standardized by analysing the inter-probe differences by all probes measuring the same spot.

5.5 Calibration procedure for NIR application

NIR probes/sensors provide a secondary measurement, i.e. to obtain quantitative moisture profiles the measured NIR data should be related to absolute moisture values. This is accomplished with the use of a calibration model which requires that a calibration data set is measured offline in laboratory conditions. It is very important that the laboratory samples are representative of the sample measured by the NIR sensor, including measurement conditions and the samples covering the entire range of variation ever produced by the process, i.e. moisture level and paper quality range. Errors in the calibration procedure are the limiting factor for the measurement accuracy but taking all aspects into account, the best possible accuracy in an NIR application is gained. The calibration set consists of NIR spectra of wet paper samples as multivariate explanatory (dependent) variables and the corresponding moisture weight percentages of the samples as an explained (independent) variable. From these, estimates for the moisture content of paper using the NIR spectra measured inline during the printing process are obtained.

The calibration measurements were conducted using the commonly known loss-on-drying method [Papers II, III and V]. First, the NIR spectrum and weight of the sample were measured prior to wetting at room temperature. Second, the paper samples were held in a humid chamber for the duration of 30–40 min so that their moisture levels were raised up to 8–12 wt% before they were placed on the microbalance and the drying process was started. The paper samples were then freely dried in room temperature and 20 % RH, and their NIR spectra and weight were measured simultaneously 10–20 times until a stable condition with regard to the paper mass was achieved. Third, the paper sample was heated with a halogen lamp at 105 °C until its weight reached a minimum level. This value was interpreted as the dry weight of the paper. At all

different moisture levels, the average value of the two readings (microbalance and NIR response) was paired with the corresponding spectrum. To prevent evaporation, the sample was placed between two large borosilicate glass sheets during the NIR measurement. Representative measurements were obtained via spatial averaging: the sample was manually scanned below the illumination spot on a horizontal black non-reflecting surface during the collection of spectra and all spectra were subsequently averaged.

In the online measurements, to account for the different light scattering properties of non-image and printed paper surfaces, separate calibration sets were collected. Moreover, the same loss-on-drying measurement procedure was made for the so-called process samples with wet ink layers. For the wet ink film, the samples were taken from the printing machine during running before the heatset offset dryer and the loss-on-drying procedure was immediately started. The moisture percentages of the calibration samples were then calculated using the Equation 5.2,

$$Moisture(\%) = 100 \times \frac{m_{wet} - m_{dry}}{m_{wet}} \tag{5.2}$$

where m_{wet} is the weight of wet paper, at each stage of drying, and m_{dry} is its dry weight. To mitigate the effect of measurement error, the loss-on-drying measurement was repeated five times with different paper samples, each having a dry mass between 200–400 mg. The calibration procedure was performed by estimating the bias and slope coefficients, i.e. the coefficients $\boldsymbol{a}$ and b, in the linear Equation 5.3,

$$\boldsymbol{y} = \boldsymbol{a} + b\boldsymbol{a} + \boldsymbol{e} \tag{5.3}$$

using least-squares (LS) regression. Here, the elements of the vector $\boldsymbol{y}$ contain the moisture percentages of the calibration samples calculated using Eq. (5.2). The vector $\boldsymbol{a}$ contains the areas of the water absorption peak calculated for each spectrum as the area between the linear line and the NIR spectrum as illustrated in Figure 9. The linear line (left) is fitted between two points which are calculated as the average log (1/R) values in the wavelength ranges coloured in yellow. The vector $\boldsymbol{e}$ contains the model errors which are here minimized in least-square sense.

The calibration set is visualized in Figure 9 (right-hand image). The actual moisture percent values on the horizontal axis were calculated using Eq. (5.2), whereas the moisture values on the vertical axis were estimated for the same samples using the linear model of Eq. (5.3). Ideally, in the absence of noise and measurement errors, the dots should be located on the solid diagonal

line drawn in the figure. However, due to the random nature of the measurement, they exhibit variance around the diagonal. The height and area under the absorption peak, corresponding to presence of water, decrease with time (due to evaporation of moisture from the substrate).

As opposed to using multivariate calibration models with the whole effective range of 1 000–2 100 nm, the wavelength range of interest was reduced to cover the water peak area between 1 850–2 050 nm in the quantitative analysis of moisture content. The baseline correction was performed from both sides of the water band, namely between 1 840–1 890 nm and 2 010–2 050 nm, respectively. The straight line fitted between the two points eliminates the possible effect of baseline variation on the spectrum. The chosen calibration technique was robust against any changes in the offset and curvature of the spectral baseline and other interfering spectral features occurring outside the range of interest which might result from the drift of electronics, the vibration of the paper web and the use of several measurement probes.

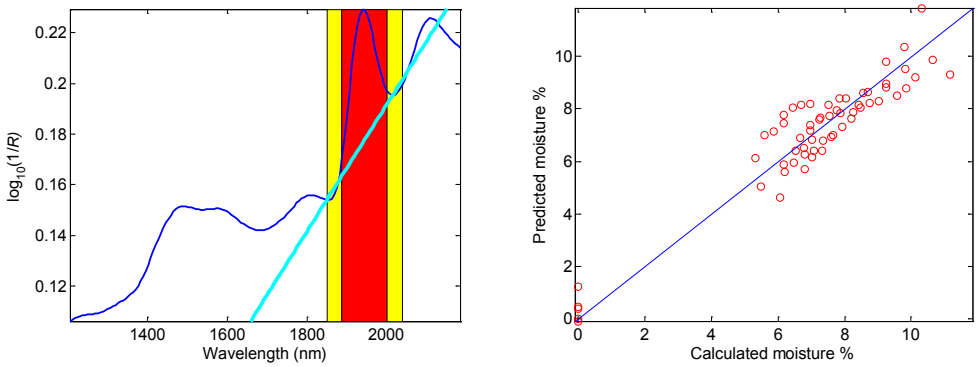

Figure 9. Visualization of the water peak area calculation (left); calculated and predicted moisture percentages of the calibration set (right). The water band area is marked with red (left) and the baseline correction bands with yellow, respectively.

5.6 Offline and online measurements

As previously mentioned, the NIR measurements were conducted both in offline and online environment. Laboratory conditions (T = 23 °C and 50% RH (relative humidity)) were used to compare different fountain solution compositions with their evaporative and permeative characteristics.

The measurement system was found to be suitable for online measurement of moisture in a heatset web offset environment. The printing trials were carried out at the (former) Forest Pilot Center Oy, Raisio, Finland on a Heidelberg Web-8 heatset web offset printing machine with five over five printing units, i.e. with application potential for 5 colours, as well as fountain solution, simultaneously applied to both sides of the paper. Kodak Gold (DITP Gold – positive plates) printing plates were used. The press room conditions were held constant, maintained at 50 % RH and temperature, T = 23 °C. The width of the paper web was 500 mm. Online measurements compared to offline measurements were easier to perform since the new measurement spots created due to the high speed of the machine excludes the possibility of the measurement spot heating up the sample. The mobile sensors were mounted into different positions along the printing line depending on the target of each sub-study (Figure 10).

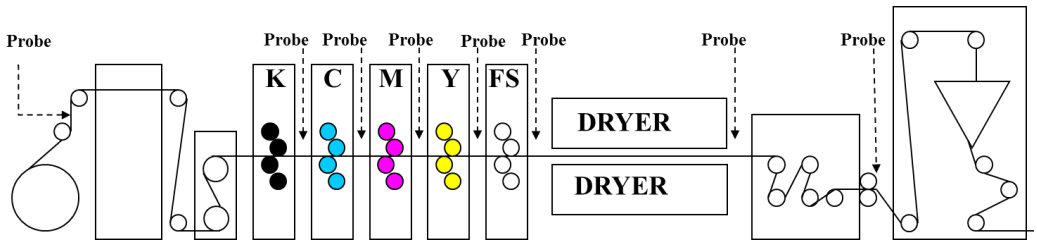

Figure 10. Measurement probes as mounted on the printing machine. Simplified schematic of the printing machine at FPC. The probes located (from left to right) at the unwinder, between the printing units, after drying and after silicone application depending on the trial topic.

6 Results

In this thesis, the presented experiments were performed to study liquid transportation and distribution in porous pigmented coated structures. Laboratory scale measurements were performed and were implemented also in a large scale pilot printing environment. The final stage was to direct the moisture related issues toward a real case of a heatset offset printing defect, and so to test the functionality of the hypotheses when drawn into practice.

6.1 Structure analysis

Both the surface and the bulk structure of the substrates were studied each depending on the research sub-topic.

Surface roughness was characterized by traditional parameters, the square root of height variance (squared deviations) from the mean plane and effective surface area with respect to the projected area as a percentage increment. The surface profile is compared to a Gaussian distribution and the deviations from it indicate, for example, whether the surface is more monotonal (narrow height distribution) than a broader Gaussian one. Figure 11 presents a cut-off portion of a paper surface showing its heterogeneous character [Paper IV].

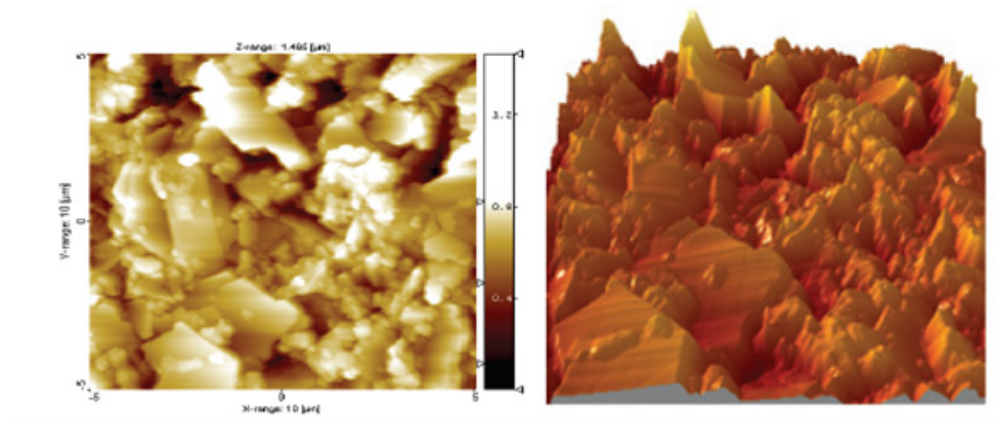

Figure 11. Height image (left) and 3D image (right) of a coated paper sample as measured by AFM. The image size is 10 μm × 10 μm.

Figure 12 represents mercury intrusion porosimetry data for a paper calendered to different levels [Paper III]. It is well known that different calendering conditions create different pore structure for papers. The peak to the right at larger pore diameters represents the

basepaper/coating interface and basepaper pore structure giving the paper its imbibition volume properties. These larger connected pores also control the permeability properties of the underlying basepaper. The smaller peaks to the left represent the coating pore structure and give the paper its surface imbibition rate properties. The reduction in specific pore volume signifies that the calendering strongly affects the basepaper peak. The structure becomes denser as a result of heavier calendering conditions. The basepaper peak reduces in both volume and pore diameter as the calendering pressure conditions are increased. The coating structure peak is also affected by the calendering conditions both in terms of total pore volume and pore diameter.

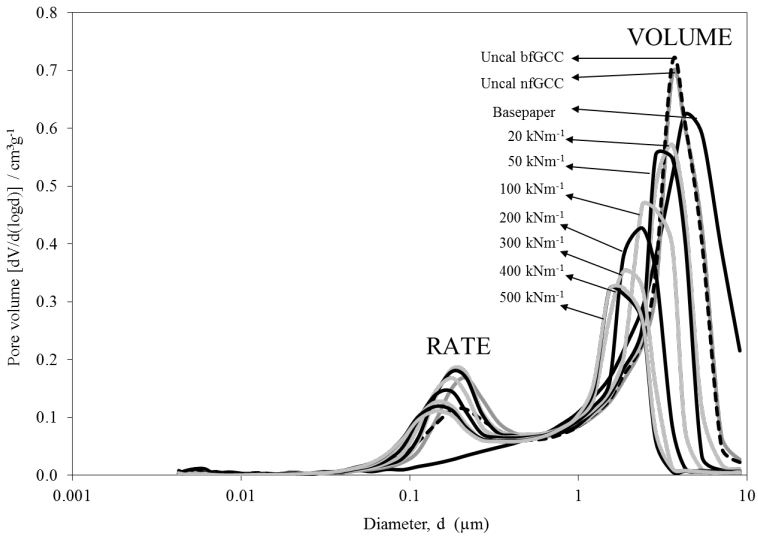

Figure 12. Pore size distribution of the paper samples showing both the coating (left) and the coating layer-basepaper (right) peaks. bfGCC stands for broad particle size distribution fine Ground Calcium Carbonate and nfGCC, narrow size distribution fine Ground Calcium Carbonate, respectively. The calendering series is for the nfGCC paper [Paper III].

Figure 13 illustrates liquid permeability results of calendered samples [Paper III]. The permeability is controlled by the larger connected pores in the structure. In the printing process, the permeability properties of the paper are important both in terms of liquid and vapour, in that the coating should not take up too much fountain solution by pressure penetration and long term capillarity, but should be permeable enough to allow rapid drying without disrupting the structure.

For flow in the *z*-direction, in this example, the basepaper displays the higher permeability in the layered structure in contrast to the coating. A bfGCC (broad particle size distribution fine Ground Calcium Carbonate) coating exhibits clearly lower permeability compared to the nfGCC (narrow size distribution fine Ground Calcium Carbonate). Regarding permeability, the coating cannot respond as rapidly to the increase in fountain solution volume, as the coating, with its lower permeability, will not let the pressure act to force the liquid in. The different calendering levels of the nfGCC coated paper present a decreasing permeability as a function of increasing linear load in the calendering nips. The larger peaks of the porosimetry differential curves presented in Figure 12 follow also this trend.

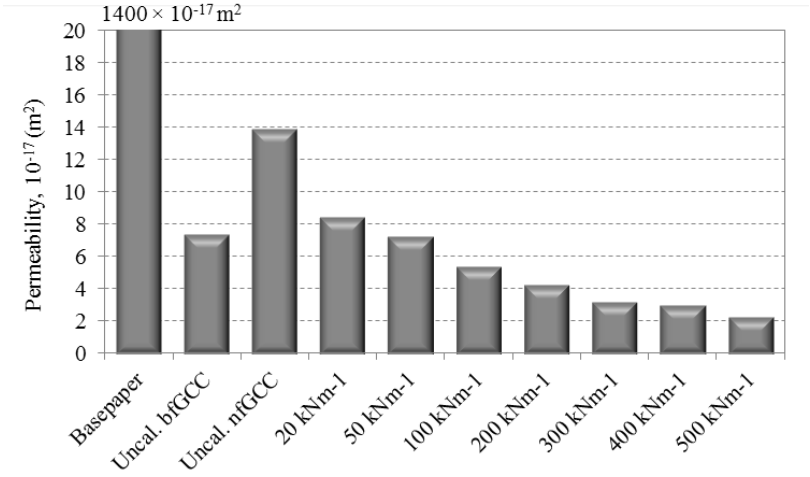

Figure 13. Liquid permeability results. The calendering series is for the nfGCC paper [Paper III].

6.2 Liquid transportation (droplet wetting) in porous media (laboratory scale studies)

First, the liquid behaviour on paper in the *xy*-plane (horizontal with the plane of the paper) was studied. In one of the sub-studies, the wetting evolution of IPA and surfactant solutions was compared [Paper IV]. The contact angle evolution for the IPA-surfactant-water mixtures is presented in Figure 14. It can clearly be seen that the amount of IPA in the solution greatly affects the contact angle on short timescales. Even a small amount of IPA (2.5 wt%) decreases the contact angle. This agrees with the results presented in previous studies [Gojo *et al.,* 1998]. All surfactant-IPA mixtures show a strong concentration-dependence, this being dependent also on the surfactant type [Paper IV]. The wetting evolution levels out after ~1 s when the surface

becomes saturated. The long timescale kinetics observed can be attributed to a more structure-dependent wetting.

Since the vapour pressure of IPA is higher than that of water, the wetting is enhanced. This is explained by Marangoni flow, where the droplet spreading is associated with the formation of a primary film of ~10 nm thickness [Bascom *et al.,* 1964], due to the vapour pressure and surface tension gradients. This film thickness is of the order of the finest pores in the paper surface [Gane *et al.,* 2000].

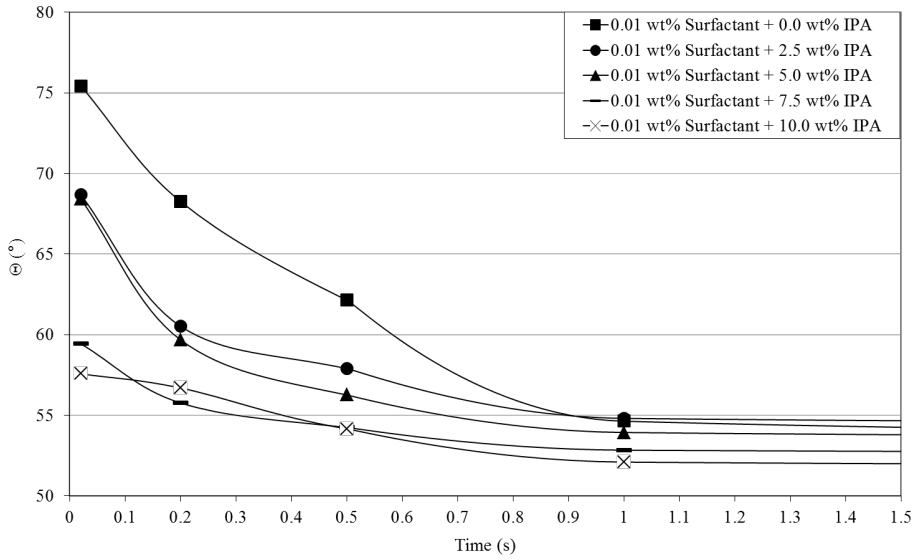

Figure 14. Wetting by solutions with 0.01 wt% non-ionic surfactant as a function of IPA concentration. The contact angles are corrected for the apparent effect of the surface roughness of the coated paper. Note that the lines do not represent any function but are guides to the eyes [Paper IV].

The liquid transportation within a porous matrix involves both penetration into the substrate and subsequent evaporation from the sample. In one of the publications, model water-based fountain solution mixtures based on IPA and surfactant, were compared [Paper I]. The liquids were applied as sessile droplets on a porous pigment tablet surface without any external pressure. The droplet was placed on the tablet surface and an immediate imbibition occurred (as characteristic for contact angle measurements).

In Figure 15, dynamic NIR diffuse reflectance spectra of a dry and wetted pigment tablet are presented. The spectra at different wetting times give an estimate of the relative moisture content in the pigment tablet. The relative differences of the curves reveal the rate of imbibition and evaporation. As the evaporation and imbibition of the liquid becomes slower, an apparent increase in reflectance (decrease in absorbance) is observed.

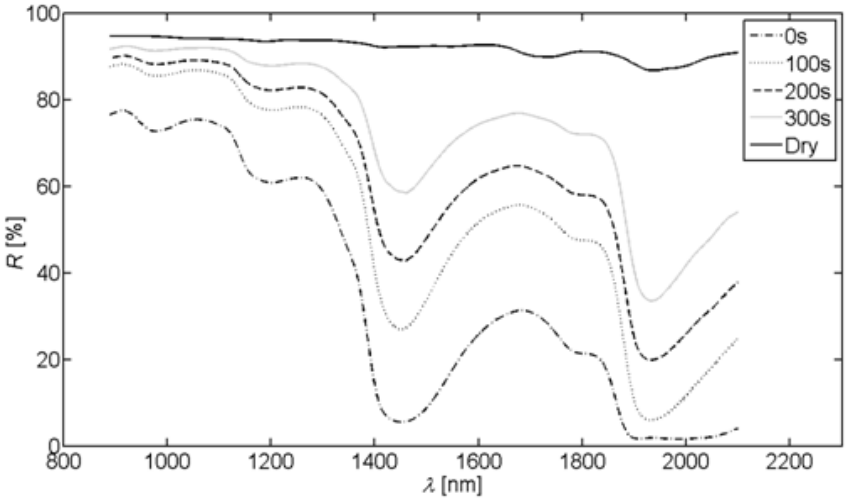

Figure 15. Dynamic NIR diffuse reflection spectra of an unwetted ("dry") and a wetted pigment tablet, as exemplified by a 1 wt% surfactant in water solution. The studied wavelength was 1 450 nm [Paper I].

In Figure 16, the imbibition and evaporation of liquids inside a pigment tablet (below and from the tablet-air interface surface) are presented [Paper I]. The point $t = 0$ represents the situation where the droplet is no longer existing on the surface but is imbibed within the structure and adsorbed on the uppermost surface layer. Initially there is an almost stable regime observed, which corresponds to the situation where further liquid transport has reached an equilibrium filling level of the surface pores and further transport is controlled by diffusion. At t = 200–300 s, depending on the liquid, the evaporation stage dominates as liquid near the surface can no longer be replenished. This phase includes both further liquid transport inside the tablet and evaporation from the inside of the tablet to the surface and then to the atmosphere. The point where the initial imbibition starts to level out corresponds to the maximum surface moisture content. It should be noted that the drop in absorbance is partly due to transport restriction further inside the tablet (deeper than NIR detection limit) and the evaporation from the tablet

surface. At t = ~500 s, depending on liquid, the levelling of the curve corresponds to the state where the liquid has imbibed deeper than the NIR detection limit and the moisture evaporation slows down.

The strongest change in intensity is observed for the 1 wt% surfactant in water solution and it is referred to droplet imbibition into the tablet. The surfactant acts to reduce the surface tension of water, so the vapour pressure differential across the liquid-vapour boundary is reduced. Compared to alcohol-based solutions, it is supposed that the surfactant does not evaporate from the tablet but adsorbs or is deposited onto the pigment surface [Tåg *et al.,* 2009].

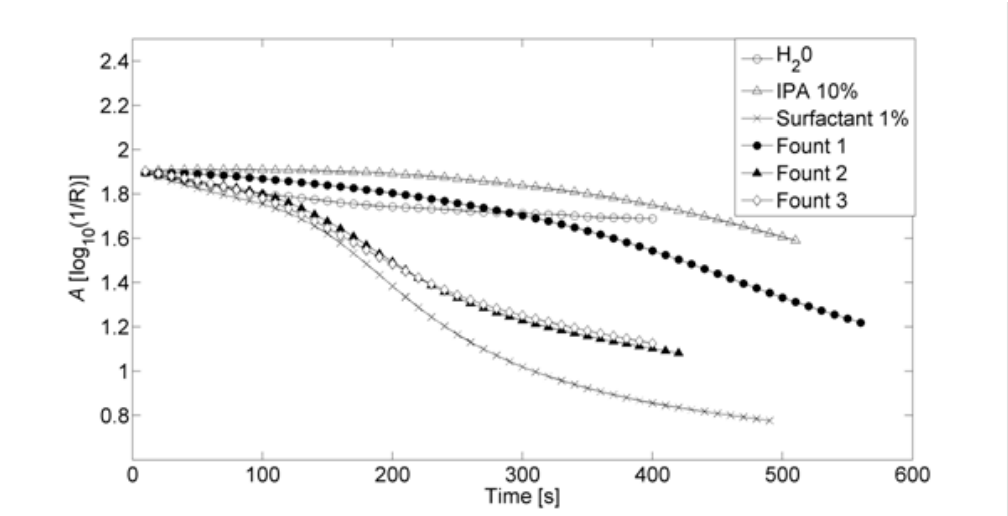

Figure 16. Imbibition and evaporation of model fountain solutions as droplets into model coating tablet structures analysed with a NIR single point probe [Paper I]. Fount 1 is an IPA based fountain solution (6 wt% IPA + 3.5 wt% concentrate), whereas Fount 2 and 3 (3 wt% concentrate) are alcohol-free fountain solutions.

The same evolution in liquid water and moisture change is observed for the two alcohol-free fountain solutions (Fount 2 and 3). The slow imbibition and evaporation of water is observed as an almost linear curve. In the samples containing isopropyl alcohol (10 wt% IPA and Fount 1), linear regions up to 150 s are observed, which can be related to the fast evaporation of the alcohol. The linear region is followed by a decline, which is interpreted as the imbibition/evaporation of the water phase. The first region is thus related to the evaporation of the more volatile component and the second stage to the other components. The faster decline for

Fount 1 than that of the 10 wt% IPA solution can likely be attributed to other unknown additive(s) in the Fount 1 mixture. The adsorption of species on the surface influences the surface chemistry, and hence the adhesion and the interaction with other substances will also be affected.

The droplet wetting was also monitored with hyperspectral imaging [Paper IV]. Moisture maps were generated by calculating the water band areas from the spectra at each spatial pixel and displaying them as an intensity image.

The lateral wetting occurs for as long as it takes for the surface area of the droplet to become fixed. The first image after contact (t = 30 s) shows the situation when the lateral wetting on the tablet surface has stopped. This stage is followed by the drying procedure and droplet internal to surface diffusion. The droplet contraction takes place and the receding interface is shown in red in Figure 17. This phase can also involve capillarity competition between the pore structure and the droplet surface curvature. The droplet shrinkage due to moisture loss results in an irregular wet core, dependent on the non-constricted pore system. As the droplet is drying, the droplet circumference is saturated causing a ring formation, the retreating meniscus acting in competition to the tension within the meniscus during retreat along the surface [Deegan *et al.,* 1997].

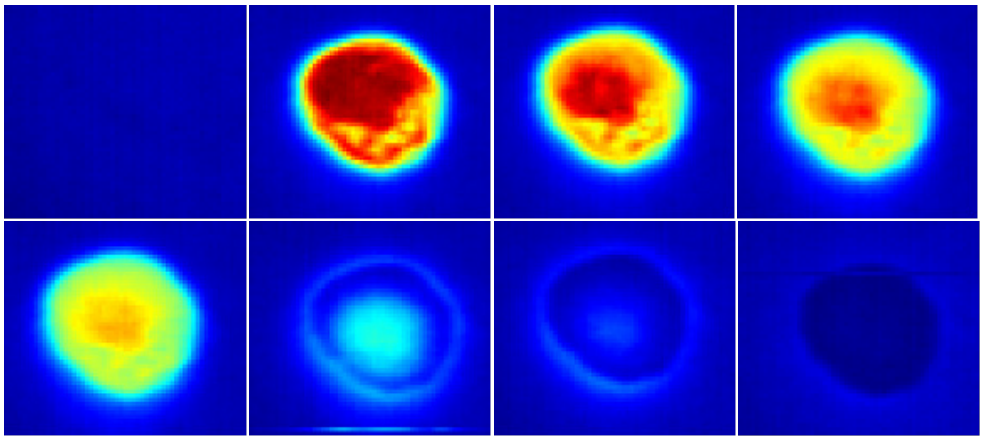

Figure 17. Droplet wetting on pigment tablet studied with hyperspectral NIR imaging. The droplet contact times from left to right and up to down are: t = 0 s, 30 s, 60 s, 90 s, 2 min, 9 min, 12 min and 30 min, respectively. Red colour means a wet surface and the colour turning blue means drier [Paper IV].

6.3 NIR calibration measurements

In order to be able to define the absolute moisture content changes, e.g. in a paper during processing, a calibration set is needed [Paper II]. In Figure 18, the results from two different procedures for non-image area and image printed area are presented [Paper V]. Process samples for calibration were taken directly from the printing line. The printing machine ran in full speed after which the machine was run down to zero speed and samples were taken from the paper web before the dryer, i.e. the printed areas were still wet. The same procedure was conducted for non-image areas. Figure 18 presents the calibration curves for both non-image and cyan (fulltone area, 100 % ink raster area) printed paper with two calibration methods ("dry" laboratory samples previously described (left graph) and wet process samples (right graph)).

It can be seen that the dried ink film on the paper developed the same calibration curve for both printed image and non-image samples (left graph), i.e. the drying profile is exactly the same for both samples. The spectral baseline was, however, somewhat higher for printed paper but this is eliminated in the baseline correction. It can now be concluded that when the calibration procedure with the humidity chamber is done on non-image paper vs. dried printed paper, the already dried cyan ink does not distort the NIR moisture measurement.

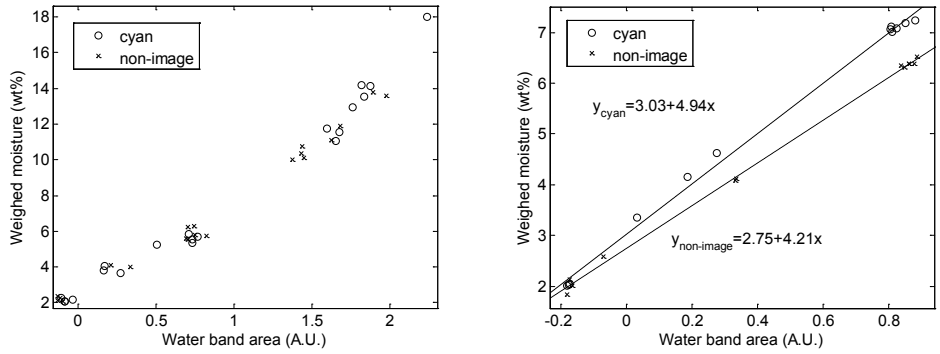

Figure 18. Calibration curves for non-image and cyan printed areas, respectively. Laboratory calibration curves for both areas (left) and on-press calibration curves determined at the printing machine (right) [Paper V].

However, in the case of the wet (liquid) ink film, the ink affects the calibration curve with a slight offset and a slope difference (right graph). The difference is more pronounced when measuring higher moisture values. The water band area for the printed surface is smaller than the

area for a non-image surface when the experimental moisture content is the same. The assumption made here is that the contribution of volatile compounds is negligible. Note that the ink in its wet state contains emulsified fountain solution while the laboratory ink is “pure” in that sense.

In the calibration measurements, also an increase in reflectance (reduced absorbance) was observed. This increases the differential between the moisture peak and the background when the moisture is at the surface. Thus, when the same calibration model is used for both surfaces, the printed paper (wet liquid ink state) is seen to be apparently drier. One should also note that in laboratory conditions, the sample is moisturized homogeneously throughout the structure since the paper is in the humid chamber for 15 min. At the printing machine, the wet ink is applied on the surface of the paper, resulting in high moisture content in the uppermost surface layers.

6.4 Laboratory printing trials

Paper strips were printed in the laboratory with the Prüfbau technique and fountain solution and cyan ink were applied pair-wise in order to compare the response of the NIR signal [Paper V]. The cyan ink was “pure” in the sense that it did not contain any emulsified fountain solution. It should be highlighted that in the case where fountain solution was applied onto ink, the ink layer was dry in order to avoid sticking of ink onto the printing roller. In all other cases, the ink was in the liquid state (wet) during the measurement.

First, very logically, when fountain solution is applied on the paper, the moisture content is increased (Figure 19). It is also further increased when another fountain solution layer is applied in addition to the first fountain solution application. It was expected that the moisture content of “dry” and printed paper should be at the same level due to no emulsified fountain solution within the ink. Interestingly, the response of the NIR signal shows a higher moisture content for the printed sample compared to the “dry” paper. It was also expected that the moisture content should be the same when fountain solution is applied under and on top of an ink film. However, this was not the case. When fountain solution was applied under the ink, a higher moisture response was obtained. Water on ink reduces the refractive index contrast with air, and so reflectance decreases. Thus water on top appears less NIR absorbing as the penetration of the NIR again increases. Again, it needs to be highlighted that the ink layer was dry in the case where fountain solution was applied on top of the ink and wet in the case where the fountain solution was applied under the ink.

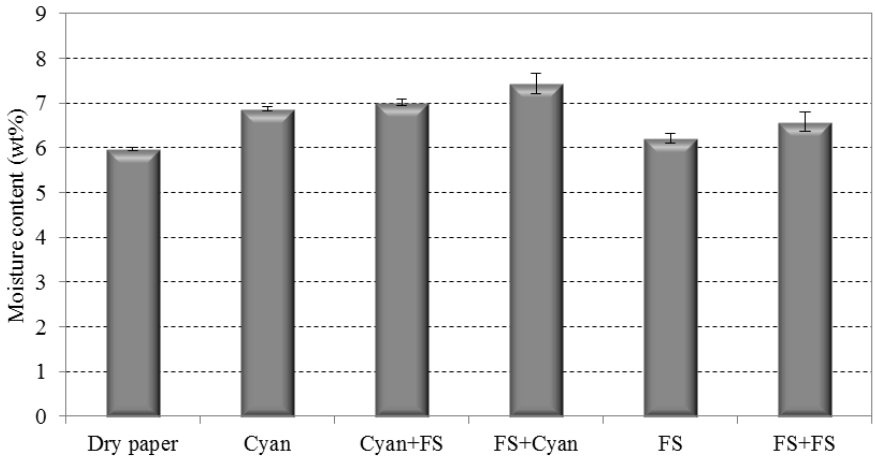

Figure 19. Moisture determination of non-image and cyan printed surfaces. The term "dry paper" refers to a non-rewetted substrate. The cyan calibration curve was used for the printed sample and the non-image calibration curve for the non-image sample. FS stands for fountain solution [Paper V].

6.5 Reference spectra for studied substrates

Reference spectra for each studied material were conducted in order to trace possible spectral features, disturbing the measurements [Paper V]. Even more importantly, the reference materials were analysed in all different states they appear in the process, e.g. wet and dry ink on paper etc.

In Figure 20, the NIR absorbance spectra for the non-image paper (both as dry and wet), a dry ink film and wet ink film on the paper and a "pure" ink (i.e. containing no emulsified fountain solution) are presented. The nfGCC non-image wet and nfGCC cyan wet ink samples were measured at the heatset offset printing machine, the spectra determined immediately as the samples were cut from the paper web before the dryer and placed under the NIR probe. The other samples were measured in the laboratory at equilibrium state with regard to ambient conditions. The conditions were, however, exactly the same, i.e. all samples were measured at T=23 °C and 50 % RH. The cyan ink layer on the paper surface was thus dry in the sample "nfGCC, cyan (dry ink)" when compared to the process sample ("nfGCC, cyan (wet ink)"). The samples were heated to near zero moisture level, and to prevent re-moisturizing from ambient air, they were placed between two borosilicate glass slides during the NIR measurement. Note that the "pure" cyan ink (wet) was measured in transreflectance mode as a thin wet liquid ink

film between two glass plates and with the white reference placed underneath. The word "purity" is used in the sense that the ink contained no emulsified fountain solution, which can be concluded due to no absorbance either at 1 450 nm or 1 940 nm.

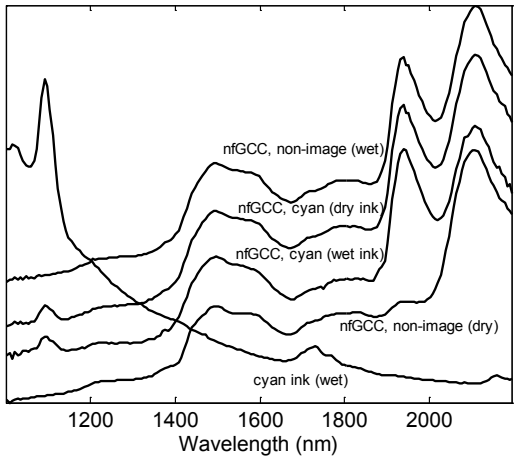

Figure 20. NIR absorbance spectra for the "dry" and wet paper, dry ink film and wet ink film on the nfGCC coated paper, and "pure" ink (i.e. containing no emulsified fountain solution). For better visualization, baseline offsets were added to the spectra [Paper V].

It can be seen that the cyan ink exhibits relatively strong absorbance at 1 100 nm, a moderate bimodal absorption band between 1 700–1 800 nm and a sloping baseline. The spectrum is relatively flat in the wavelength range 1 900–2 000 nm. Thus, the characteristic absorption features of cyan ink do not have an effect on the NIR moisture measurement when the baseline-corrected water band area between 1 900–2 000 nm is regressed against the moisture percentage of the sample. This statement is true if, for simplicity, the measured spectrum is assumed to be a linear combination of pure analyte spectra (assumption of generalised Beer-Lambert's law).

The bimodal peak between 1 700–1 800 nm corresponds to the oil in the ink. It is not observed in the spectra for ink printed on paper partly because the solvent is evaporated in the dryer and partly due to the low concentration of the oil in the wet ink film. It should be noted that, in Figure 20, baseline offsets were added to the spectra to make them visually distinguishable from each other.

The amount of moisture in paper may be visually discerned by observing the intensity of the water absorption band at 1 950 nm. The process sample with wet ink layer ("nfGCC, cyan (wet ink)") has the largest water absorption band. The dried sample ("nfGCC, non-image (dry)") has only a small bump in this location, as expected.

Also for process liquids, namely ink, fountain solution and silicone, the reference spectra were measured [Paper II]. The NIR spectra of the aqueous fountain solution are virtually identical with the spectrum of pure water (Figure 21). Thus, in a spectroscopic sense, the fountain solution may be treated as water from the perspective of the measurement. It is thus assumed that the spectral signals of the other components, i.e. the inks, the fountain solution and the silicone emulsion, do not interfere with the signal of interest, namely the strong absorption spectrum of water (marked with a light blue bar). The presence of e.g. IPA, however, has an influence on the amount of moisture the paper is able to pick up, and the relative evaporative loss (See also Figure 16). Furthermore, the presence of ink also has an influence on how much moisture the paper picks up, as shown in one of the sub-studies [Paper V]. The effect of silicone application can also be detected with the NIR method as an increase in the moisture level [Paper II]. This is expected since the silicone emulsion is mostly water.

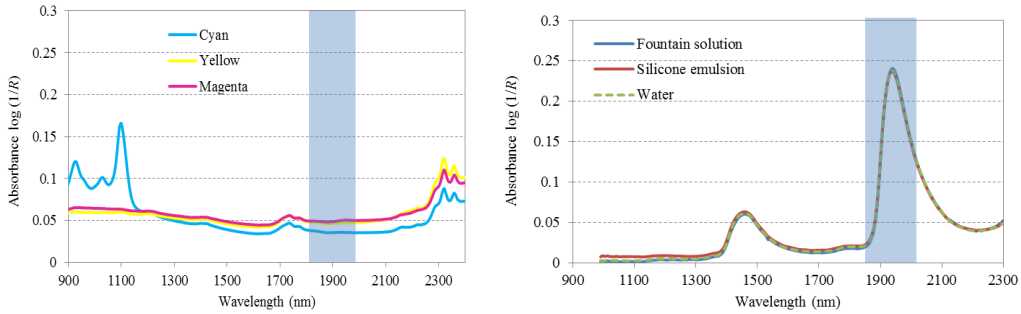

Figure 21. NIR spectra of magenta, cyan and yellow inks (left). NIR spectra of a fountain solution and a silicone emulsion (right). The analysed water band area is marked with the light blue bar. The spectra were measured in diffuse transreflectance mode [Paper II].

6.6 Full-scale heatset offset printing studies

The up-scaling of the measurements was conducted on an 8-page heatset offset printing machine. Several machine parameters, such as, the machine speed, fountain solution feed, drying conditions and silicone application were studied in order to increase the understanding on how

the process is able to modify the temporal moisture profiles accounted on the printing press [Paper II]. The analysis of printed image and non-image areas and their individual role in the layer formation was enabled with numerous print layout modifications and depending on the position of analysis.

As well known, the offset printing process influences the moisture content of paper by applying ink and fountain solution on it. The subsequent drying obviously also affects the moisture content. Figure 22 shows an example of the changes in moisture content during printing of paper measured with NIR, fully supporting hypothesis III.

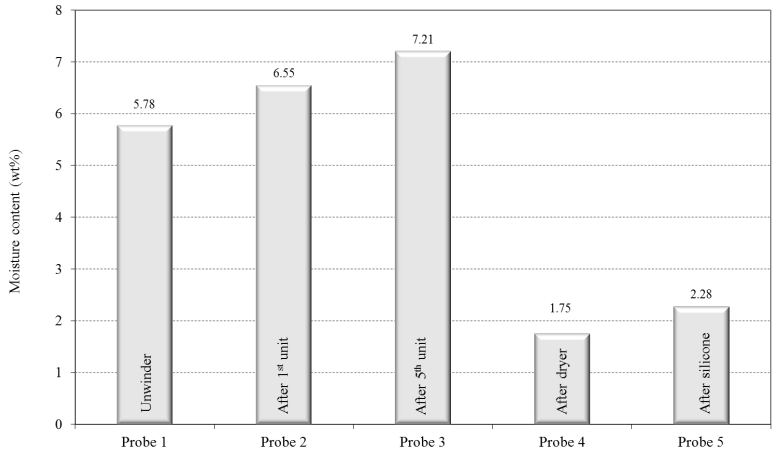

Figure 22. Moisture contents of the paper during the printing process. Probe 1 at the unwinder, probe 2 after the 1st printing unit with only the fountain solution application, probe 3 after the 5th printing unit, probe 4 after the dryer, probe 5 after the silicone application. The printing speed was 32 000 rph (5.6 ms^{-1}) and the web temperature was 120 °C (paper web temperature was measured inside the dryer) [Paper II].

The results clearly and logically show that:

1) the more printing nips the paper web passes, the more liquid water is transferred to the paper,

2) the dryer dries the paper, and

3) application of silicone acts to re-moisten the paper after the dryer.

The figure also gives the relative response of liquid transferred to the paper by capillarity and permeability in the first units and pressure permeation primarily in the latter units.

6.6.1 Printing machine speed

In Figure 23, the amount of water transferred to the paper is studied as a function of printing speed [Paper III]. The study was conducted on non-image areas of the printed sheet. It needs to be highlighted that as the printing machine speed is increased, the machine automatically compensates the delivery of the fountain solution volume linearly by increasing the fountain solution ductor roller speed. The initial pick up by the paper is greater than in the subsequent units. As the printing speed increases, less fountain solution is transferred to the paper. The rough surface of the paper acts to reduce the print nip pressure by increasing the non-contact volume. The hypothesis I, hereby suggested, relates to the comparison between rougher and smoother paper grades. The rougher surface displays a greater void volume in the printing nip, which may not be filled by the available volume of liquid (fountain solution) at the first or early print stations. A smoother surface will form a thin continuous liquid film more readily in the nip, once flooding of the nip has occurred, and thus experience the full transmission of the nip hydraulic pressure acting on the liquid and via the liquid into the paper surface pores, whereas in the case of a rough surface the liquid will not transmit the hydraulic pressure, but rather flow within the unfilled surface roughness. Thus, the smooth surface will experience additional pressurized permeation, whereas the rough surface will only exhibit capillary imbibition and surface void filling. We can see, therefore, that, unless the surface of the coating is extremely smooth, the mechanism of fountain solution uptake rate is predominantly driven by capillary pressure. Thus, uncalendered and matt coated papers do not have dominant pressure-driven permeation at the liquid volume levels normally encountered on a press. It can also be seen that as the printing speed increases, the drying efficiency of the paper in the heated oven is decreasing.

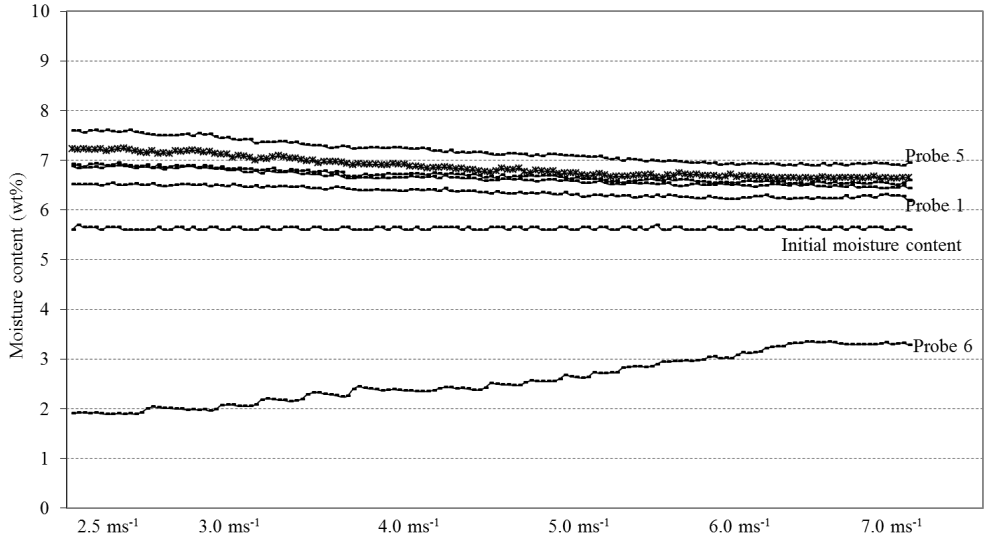

Figure 23. Changes in fountain solution pick-up by paper as a function of printing speed spread over time for the uncalendered nfGCC coating. The printing speed was 13 000 rph (2.5 ms^{-1}) in the beginning of the trial point and 40 000 rph (7.0 ms^{-1}) at the end with continuous speed change of the fountain solution delivery to the printing plate. Probe 1-5 located between the printing units and Probe 6 after the dryer [Paper III] (See schematic in Figure 10).

6.6.2 Fountain solution feed

In Figure 24, the dosage of fountain solution was adjusted from a minimum value to its maximum at a given printing speed [Paper III]. The study was conducted on non-image areas of the printed sheet. As the dosage level is increased, the amount of fountain solution transferred to paper increases linearly. The strongest inclination is seen for Probe 5. This supports the hypothesis that the volume of liquid must be equal to, or exceed, the blanket-coating contact volume before significant pressure-driven permeation can occur.

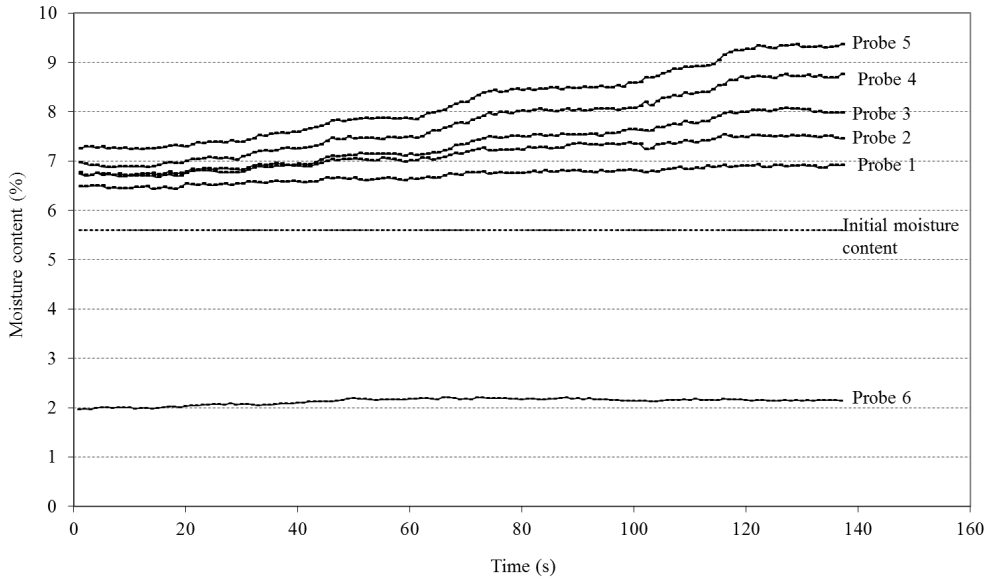

Figure 24. Fountain solution pick-up by the uncalendered nfGCC coated paper as a function of dosage at constant speed. The dosage level of fountain solution was changed from minimum to maximum. The printing speed was 18 000 rph (3.0 ms^{-1}). Probe 1-5 located between the printing units and Probe 6 after the dryer [Paper III] (See schematic in Figure 10).

In Figure 25, the results from printing of coated papers with different calendering levels are presented [Paper III]. The liquid water uptake by the paper as a function of printing units passed can be divided into three regions. The study was conducted on non-image areas of the printed sheet. The samples move from an open/initially unwetted structure to partly filled and finally to a surface saturated structure. In the first region (I), the paper is initially wetted and strong capillary forces act to imbibe the liquid inside the paper leaving the surface void volume essentially empty until entering the second unit. In the second region (II), the paper structure becomes partly liquid-filled and surface saturation takes place, and after the second unit further transport inside the paper occurs but the liquid volume compared to the surface void volume becomes equalized when entering the third unit. In region three (III), the linear trend for the last three printing units indicates a saturated surface which takes up more liquid only via film splitting and permeation. At surface saturation, a "calendered equivalent plane" is created. The transition between region II and region III is bound to be less distinct, but by definition has to exist simply in terms of mass balance.

For Probe 1 the liquid uptake is lower for the calendered samples compared to the uncalendered sample. Within the different calendering levels, there are no significant differences in liquid uptake in one studied unit. However, the liquid uptake increases as a function of paper passing further printing units. These findings fully support hypothesis II and conclude that the mechanism of liquid transfer in subsequent units is controlled by splitting of the liquid film and the amount of permeation that is able to occur as a function of permeability, which necessarily for calendered coated papers is very low.

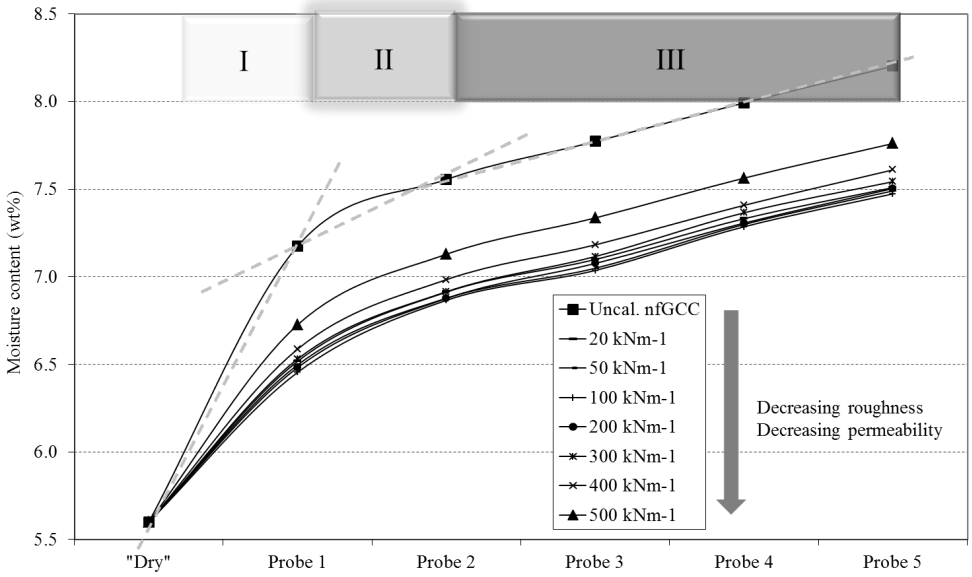

Figure 25. Fountain solution uptake by coated paper. The paper coating consists of 100 parts nfGCC pigment and 11 parts latex applied as a single coat (18 gm^{-2} per side). The printing speed was 18 000 rph (3 ms^{-1}). The figure presents the liquid uptake for papers calendered to different degrees using different linear loads indicated in the legend [Paper III]. The porosity related values of the papers can be found in Figure 12 and Figure 13. Note that the lines do not represent any function but are guides to the eyes.

6.6.3 Printing layout

Five measurement probes (Figure 26) were mounted in the cross-direction of the paper web after the 5th printing unit [Paper V]. The measurement probes were placed to measure simultaneously printed and non-image areas. The middle probe measured the borderline between the two areas.

The results reveal that the edge between the printed and non-image area has the highest moisture content (independent of the calibration curve used). This indicates that the fountain solution applied on top of an ink layer partly remains on the ink layer but is also pressed to the side due to the pressure in the printing nip and likely reticulation for the hydrophobic ink surface. Also, in case of a printed image, the end of the print probably will be wetter resulting in tail edge piling/picking as fountain solution is squeezed to the end of the print as well as sideways. The proposed reasons to this can be a combination of an interfacial tension effect resulting in surfactant concentration drawing fountain solution to the borders or the fountain solution applied on top of ink is squeezed towards the borders since the ink applied from a previous station hinders the penetration of the fountain solution applied in subsequent units.

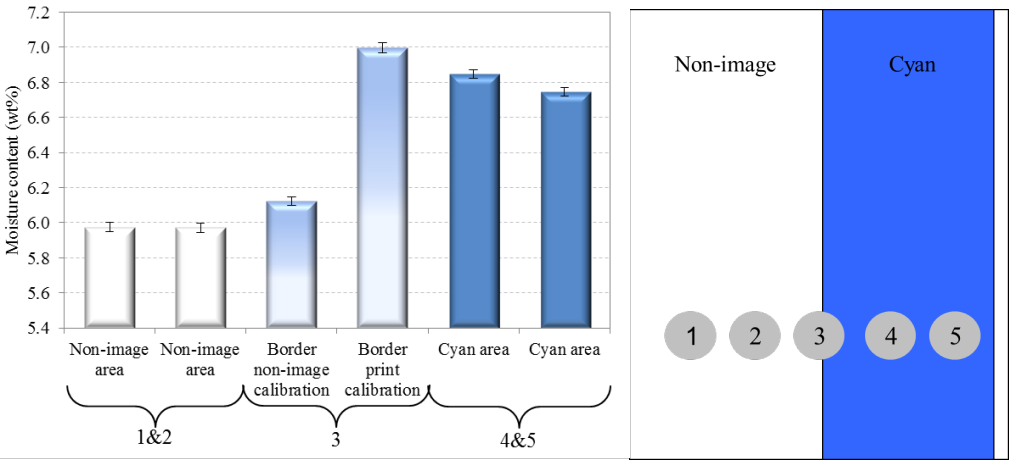

Figure 26. Moisture content of cyan print vs. non-image vs. border line (of image in machine direction) after the 5th printing unit. The studied paper was a double coated glossy paper. The border line measurement spot was calibrated both with the non-image and printed surface calibration curves [Paper V].

6.7 Depth of fountain solution penetration by independent tracer technique

The aim of the moisture sensitive NIR measurements was to be able to detect small variations in the paper moisture content in heatset offset printing, because the printing technique and the subsequent print quality are highly sensitive to moisture variations in the surface layers. The liquid/moisture in the form of fountain solution applied on the paper will penetrate into the paper, partly due to capillary action and partly due to the pressure pulse in the nip, before the

sample is dried in the dryer. In order to detect the penetration depth of the applied liquid, the tracing element (LiCl) was added.

Figure 27 shows the cross-section of non-image areas at three different fountain solution feed levels, increasing from left to right (1.-3.) and a printed sample (4.). Obviously more fountain solution is transferred as the feed is increased. It can also be seen that the fountain solution (marked with green colour) transferred in the printing process does not penetrate into the base paper but is imbibed by/within the coating layer. The penetration depth of the fountain solution in the image area is even more surface concentrated.

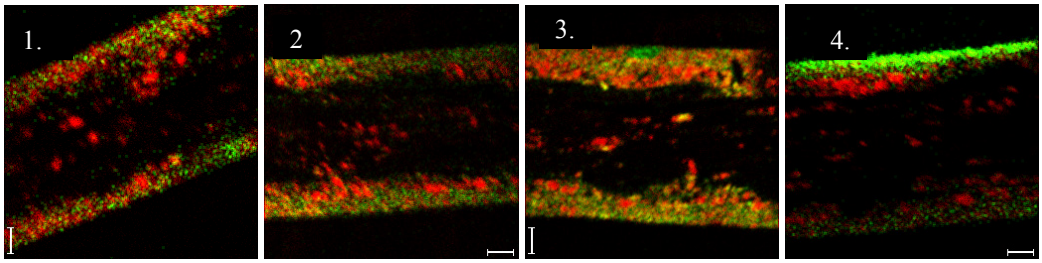

Figure 27. ToF-SIMS cross-section images showing the Li^+ ion distribution in green in the non-image area of a double coated paper (70 gm^{-2}) with low (1.) medium (2.) and high (3.) fountain solution dosage as well as a cyan image area with low fountain solution dosage (4.), respectively. The Ca^{2+} ion is marked with red. The scale bar is 10 µm.

Figure 28 demonstrates the distribution of the fountain solution/Li^+ ion in the cross-section. It can be concluded that the liquid did imbibe into the outer surface layers before the paper went into the drying section. But, it can be seen that the fountain solution transferred in the printing process did not penetrate deeper than 20 µm into the studied paper sample. Thus the liquid did not reach the basepaper though the dosage level was at its maximum. For lighter coat weight, however, clearly the penetration would easily have reached the basepaper. The implications for LWC paper usage in respect to moisture content of the responsive basepaper fibres are borne out in practice, where fluting (waviness) of the printed web is readily identified under heatset conditions.

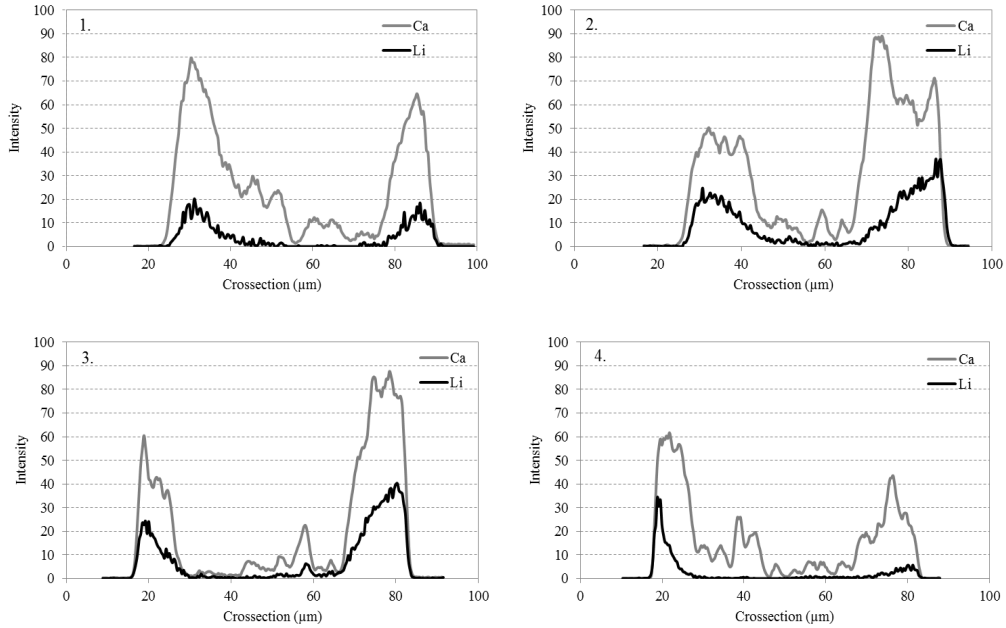

Figure 28. Li^+ ion distribution as a line profile in the cross-section of the non-image area of a double coated paper (70 gm^{-2}) with low (1.) medium (2.) and high (3.) fountain solution dosage as well as a cyan image area with low fountain solution dosage (4.), respectively. The double coated (70 gm^{-2}) high coating thickness paper, as illustrated here, contains all the fountain solution in the coating layer.

6.8 Drying conditions – moisture variation and its relation to waving – NIR implementation

Figure 29 presents the difference in moisture content determined from a green printed (rastered 100 % cyan and 100 % yellow giving the sum of green) versus a non-image area. The web temperature in the dryer was adjusted from 120 ºC to 170 ºC. It can be observed that the relative moisture content difference (uneven moisture profile) between the two areas is decreased as the paper web temperature is increased.

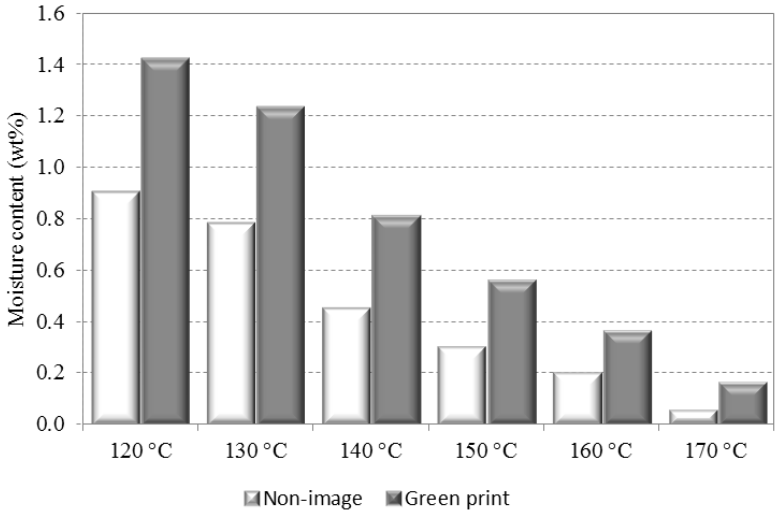

Figure 29. Moisture content of printed (green patch) and non-image area as a function of drying conditions for a double coated paper with a basis weight of 70 gm^{-2}.

The implementation of the NIR measurement system was directed to one concrete printability defect, namely waving. The waving tendency was seen to be strongly dependent on the drying conditions with the chosen press configuration and the studied substrate (Figure 30). A maximum waving was reached at 130 °C, whereafter it decreased as a function of web temperature reaching its lowest value with the highest web temperature. Combining the moisture response in Figure 29 with the waving tendency in Figure 30, it can be concluded that the smaller the relative moisture difference between the non-image and image areas is, the lower is the waving tendency. These results fully support hypothesis IV, that the unevenness of moisture can be monitored and related to the waving tendency of paper.

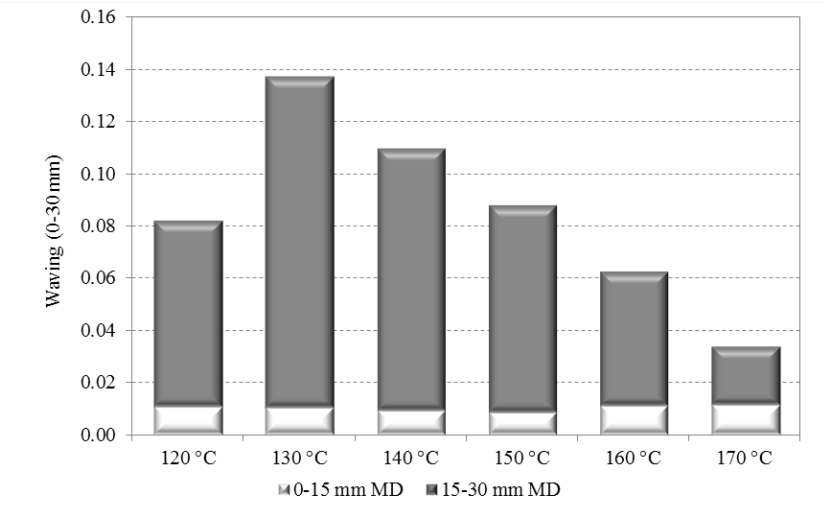

Figure 30. The influence of paper web temperature on the degree of waving (web temp profile vs. waving in machine direction). A double coated paper (70 gm^{-2}) was used in the trials. The degree of waving was determined with the ViWa measurement device. MD refers to the machine direction. The results are still unpublished.

6.9 Sensitivity of the NIR moisture measurement device

6.9.1 Figures of merit

Some commonly known parameters are used to describe the performance of the measurement device. In the sensitivity measurements, both electronic noise (NIR instrument) and process noise (printing machine) were measured. The noise level was defined to be the standard deviation (SD) of the predicted moisture time profile during stationary process conditions. In this study the moisture detection capability is described by the *lowest moisture limit of detection* (LOD), which is the lowest detectable change in moisture level. The detection limit was estimated from the average of moisture and the standard deviation. Here, the standard deviation was multiplied with a factor three to get the LOD.

Obviously detection limits are dependent on both the signal intensity and the noise. Due to the noise, it is not clear how much moisture there actually is in the matrix. The *lowest limit of quantification* (LOQ) is the limit at which one can reasonably tell the difference between two different values, i.e. the smallest measurable change in moisture level. Here, the quantification

limit was estimated from the average of moisture and the standard deviation, the standard deviation being multiplied with a factor ten to get the LOQ.

It needs to be highlighted that these parameters can be drastically different between laboratory and process conditions. Due to this, the abovementioned parameters in process conditions are described with the process detection limit (PDL) as well as process quantification limit (PQL), respectively. The STD, LOD and LOQ parameters were calculated for the extracted noise.

The different probes had slightly different signal-to-noise ratios (SNRs). On average, the PDL=0.07 wt% and PQL=0.21 wt% for measurements carried out in process conditions. In printing process conditions, the varying sample-to-probe distance due to flapping paper will increase the figures somewhat, but one should note that the NIR-method is still highly sensitive as the figures show. In laboratory conditions, the LOD and LOQ for the moisture level of stationary paper were less than 0.032 wt% and 0.107 wt%, respectively.

As stated, variations in the LOQ values exist. Paper samples are spatially inhomogeneous but variations also occur due to small illumination and detection spots. The SD, LOD and LOQ values depend mainly on the following variables:

- Integration time which decreases SD
- Number of averaged consecutive spectra which decreases SD
- Number of non-linear or noisy pixels in the detector array which increases SD

6.10 Effect of internal and external stimuli on moisture measurements with NIR

6.10.1 Moisture sensitive wavelength band

It is very important to choose which water-sensitive peak is investigated. In these measurements, the 1 450 nm water absorption band displayed a slightly lower noise level than the 1 940 nm peak. However, the 1 450 nm region can, depending on the substrate composition, be partly overlapped by the cellulose band (1 490 nm). The choice of the analysed water band has been marked in each case and the reason for the choice is one of the abovementioned factors

e.g. the 1 450 nm band suited better for the pigment tablets (containing no cellulose) and in the case of paper analysis, the 1 940 nm band was preferred.

6.10.2 Temperature

Figure 31 shows the effect of sample temperature on NIR spectra. The cold sample was measured in 20 °C and the hot sample as 70 °C. The water bands at 1 450 nm and 1 940 nm are shifted towards smaller wavelengths when the sample temperature is increased, i.e. if the same calibration model is used over a large temperature range, too large moisture levels are erroneously given for warmer samples. The effect is more pronounced at high moisture contents (right image).

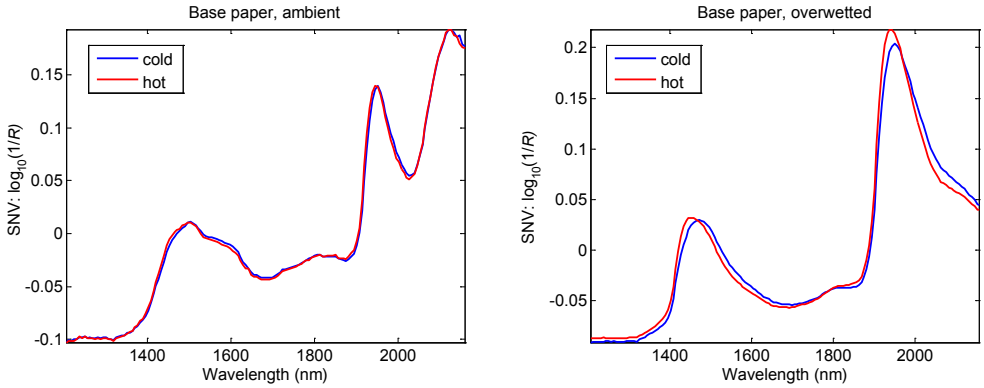

Figure 31. The effect of sample temperature on the NIR spectrum of a paper sample at two different moisture levels. Paper measured in ambient conditions (left) and as over-wetted (right). SNV (Standard Normal Variant) transformation done on spectra for better visualization. Cold refers to 20 °C and hot to 70 °C, respectively.

Hence, if the measured sample has a higher temperature, e.g. moisture determination directly after a heatset offset dryer, a shift in baseline occurs and the peak moves slightly towards shorter wavelengths and tends to become broader in shape (Figure 32). This has also been shown by Burns [2001].

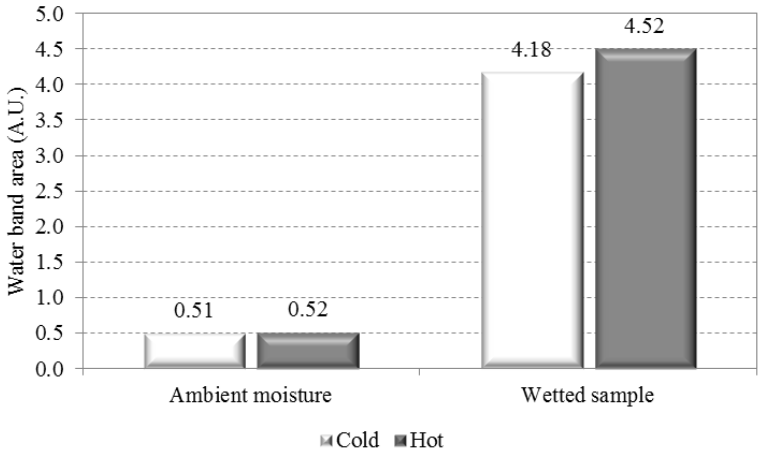

Figure 32. The effect of sample temperature on the analysed water band area around 1 940 nm. Cold refers to 20 °C and hot to 70 °C, respectively.

6.10.3 Drying of sample with NIR beam during measurement

Sample movement during the measurements is an important limiting factor, known since the formation of the paper induces noise in the NIR spectra and movement effectively changes the area projection of the formation. In the laboratory measurements, the measured sample was manually scanned. The moving web in the process conditions obviated the need to scan with the probe, thus simplifying the data collection for the online measurements. As well, the power capacity of the IR-source optical fibre was low and the detector integration time correspondingly long and thus the heating of the sample during the measurements was considered negligible.

6.10.4 Borosilicate glass window

A borosilicate glass plate was used when producing the calibration curves for the different substrates. The reason to use the glass plates was to avoid evaporation of liquid from the measured sample. The influence of the borosilicate glass window on the NIR spectra was determined by measuring a set of paper samples with and without the glass (Figure 33, left). It was found that the presence of the glass window increases the spectral baseline, i.e. light is lost to specular reflectance and/or absorption by the glass window. However, this baseline shift is a constant over the spectral range of interest.

The water band area, therefore, yields larger values when the measurement is conducted through the glass window, i.e. if the calibration model is constructed with a glass window, moisture values are subsequently underestimated for process samples (Figure 33, right). A correction factor according to the bias created by the borosilicate glass plate was implemented in the analysis.

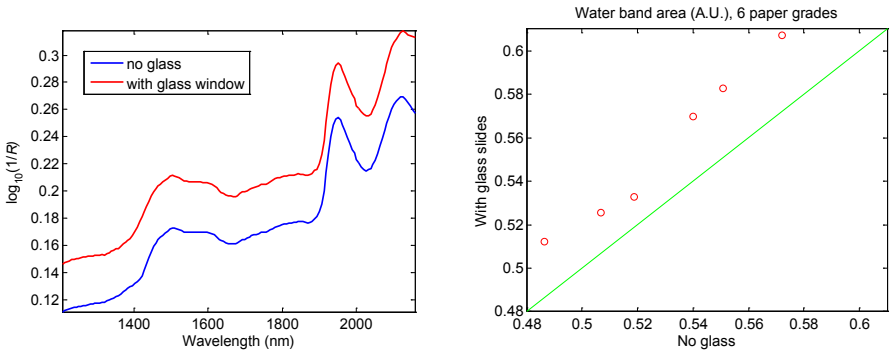

Figure 33. Examples of the log(1/*R*) spectra of a paper sample measured with and without the borosilicate glass window (left) and the bias effect of borosilicate glass on the water band area determined for six different paper grades (right).

6.10.5 Condensed liquid (vapour)

As previously mentioned, together with liquid imbibition into the paper substrate, there is always evaporation taking place. The heatset offset printing environment involves heating gradients in the printing units. Though the measurement distance between the probe and the sample was great (165 mm), the possible effect of water vapour or condensed liquid on the spectral response was investigated in laboratory scale.

Firstly, water was boiled in a decanter glass such that the hot vapour rose into the optical path, and, secondly, droplets of water were sprayed into the optical path through a nozzle. As seen in Figure 34, water vapour has spiky, multimodal absorption bands at 1 380 and 1 880 nm (marked with black arrows). The presence of water vapour distorts paper moisture measurements. When the water band area (1 900–2 000 nm) is calibrated to represent moisture wt%, the presence of vapour has a decreasing effect on the estimated moisture value. This is due to the fact that the absorption band of vapour is next to the absorption band of liquid water. Therefore, the apparent area between 1 900–2 000 nm is decreased. The paper moisture seems to

be about 0.1 wt% lower when water vapour is in the optical path. Thus, the effect was concluded to be small, if there would be vapour present. However, such an effect was not observed in the conducted measurements.

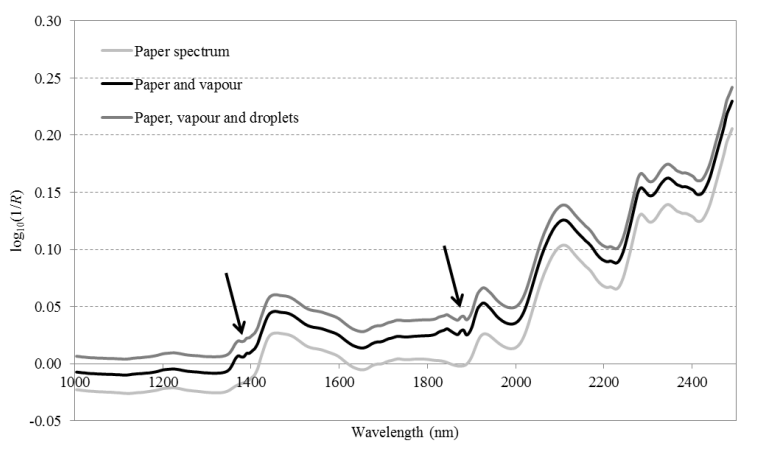

Figure 34. The effect of vapour and condensed liquid on NIR spectra. The black arrows show the vapour spikes.

6.10.6 Influence of dry ink film on moisture determination – laboratory study

Hyperspectral imaging of cyan printed papers showed that a dried cyan print does not disturb the measurement of moisture (Figure 35), i.e. the cyan absorbance band is seen (left) but the corresponding water band remains unaffected (middle). Cross sectional line profiles of both areas are also shown in Figure 35 (right). As previously shown, cyan does have an absorbance peak at 1 100 nm but it does not affect the water band (1 940 nm) and thus the inks are, from a spectroscopic viewpoint, transparent in that region unless a very large amount (400 %) is applied. It was also seen that, a dried ink layer of magenta or yellow does not affect the measurement of moisture either (results excluded).

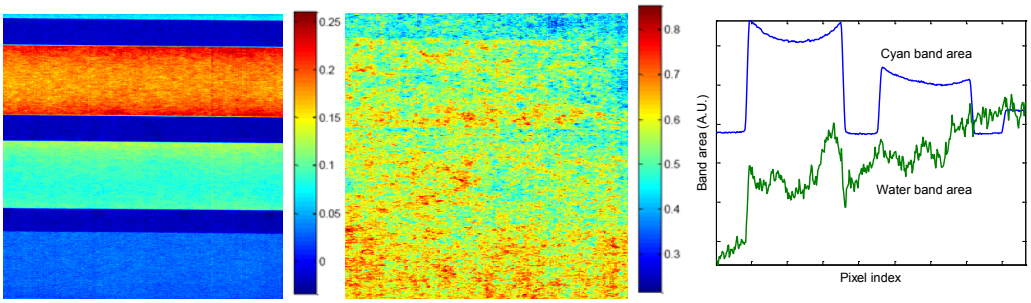

Figure 35. Baseline corrected area of the cyan wavelength band (1 060–1 120 nm) (left) and water band (1 900–2 000 nm) (middle). Cross sectional profile of both areas (right). The printing intensities from top to down were 400 % coverage of cyan (application of 100 % cyan from four units), 50 % and 20 % coverage, respectively. The ink patches were analysed as dry prints.

6.10.7 Ink Intensity

The influence of ink intensity/coverage level on the measurement of paper moisture content from a dry print area was determined. The moisture content was determined from different printed areas where the ink coverage differed from 10 % to fulltone, i.e. 100 % rastered. Figure 36 shows that the cyan ink absorbs strongly at 1 100 nm. According to this result, also the cyan density level could be quantified. The right graph shows the water band area around 1 940 nm at the same coverage levels. It can be concluded that the cyan ink is in a spectroscopic sense transparent at 1 940 nm and hence, the moisture measurement is undisturbed by the ink.

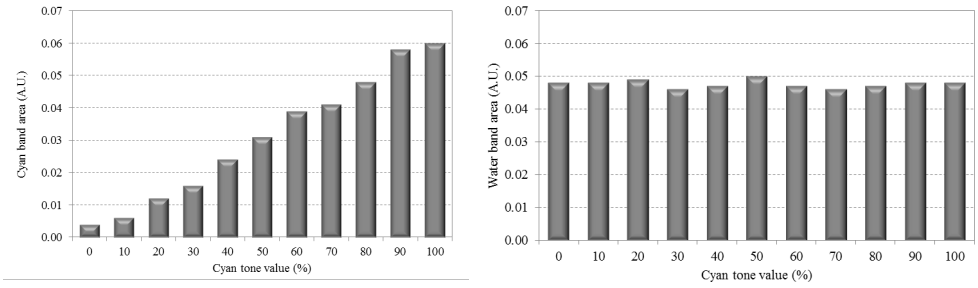

Figure 36. The influence of cyan ink coverage on the cyan absorption peak (cyan band area) at 1 100 nm (left) and on the water band area at 1 940 nm (right).

The same test was carried out for the other primary process colours as well. The results from dry magenta and yellow printed areas showed same results as for the dry cyan print, i.e. the ink

does not disturb the measurement of the moisture. However, as seen in Figure 37, a dry black print distorts the measurement of moisture. Black ink absorbs NIR radiation at 1 940 nm and thus the water band area is decreased with increasing black ink amount. Therefore, if there is black ink in the image studied, it is important that the amount is constant.

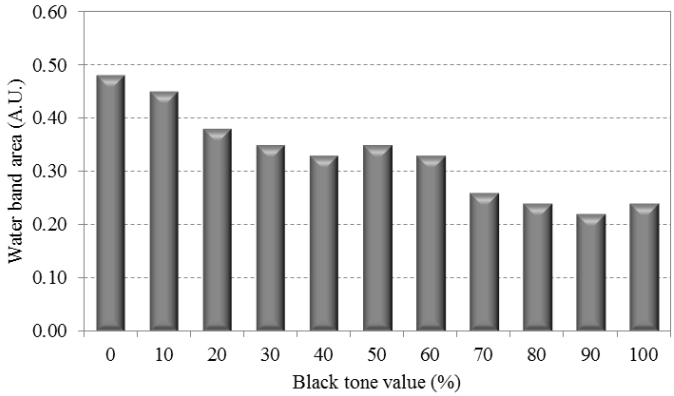

Figure 37. Changes in water band area (1 940 nm) as a funtion of black ink coverage.

6.10.8 Amount of emulsified water in ink

The hydroscope test device [Voltaire *et al.,* 2007] was used to add drop wise fountain solution into the ink under shear to form an emulsion [Paper V]. The aim of the test was to investigate if the NIR probes also detect emulsified fountain solution within the ink. The fountain solution was added until the ink was saturated, which was visually observed as droplets floating on the ink in the roller nip. At that point, the liquid addition was stopped and the evaporation of the emulsified fountain solution took place. As seen in Figure 38 (left), a steep increase in the moisture level of the ink is observed at t = 180 s to the saturation point at t = 220 s, thereafter the fountain solution was let evaporate from the ink. The corresponding spectra at three different states are also presented in Figure 38 (right) According to the results, an increase in fountain solution content as an emulsion within the ink can be detected with the NIR measurement.

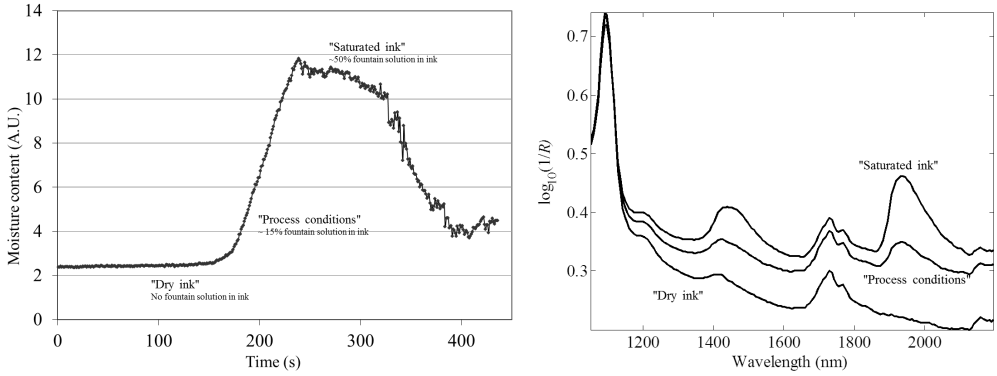

Figure 38. Ink-fountain solution emulsification. Fountain solution addition to ink (left) and corresponding spectra at three states (right). The abbreviation A.U. denotes absorbance units. The depicted moisture level is linearly proportional to the baseline-corrected water absorption band area between 1 890 – 2 000 nm, and it is assumed also to be proportional to the true moisture level. The measurement was carried out as a transreflectance measurement from the roller surface.

6.10.9 Information depth

Total NIR reflectance measurements were performed by integrating sphere measurements. The information depth of the NIR signal was measured for wet and dry print on coated paper samples as well as for non-image areas. In Figure 39, the information depth is plotted as a function of wavelength. It can be seen that the spectra are affected by the ink in the lower end of the NIR wavelengths. However, the spectra are identical in the spectral range where the moisture analysis is performed, i.e. around 1 940 nm.

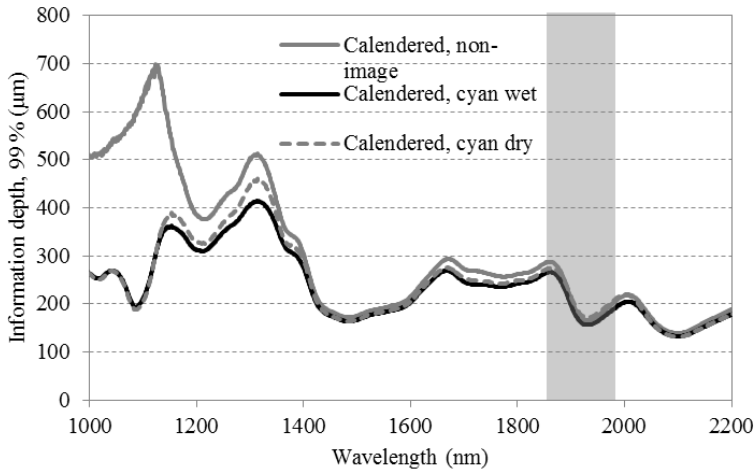

Figure 39. Information depth. The *y*-axis refers to sample thickness which reflects 99 % of light power reflected by an infinitely thick sample.

Figure 40 shows the information depth in paper as a function of reflected light power. When going deeper into the coated paper from the top surface, the remaining light power decreases monotonically as a function of the depth. It can be concluded that the information depth is identical for all printed samples on a given substrate, whether the ink is wet or dry or whether the studied area is a non-image one. The results confirm that 50 % of the information is collected from the first top 20 µm.

A reflectance conversion $R=I_{sample}//I_{\text{white ref.}}$, where I_{sample} is the sample raw signal and $I_{white\ ref.}$ is the white reference (Spectralon) raw signal (both are corrected with black reference (noise)), has been made to the integrating sphere measurement data. The information depth was determined using the Kubelka-Munk theory [Kubelka and Munk, 1931] which has been used in the determination of the optical properties of paper [Pauler, 1986] and prints [Pauler *et al.,* 2001].

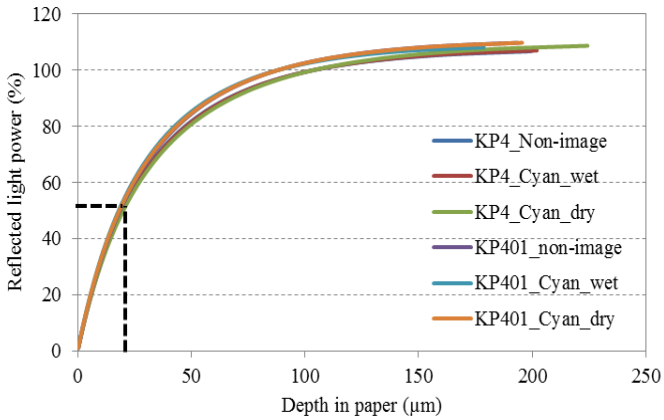

Figure 40. Average information depth of NIR signal in the wavelength band 1 750 – 1 850 nm of a woodfree fine basepaper applied with a single 12.5 + 12.5 gm^{-2} two sided coating. KP4 refers to an uncalendered sample while KP401 is calendered with a 500 kNm^{-1} linear load (Metso Optiload 4 + 4 nips). The diffuse reflected light power is scaled so that it gets the value 100 % at the thickness of the paper sample i.e., KP4: 103.4 µm and KP401: 87.8 µm, respectively. The results are still unpublished.

6.10.10 Pore volume and moisture level

According to Figure 40, a more closed structure has a slightly lower penetration depth compared to a more open one. A more closed structure absorbs more of the incident light compared to an open structure leading to a change in the spectral baseline. A structure having higher moisture content also absorbs more of the incident NIR signal.

6.10.11 Specular reflectance

The change in specular reflectance for non-image and wet cyan printed samples are presented in Figure 41. As observed, the specular reflectance significantly increases when the ink layer is on top of the paper, especially for the more porous and permeable uncalendered paper. For the hard calendered paper, the wet ink film does not significantly affect the specular reflectance. It should also be pointed out that the specular reflectance is relatively stable in the whole NIR region, somewhat increasing towards the longer end. However, in the wavelength region of interest, i.e. the water band area around 1 940 nm, it is almost constant.

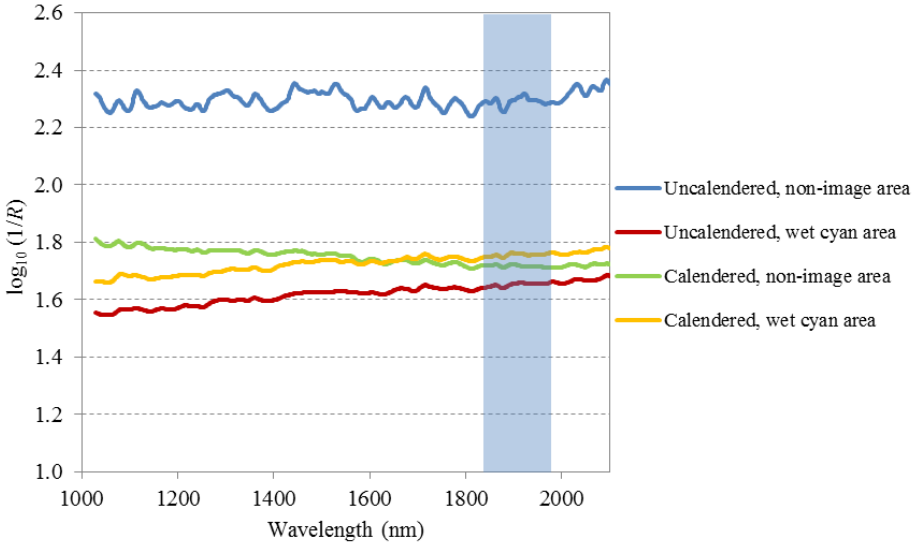

Figure 41. Specular reflectance spectra for two papers; an uncalendered paper and a heavily calendered paper (500 kNm^{-1} linear load (Metso Optiload 4 + 4 nips)). The papers were applied with cyan ink and measured when wet. Note that the cyan ink was applied with a hand-held printing device resulting in a significantly thicker ink film (ink density: 2.5) than under process conditions (ink density: 1.45). The water band area (1 940 nm) is marked with a light blue bar.

7 Discussion

Model pigment tablet structures as well as coated papers were used throughout the study. A thorough analysis of the surface and the internal structure of each of the substrates was conducted.

The wetting of liquids on and into porous structures has been studied in detail both in laboratory and process environments. The wetting was studied with both a sessile droplet approach as well as being applied as a liquid film under pressure. The wetting was defined as changes in total moisture content of the chosen porous medium.

The laboratory tests continued with up-scaling into full scale pilot printing trials, where also machine related parameters and their role in liquid transportation and distribution were investigated. The NIR technology, being applied as moisture sensitive probes, has been evaluated in this in-line context, and critical factors isolating the various contributions to the characteristic data have been analysed in depth.

7.1 Wetting and substrate structural analysis

Wetting of liquids on solid surfaces is a very commonly used method to describe the interfacial characteristics and interactions between the two media. As previously discussed, the sessile droplet technique is a useful method but sets challenges when it is applied on a porous substrate under ambient air conditions.

The surface properties of the substrate are of key importance in order for wetting to take place or not. The transport mechanisms depend on the surface structure and the pore size distribution, which cause local variations in transport rates, since paper is heterogeneous with respect to species content and features of different length scales. Clearly, the nature of the pore space influences transport by dictating both the nature of the interactions and the availability and directness of paths across and within regions throughout the void space.

A real paper surface is far from smooth, but is characterized by surface asperities of different heights and pores extending into the bulk. Hence, it is recognized that it is not possible to determine a true contact angle for imbibing surfaces, due to the probability of liquid passing laterally within the sub-surface. This influences the three-phase-contact at the apparent wetting front, i.e. the liquid droplet boundary is in contact with solid, air, and in some cases further liquid (Figure 42). The concept of surface roughness in the Wenzel model is, therefore, not possible to

define for a porous substrate unless a detailed nano-scale distribution of the liquid in the surface and sub-surface pores would be known. This is impossible as the increased exposed surface is a function not only of measured surface roughness but should include that expressed also internally in the pore structure as the liquid is also imbibed, leading to lateral just sub-surface spread. An application based only on surface roughness measure thus delivers only an apparent or "equivalent" contact angle, which represents the contact angle that would occur if the surface roughness effect was acting alone without coupling laterally with the pore structure, a situation which is, in relation to the true structure, unreal.

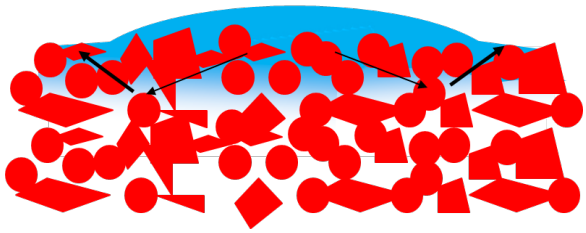

Figure 42. Contact angle / liquid droplet imbibition behaviour on nano/microporous material.

The results obtained here follow previously published data showing the preferential wetting of smaller pores in the structure with subsequent filling of big pores. This was also proposed by Gane *et al.,* [2000] and Koivula *et al.,* [2012]. The importance in taking into account both the surface features as well as the internal pore structure when discussing liquid wetting of heterogeneous porous media has hereby been reviewed and experimentally shown. Since it is the interfacial characteristics which play the key role, an individual analysis of the liquid and solid properties is not enough. For example, the liquid surface tension affects wetting but it is also dependent on the surface energy of the solid, creating the adhesion between these. The study showed that the wetting behaviour of offset fountain solution will depend on both surfactant and IPA as both molecules will be at the liquid-air interface and will thus affect the interfacial tension properties [Paper IV]. The work showed that by optimizing the liquid properties to fit the characteristics of the paper, most favourable dosages of individual components can be defined.

It was found that the measurement of contact angles is a complement to NIR when studying wetting [Paper I]. The NIR and contact angle studies concluded that capillarity is extremely rapid when the droplet comes into contact with the coated substrate and is defined by the contact area.

The imbibition/evaporation behaviour as a function of time was seen to be different for the studied solutions. The IPA based solutions exhibited a mechanism based more on evaporation while the surfactant mixtures displayed a behaviour more related to imbibition. From these results, a schematic series of events occurring during the imbibition of a droplet and subsequent evaporation of liquid(s) in porous structures, exhibiting a planar surface to air, was created (Figure 43).

Phase I represents the initial wetting once the liquid droplet has been introduced on the sample surface. As the droplet comes into contact with the surface, wetting is initiated. The initial wetting is related to the nano-second timescale for filling the outermost surface voids, to micro- and milli-seconds in relation to the filling of the just sub-surface structure of the coating [Schoelkopf *et al.,* 2000]. This phase corresponds to the highest speed of lateral wetting, indicating once again the linked roles of surface structure and pore structure, and the likely lateral liquid transportation sub-surface as an added effect on top of that of surface roughness alone [Koivula *et al.* 2012]. In case of droplet wetting, the penetration rate of such droplets, whose volumes exceed that of the capacity of the upper structure layers, is dominated by permeability, and thus square root time related in the longer term regime [Gane *et al.,* 2000].

Phase II describes the wetting at longer time scales (milliseconds to seconds). Apparent contact angle values are determined between this and the previous regime, i.e. phase I and phase II, recognizing the incomplete nature of the solid boundary of a porous material. Initially, the liquid is removed from the top layer by the dominating mechanism of capillary imbibition. This imbibition occurs according to a preferred pathway mechanism [Gane *et al.,* 2000] leading to a very rapid equilibration of selectively filled pores within the surface layers of the porous medium. During phase II, droplet surface evaporation is also initiated.

Phase III corresponds to the state when the droplet has fully wetted the substrate. In this regime, evaporation is the subsequent dominating factor for liquid weight loss from the porous medium, this being even more marked when the liquid mixture contains fast evaporating additives, such as IPA. Phase III can only progress by liquid evaporation if liquid is transported inside the tablet to replenish the solid-liquid-air interface. The evaporation continues and the liquid content of the interfacial region remains steady but partially depleted.

Characteristic for phase IV, is the slower evaporation of the liquid (water phase) via the surface. The water diffusion inside the tablet is continuing and the moisture transport occurs as

evaporation from the inside of the tablet to the solid-liquid interface(s) combined with retreat of the wetting front, and finally to the atmosphere. The interfacial water content depletes, and this continues until bulk fluid is exhausted.

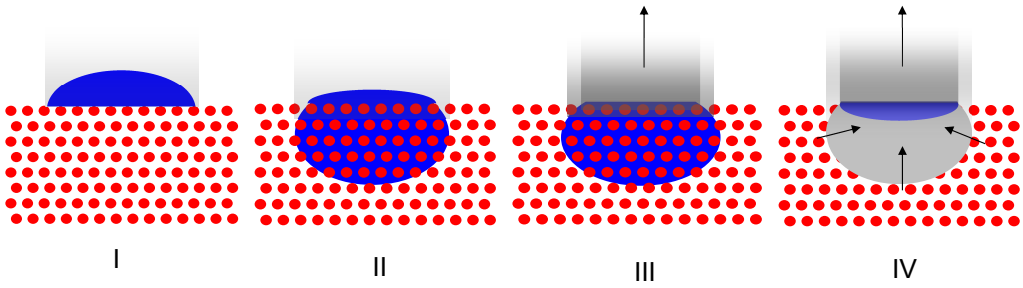

Figure 43. Liquid – vapour transition in a coating [Paper I]. The shape of the imbibed liquid distribution within the medium is in context with the work of Gane *et al.* [2000] in which they showed an ellipsoidal distribution of dyed water within a tablet structure similar to that used here.

As the liquid is applied on paper as a liquid film, under process conditions, the results indicate that the surface void roughness in the first nip is of great importance [Paper III]. This void roughness plus the permeable coating structure means low pickup despite the high permeability at the surface at the first printing unit. However, for smooth surfaces, or sufficient fountain solution feed, the solution is drawn into the coating after the nip to a point where the surface menisci balance, or excess remains, respectively, i.e. they are level with the surface or a film remains, depending on the coating capacity and imbibition rate. This makes then a "saturated equivalent plane" so that the subsequent dynamics on a relatively non-permeable surface is that of film split followed only by capillarity until the next planar contact, and so on (Figure 44). Thus, subsequent units on a rough surface behave the same as a calendered surface, in the case where permeability is low, with the water transforming the surface into an aquaplane, i.e. the liquid fills the surface voids between the particles/surface roughness and saturates the surface structure [Gane *et al.,* 2007].

The conclusions, which could be drawn, are that the first printing unit delivers fountain solution proportional to surface roughness, provided the volume of fountain solution is not excessive such that pressure penetration would be initiated when the permeability of the coating is high, or the amount of fountain solution is so small as to be independent of volume filling (supporting hypotheses I and II). The subsequent units deliver fountain solution according to

film split only, in the case where permeability is limiting. Figure 44 shows these effects schematically as follows:

I) the surface voids are progressively filled at the first unit and capillarity is initiated. Then,

II) the capillarity acts to imbibe liquid to the level of the surface profile between units, and

III) the subsequent units deliver according to film split dynamics a fixed amount of fountain solution, provided permeability is low, and each time this gets imbibed by capillarity to create menisci at the surface profile level provided coating pore volume capacity is sufficient and the volume of fountain solution is not excessive in relation to the capillarity present.

Deviation from this model can occur at step III) if the surface is highly permeable, such that pressure penetration, developed in the case where an excessively high volume of fountain solution is delivered to the surface, will cause additional pressure permeation to occur in the nip.

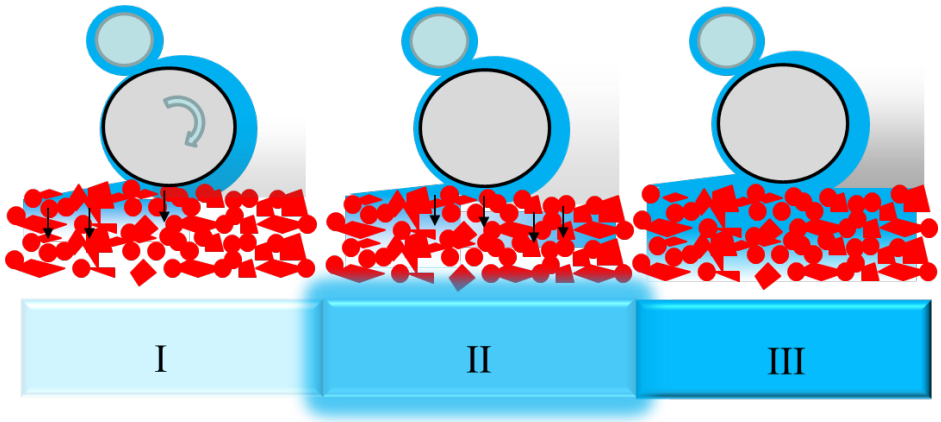

Figure 44. Fountain solution transfer to a coated paper surface when surface saturation can occur. First unit is surface roughness dependent, and subsequent units show further capillary transport and permeation inside the coated paper, with retained amount at the surface dependent on film splitting at the blanket roller-paper coating interface. The image series highlights also the background evaporation between the printing nips. See also Figure 25.

Hoyland and Field [1977] suggested that water transfer to paper is a sum of capillary flow and penetration into fibres, the capillary flow being the major process. However, the capillary

flow in uncoated paper has been questioned when the water amounts are small [Trollsås and Eriksson 1992], though the effect of nano-porous coatings, i.e. having the majority of pore diameters < 100 nm (typical of coated fine papers), biases the action towards rapid capillarity [Ridgway *et al.,* 2006]. Trollsås [1995] concluded that an increase in surface roughness of the paper decreases the water uptake. Skowronski and Lepoutre [1985] claimed, however, that an increase in surface roughness increases the water uptake. These different views can be reconciled by considering water film thickness differences in respect to the pressure profile in the printing nip, and highlights the interdependency of the porous medium, the liquid involved and the process application [Kananen, 2003; Paper III] The surface properties of paper and blanket together are, therefore, important factors for the amount of solution transferred, imbibed and permeated within the process.

A decrease in moisture content of a paper should reduce the dynamic capillary pressure and the capillary transport velocity [Salminen, 1988]. Therefore, if the water sorption is diffusion controlled, as, for example, in the case of extremely dense paper, the water transport rate is increased by diminishing the moisture content. Salminen has also shown that during pressure penetration, the effect of capillary forces is minimized in favour of pressure-driven permeation, and the transport rate is independent of the moisture content, which is also in good agreement with the results in this study. However, in the case of coated paper, the penetration is dependent on the moisture content in relation to the permeability. According to Salminen, the effect of calendering on the water sorption characteristics of a paper depends primarily on the decrease in the apparent pore radius, the surface roughness and the total pore volume, which could also be concluded in this work.

7.2 Implementation of NIR in printing processes

One focus in this thesis was to establish a measurement system which is able to monitor rapid changes in moisture content of the paper. It was also agreed in the planning of the construction of the measurement heads (probes) that the system should be sensitive to surface water, the level of which is critical for achieving a good print quality in the offset printing process. Another aim was to be able to follow the moisture evolution at several different positions in the process and to obtain real-time information of the process behaviour. Previous research has presented similar approaches with NIR applications but so far no publications have focused on the determination of moisture also in printed ink areas, arising either from previous non-image area fountain solution applications and/or from the emulsified water carried in the ink.

The offset process as such is complex, since both ink and fountain solution are transferred through multiple roller nips to the paper. At the printing plate, these two chemically totally different liquids are mixed to create an emulsion. As previously mentioned, the areas without ink contain the water based fountain solution and the inked areas the emulsion of ink and fountain solution. What also is characteristic for the offset printing process is that the process colours are applied wet on wet. This layered structure is wet until it reaches the dryer, after which the solvents in the ink and the fountain solution are rapidly evaporated. The printed and dried product takes up moisture again as it is cooled in the chill roll section and during the subsequent application of silicone. All these different phenomena happen within about two seconds, and thus it is obvious that the requirements set for the substrate in order to survive the processing are very high. These factors clearly also set challenges for measurement devices to be able to understand fully what occurs and at which stage. Moisture measurements, as such, are critical mainly in terms of moisture level instability in the environment and its distribution within the material.

Problems in print quality (here mentioned waving), have been proposed to be a result of uneven moisture distribution in the printed sheet. Exposure to high heat creates a differential moisture loss/retention across the web between image and non-image areas. The difference in moisture content of non-image areas and image areas was also shown in this work. One suggested solution to reduce waving is to use excessively high dryer temperatures [Mochizuki and Aoyama, 1981]. Research has also shown that lower press speeds and extended dwell time in the dryer reduce waving [MacPhee, 2000]. Also the drying profile has been shown to have an effect on waving, running the printing machine with the lowest possible exit web temperature reduced waving. One of the hypotheses in this work was that part of the waving tendency in the heatset web-offset process may be due to an uneven moisture profile in the paper, either prior to or generated within the printing process. The work identified one of the sources for waving appearance and the influence of drying conditions on the waving magnitude (supporting fully hypothesis IV). Moisture transport is obviously also one of the factors contributing to the process efficiency improvement, i.e. over-drying would lead to high energy consumption. The findings relating to the uneven drying of the paper and the uneven moisture removal of the printed paper, gives clear indicators as to what is needed in an attempt to prevent or reduce the waviness, namely a liquid barrier, so that the applied liquid in the printing units cannot enter the paper, but also a thermal barrier so that the heat in the dryer does not affect the internal moisture of the paper [Gerstner *et al.,* 2010]. However, the trend towards carbonate and narrow particle size

distribution coatings supports the observation of increased permeability, providing less protection from liquid permeation, which will affect that the fountain solution is forced deeper into the structure according to the findings and hypotheses presented here.

In the present study, and in the development of the measurement system, the variability in moisture in the different layers set high requirements on the measuring device performance and characteristics. Another element is the variability of the layer thickness of the base paper, coating layer and the ink and fountain solution layer(s). These affect the measurement information depth obtained. The higher the wavelength range used, the shorter is the information depth [Wieliczka *et al.,* 1989], which determined NIR to be the optimal choice for this study. Longer wavelength (1 940 nm) photons are more likely to be absorbed, therefore they will not (on average) penetrate as far as shorter wavelength (1 450 nm) photons. The counter argument applies to scattering, as shorter wavelengths tend to be scattered more. Thus, the use of NIR has the advantage of moving the system away from scattering more toward absorption. In this way, the spectroscopic limit of absorption in proportion to specific material present in a homogeneous molecular mix is more closely reached.

In order to trace the location of the penetrated fountain solution, tracer agents were added to the fountain solution. Choosing an appropriate tracer depending on the characteristic property studied is important for correct interpretation of the data. Lithium was chosen due to its high detection sensitivity. However, small traces of lithium were also found in the reference materials, such as ink and to a lesser extent coated paper. This was not a drawback in respect to determining the penetration depth of fountain solution, as ink penetration is generally less deep [Oittinen, 1976; Rousu *et al.,* 2000]. However, for quantitative analysis of fountain solution transferred in the printing press, a tracer not existing in the reference materials would have to be used (this is a subject for further work). It was found, that, in our case, the penetration of fountain solution was less than 20 µm, i.e. within the region where the majority of the moisture information was collected (50 % of the information collected originated from the first 20 µm (Figure 40)). This range spans the coating depth – typically 10–20 µm - and is likely, therefore, also to incorporate some information from the coating-basepaper interface.

The role of ink film thickness on specular reflectance has been studied by Preston *et al*. [Preston *et al.,* 2002]. They concluded that an increasing ink film thickness generally extends the gloss development time, but does not necessarily increase the final gloss level. Higher ink film

thicknesses result in longer ink filaments and thus a rougher initial printed surface. Thicker ink films also have a slower ink tack development time and are generally rougher. So, in this context, a dry rough surface diffuses incident NIR light (Figure 45, left image), while when wet ink and water fill the surface voids and smoothen the surface, it results in a higher specular reflection (Figure 45, right image). This was also confirmed in this study (Figure 41).

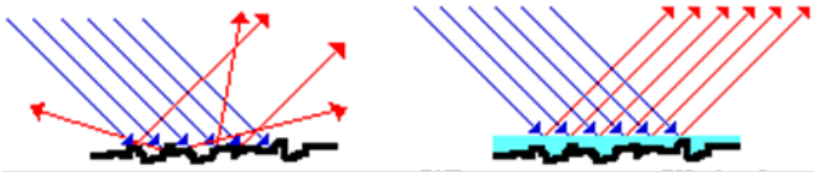

Figure 45. Reflection from a dry versus a wet paper surface.

In Figure 46, the change in NIR response is presented as the measurement probe is scanning between cyan printed and non-image areas [Paper V]. The scattering and reflectance properties of cyan printed and non-image samples are obviously different. It may be assumed that an equal proportion of all NIR wavelengths are specularly reflected, i.e. specular reflectance is not wavelength selective (referred to Figure 41). Thus, the effect of increased specular reflectance may be observed as an increase in spectral baseline (absorbance units). The light scattering effect (multiplicative error) which changes the amplitude of the water peak, is likely either to be a multiple reflection effect within the continually changing refractive index of an ink layer as it loses its diluent vehicle and/or an exchange of the water distribution in the pore structure by the displacement by the ink vehicle [Ridgway *et al.,* 2011]. Thus, this problem can be solved by simple baseline correction or by using separate calibration models for the respective areas in the printed sheet or for different paper types.

The cyan-printed area has a larger spectral baseline absorbance than the non-image area (Figure 46, right). It, thus, back-scatters less light than the non-image area, although some light penetration may be lost to specular reflectance. Additionally, some light may also be lost because of the strong absorption of water and the weak absorption of the cyan ink.

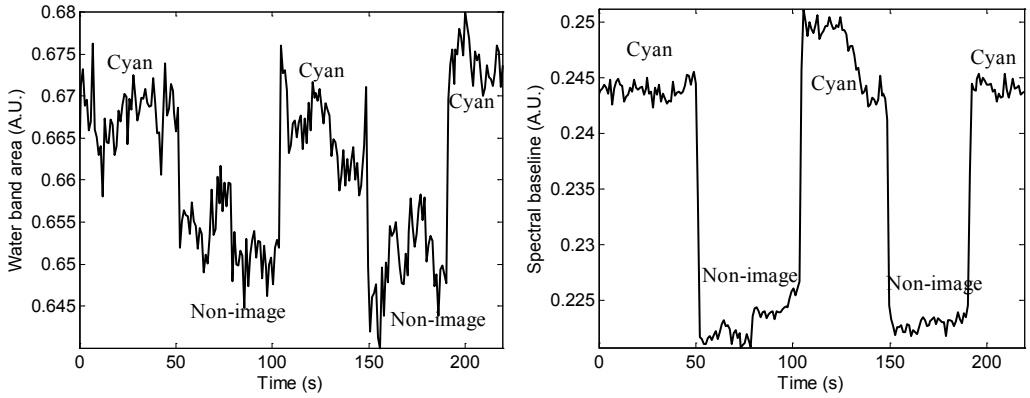

Figure 46. Probe scanning: sequence = cyan – non-image – cyan – non-image - cyan as the press runs. Baseline-corrected area of the water band between 1 890–2 010 nm (left). Spectral baseline (right): mean value of the spectrum between 1 200–2 100 nm [Paper V].

A rough, porous paper can also be described by an effective refractive index, consisting of refractive indices of all components as a mixture with air [Meeten, 1986]. The effective refractive index depends on the relative proportions of the components as well as how they are physically structured. An open, porous coating will have a lower refractive index than one of identical composition, which is more closed (less permeable) and less porous. The more porous sample has more air present in the structure, which lowers the refractive index [Elton and Preston, 2006]. If there is moisture in the paper coating, the refractive index is affected, i.e. the value is dependent on both the refractive index of the paper coating and moisture. The amount of water/moisture defines the magnitude of the resultant combined refractive index. The refractive index of water is somewhat changed in the NIR region as a function of wavelength [Schiebener *et al.,* 1990]. However, when concentrating on a narrow band, the change is not significant.

The change in the specular reflectance of the samples is affected by the surface roughness differences and the refractive index. It is clear that the printed areas have a higher specular reflectance compared to non-image areas, i.e. surface roughness influences the amount of light reflected in the specular direction. Scattering and moisture (if wavelength is chosen around water bands) influence the total reflectance, respectively.

Regarding moisture measurements from printed areas, and the effect of the ink layer on the measurement results, the ink layer might affect the NIR light propagation in the following ways:

1. The ink absorbs light to some extent which changes the absorption spectrum (Figure 21).

2. The ink is mostly glossier than paper which will influence the specular reflectance (Figure 41).

3. In process conditions, during printing, the *z*-profile distribution of water/moisture in the paper matrix is changed, which affects the water/moisture amount in the absorbance spectrum (Figure 27).

These points raised above were observed during the study but the effects were not quantified, but rather simply highlighted that they may, and probably will, exist. This is also a good proposal for future work.

The abovementioned facts have been observed during the study and can possibly affect the measurement of moisture with NIR or, as here has been determined, affect the log (1/*R*)-spectrum and the water band area. The disadvantage of reflectance measurements is the sensitivity to the changes in the water *z*-profile distribution. When the water is closer to the surface, the sample will seem to be wetter.

The presence of the ink layer on the coated paper causes an additive and wavelength-independent offset in the pseudo-absorbance log(1/*R*) spectrum with the assumption that the change in light power caused by the ink layer is equal at all wavelengths. This assumption is an approximation which is justified by the facts that:

a) The ink layer absorbs very weakly over the NIR wavelengths (Figure 21). Thus, it is assumed that the absorption of the ink layer (of the thickness ~2 μm) is negligible.

b) The specular reflectance depends on the real part of the refractive index of the reflecting material. Here it is assumed that the real part of the refractive index is a very smooth function of wavelength such that it may be approximated with a constant function.

The presence of the ink layer causes, thus, an additive and wavelength-independent offset in the absorbance spectrum. If the two assumptions above are met (at least in the vicinity of the water absorption band 1 940 nm, say between 1 600–2 100 nm), the effect of the ink layer via regular baseline correction may be removed.

If there is clear evidence of multiplicative error in the NIR spectra, i.e. the effect of scatter on the NIR spectra at a given wavelength is proportional to the magnitude of log(1/*R*) at that

wavelength, a multiplicative correction of the spectral signal [Osborne, 1993] via, for example, the use of a ratio model is needed when determining moisture contents of paper. The other alternative is to prepare unique calibration curves for each sample measured. One should, however, note that a bias difference is usually constant, and relative differences within, for example, the printing process units, are highly accurate and sensitive.

It needs once more to be highlighted that the offset printing process is a dynamic process, and mimicking it in laboratory conditions is challenging. That is why online instruments provide the solution for process monitoring and understanding. However, a process cannot be described from one single measurement point, but by using a multipoint tool, a single spot and its variations throughout the processing can be monitored. Since the paper in the offset process is exposed to two chemically totally different liquids, creating areas with different properties, the areas in turn locally changing the paper characteristics, the strength in being able to measure moisture in both of them makes the device hard to beat. The NIR measurement device developed for the heatset offset printing environment, being based on diffuse reflectance spectroscopic measurements, was chosen in order to obtain a measurement with optimized sensitivity for the liquids applied on or existing in the surface layers of the paper (supports hypothesis III). Other possibilities would also have existed, e.g. transmission measurements through the whole paper, but then the resolution would have slightly decreased. Application of, for example, mid-infrared would also have been possible, but the clear reduction in information depth excluded that option [Wieliczka *et al.,* 1989]. In addition, a multipoint approach at this wavelength would not have been possible to carry out in the configuration on-line.

8 Concluding remarks

A study on liquid transportation and distribution during rewetting of porous pigmented coated structures has been conducted.

The influence of interfacial surface energy on wetting was proven to be noticeable and acted more strongly on short wetting timescales. The wetting kinetics was dependent on the individual species since all surface active molecules migrate to the liquid-air interface, and thus affect the solid–liquid interfacial energy. However, one component can dominate the wetting due to, for example, controlling the saturated state at the wetting front.

Surface heterogeneities affect both the wetting profile and the wetting kinetics, as was concluded from the results. Importantly, as reviewed in the literature, the potential roles of surface nano-pores, typical of coated fine papers (< 100 nm), and sub-surface connectivity in defining wetting and surface spreading were highlighted.

Different wetting phases, monitored as changes in moisture content reflecting the wetting mechanisms, were defined together with the factors affecting each phase for a single droplet applied on a porous substrate. The initial surface wetting and capillary imbibition within a selective network of pores was followed by vapour diffusion (defined by literature) through the void space of the paper coating. Then the equilibrium pore filling regime at the surface layers of the porous medium was established, after which evaporation on a linear time scale took place continuing while the surface volume of water depleted. Finally, the transport limitation of the retreating wetting front led to further depletion of the surface contained liquid, related to the different stages in liquid concentrations as a function of time and depth.

The study has confirmed the observations in which liquid water and moisture are transported in different stages of penetration and evaporation, also for on-press behaviour where the substrate is rewetted and thus progressively liquid-filled in the printing units.

This novel analysis provides a means of defining the pore structure characteristics of a coated paper surface and bulk in order to obtain optimal press performance in terms of preventing liquid water interference in offset printing. The controlling factors have been determined to be,

(i) the volume of fountain solution delivered in the printing nip in relation to the surface contact coating voidage, i.e. roughness,

(ii) the capillarity of the coating and its ability to remove fountain solution from the surface,

(iii) the permeability of the coating once sufficient surface film continuity is reached either in relation to fountain solution volume applied or the smoothness of the sheet, and

(iv) the capacity in respect to the pore volume of the coating.

This study developed the applicability of an online NIR diffuse reflectance spectroscopy measurement device for the printing process environment. A summary of mechanisms, when speaking about fountain solution behaviour on a printing press when in contact with a coated paper surface needs to be split into:

(i) forced wetting in the nips,

(ii) volume of fountain solution in relation to surface roughness,

(iii) permeability of the coating under nip pressure given the status of (ii),

(iv) surface spreading once forced wetting regime is complete - relates to surface energy, surface material continuity and rugosity,

(v) capillary imbibition once external pressure is removed, which relates to pore network surface energy and the distribution of fine and larger pores in relation to the connectivity (Bosanquet).

All these mechanisms and the hypotheses lie behind the results of this thesis.

It was shown that the device can be used as a moisture sensitive system for providing accurate online qualitative indicators, but, also, when accurately calibrated, for providing quantification of moisture levels, liquid distribution and dynamic liquid transfer. The sensors can determine relative and absolute water/moisture values in both machine- and cross-direction, online, from non-image and image printed areas in the layout. The results obtained in the laboratory were in agreement with, and confirmed by, process measurements.

The NIR measurements revealed moisture gradients (uneven distribution) in the web during printing and subsequent drying, which were dependent on the print image design, and process parameters such as speed, fountain solution dosage and drying. As well, the moisture measurements were implemented when studying the waving (fluting) tendency of printed paper.

The contributing factors to the NIR response outcome were defined for separate measurement areas and for the multi-layered structure of printed paper. The *z*-directional distribution of the imbibed liquid, being one of the most sensitive factors affecting the measurement result, was defined by surface chemical analysis of tracing agents.

The statistical assessment of the observations reflects the reliability, repeatability and sensitivity (limits of detection and quantification) of the measurements and clearly reflects a pattern rather than a coincidence. Thus, the results are deemed statistically significant and provide enough evidence for challenging the hypotheses set for the work.

The use of NIR probes to determine moisture contents and fluctuations can clearly be used to optimize the heatset offset printing process, and can also yield strategies toward savings in energy consumption (more tightly controlled liquid transport resulting in optimized drying), water consumption and material costs. The online possibility could even allow a process steering option for a more uniform process and shorter make-ready times.

9 Suggested further work

Greatest error sources in the current NIR method are attributed to the construction of a reliable calibration model. Although the NIR instrument itself is very stable and accurate as is demonstrated by the figures of merit, accurate quantification of the measured moisture levels requires skill in calibration procedures.

Clearly, a rigid porous structure does not present a molecular mix with the air or liquid within its pores, but rather a segregated series of zones predominating in solid and liquid, respectively in turn. Future focus could be put on the changing pore structure, the refractive index medium change as a function of pore filling.

Further quantitative tracer work could be used to support the NIR findings, taking into account mechanisms such as on-press evaporation.

Extension of the use of NIR into digital printing fields looks promising, e.g. inkjet drying control and dye adsorption.

10 Svensk sammanfattning

Papper har en viktig roll i dagens samhälle, främst för spridning av information och som kommunikationsmedel. Digital media har tagit över en stor del av nyhetsdistributionen framförallt p.g.a. dess snabba uppdatering och flexibilitet gällande innehåll. För papper måste en kontinuerlig utveckling ske för att kunna vara konkurrenskraftig och kunna möta samt uppfylla kundens krav och önskemål. Offset tryckteknikеn är den för tillfället största teknologin som producerar stora volymer av t.ex. tidningar av hög kvalitet.

I många industriella applikationer, t.ex. inom grafiska industrin, innefattar vätning av porösa material både bulkvätning, men även avdunstning och ytspridning. Genom att förstå dessa separata fenomen, fås värdefull information om processkontroll och optimering. Vätning med efterföljande torkning spelar en mycket stor roll för både kvalitet och kostnadseffektivitet (i form av t.ex. energiförbrukning). Vätsketransporten i processen är viktig att förstå för att uppnå en stabil process med möjligast jämn körbarhet och tryckkvalitet.

Denna avhandling fokuserar på heatset web offset tryckteknikеn, men analysen och resultaten kan även användas inom andra teknologier där fukthaltsmätning och kontroll är viktiga faktorer för att nå en jämn och bra kvalitet hos slutprodukten. I avhandlingen presenteras en teknologi baserad på när-infraröd spektroskopi, som används för att analysera vatten och fukthalt i porösa pigmenterade strukturer. Resultaten stöds av känsliga ytkemiska och strukturella analyser av materialen. Vätskevätningen samt distributionen i materialet, kompletterar informationen som erhållits från den spektroskopiska analysen.

Ett av målen i denna studie var att bygga upp ett mätinstrument som i realtid detekterar, från multipla positioner, signalvariationer relaterade till substratet eller till själva tryckprocessen. Information om nyprelaterade fenomen t.ex. återvätning genom dynamisk vattentransport, temporära fukthaltsprofiler, torkningsgrad och effektivitet samt stabiliseringsfasen efter torkning har erhållits. Utöver detta, separeras även områden i tryck layouten dvs. fukthaltsgradienter mellan otryckt och tryckt yta. För att åstadkomma möjligast noggranna, kvantitativa mätvärden, krävs en kalibreringsmodell som här även utvecklades för detta syfte. Avhandlingen innehåller laboratoriestudier där rena- och flerkomponent- lösningars beteende på/i porösa material i form av papper och pigmenterade modellytor studerats.

I laboratorieförsöken framkom att gränsytspänningen har en anmärkningsvärd inverkan på vätningsförloppet, främst under korta kontakttider. Situationen är dock inte helt samma i processen där nyptrycket inverkar på mängden överfört vatten samt dess penetrationshastighet. Naturligtvis spelar också papprets ytstruktur, samt porerna, en viktig roll med tanke på de ovan nämnda faktorerna. I laboratorie- och process- förhållanden separerades olika vätningsfaser samt faktorer som inverkar på dessa. För rena vätskor, kunde en initial vätningsfas urskiljas, med efterföljande kapillär absorption i det porösa materialet. Ett mättat tillstånd med efterföljande avdunstning kunde även observeras. I processförhållanden kunde en progressiv återvätning observeras som funktion av antalet passerade nyp, detta beroende på överförd vätskevolym samt bestrykningens kapillaritetsegenskaper samt strukturens permeabilitet. Dessutom analyserades inverkan av processparametrar såsom hastighet, torkningsförhållanden och fuktvattendosering, samt deras inverkan på fuktprofilen i både maskin och tvärriktning. För att sammankoppla processhändelser, testades mätinstrumentets effektivitet på ett konkret tryckrelaterat problem, nämligen materialets tendens att deformeras, sett som vågbildning, definierat i ett fenomen kallat waving. Waving beror på ojämn absorption i och evaporation av vätska/fukt ur pappret (tryckt vs. otryckt yta) och detta förlopp kunde relativt enkelt mätas med instrumentet.

Denna studie har gett djupare insikt i vätningsfenomen som sker under korta tidsintervall. En viktig slutsats var att resultaten producerade i laboratorieskala även bevisades i verklig process. Erhållen information kan användas vid substrat-optimering t.ex. i form av yt- och por-strukturen för att undvika tryckkvalitets relaterade problem i offset processen. Med hjälp av fukthaltsmätning samt processoptimering utgående från instrumentets utslag, kan variationer kompenseras och energikonsumptionen främst vid torkningsfasen regleras. Härmed optimeras även förbrukningen och kostnaderna för valda material. Även processtyrning och processoptimering var möjlig.

11 References

Abrams, L., Favorite, C.W., Capano, P.J., Johnson, R.W., Using mercury porosimetry to characterise coating pore structure and its relation to coating optical performance, in Proceedings of the 1996 TAPPI Coating Conference, USA, 185–192, 1996.

Allem, R., Characterization of paper coatings by scanning electron microscopy, Journal of Pulp and Paper Science, 24, 10, 329–336, 1998.

Al-Turaif, H., Unertl, W.N., Lepoutre, P.J., Effect of pigmentation on the surface chemistry and surface free energy of paper coating binders, Adhesion Science and Technology, 9, 801–811, 1995.

Anderson, J.G., Measuring paper moisture, Measurement and Control, 25, 4, 102-103, 105, 1992.

Arai, T., Yamasaki, T., Suzuki, K., Ogura, T., Sakai, Y., The relationship between print mottle and coating structure, TAPPI Journal, 71, 5, 47-52, 1988.

Aspler, J.S., Perron, L., Zang, Y.-H., Larrondo, L., Printing tack development and coated paper structure, in Proceedings of the Technical Association of the Graphic Arts, Rochester, NY, 162-178, 1997.

Aspler, J., Ink-water-paper interactions in printing: an updated review. In: 2006 TAPPI Advanced coating fundamentals symposium, USA, 117-146, 2006.

Aurenty, P., Lemery, S., Gandini, A., Dynamic spreading of alcohol based vs. surfactant based fountain solutions on model plate “non-image” areas, American Ink Maker, 12, 154-160, 1999.

Ausserré, D., Picard, A.M., Léger, L., Existence and role of the precursor film in the spreading of polymer liquids, Physical Review Letters, 57, 21, 2671-2674, 1986.

Banerjee, D., Schabel, S., von Spiegel, W., Thomson, M., Roskos, H.G., Measurement of paper moisture content using terahertz imaging, Das Papier, 12, 14-21, 2009.

Bascom, W.D., Cottington, R.L., Singleterry, C.R.: in contact angle, wettability and adhesion, edited by Fowkes, F.M., Advances in Chemistry Series, Vol. 43 American Chemical Society, Washington, 1964.

Béland, M.C., Mangin, P.J., Three-dimensional evaluation of paper surfaces using confocal microscopy, chapter in surface analysis of paper, ECT, SB Eds. CRC Press, USA, 1-40, 1995.

Bico, J., Marzolin, C., Quéré, D., Pearl drops, Europhysics Letters, 47, 2, 220-226, 1999.

Blayo, A., Pineaux, B., Printing processes and their potential for RFID, Printing Joint sOc-EUSAI conference Grenoble, 27-30, 2005.

Bosanquet, C.H., On the flow of liquids into capillary tubes, Philosophical Magazine, 6, 45, 267, 525-531, 1923.

Botel, A., Trends in offset - part one: opinion, Graphix, 9, 4, 18-19, 2010.

Bousfield, D.W., Pellerin, P., Toivakka, M., Modelling of short time penetration into complex porous structures, in Proceedings of the 2000 TAPPI Coating Conference, USA, Tappi Press, Atlanta, GA, 211-224, 2000.

Burns, D.A., Ciurczak, E.W., Handbook of Near-Infrared Analysis, 2nd edition, Marcel Dekker Inc., New York, USA, 2001.

Chami Khazraji, A., Bélanger, S., Mangin, P., Brouillette, F., Contribution of the magenta pigment to calcium-induced piling in web offset lithography, Proceedings of 61st Annual Meeting of the Technical Association of the Graphic Arts, Nouvelle-Orléans LA, 234-244, 2009.

Dalphond, J.E., A critical review of the main variables in offset printing: Effects on print quality, measurement and control, Pulp & Paper Technical Association of Canada, 1-47, 1999.

Darcy, H., Les Fontaines Publiques de la Ville de Dijon, Dalmont, Paris, 1-647, 1856.

Deegan, R.D., Bakajin, O., Dupont, T.F., Huber, G., Nagel, S.R., Witten. T.A., Capillary flow as the cause of ring stains from dried liquid drops, Nature 389, 827-829, 1997

de Gennes, P.-G., Wetting: statics and dynamics, Reviews of Modern Physics, 57, 827-863, 1985.

Desjumaux, D.M., Glatter, T.P., Bousfield, D.W., Donigian, D., Ishley, J.N., Wise, K.J., Influence of pigment size on wet ink gloss development, Journal of Pulp and Paper Science, 24, 5, 150-155, 1998.

Dimmick, A., Huhtala, K., Quality performance using increased moisture content at the reel with woodfree coatings, TAPPI Coating & Graphics Arts Conference Proceedings, USA, 1-20, 2005.

Dimmick, A.C., Effect of sheet moisture and calender pressure on PCC and GCC coated papers, TAPPI Journal, 6, 11, 16-22, 2007.

Di Risio, S., Yan, N., Characterizing the pore structures of paper coatings with scanning probe microscopy, TAPPI Journal, 5, 3, 9-14, 2006.

Donigian, D.W., Vyörykkä, J., Xiang, Y., The relationship between ink setting rates, backtrap piling and micro-picking, TAPPI Coating Conference, TAPPI, Atlanta, 2004

Dougherty, W.R., Acetylenic diol surfactants cut foaming and wetting problems, Adhesives Age, 32, 26-30, 1989.

Dubé, M., Chabot, B., Daneault, C., Alava, M., Fundamentals of fluid front roughening in imbibition, Pulp and Paper Canada 106, 9, T178-T182, 2005.

Elftonson, J.E., Ström, G., Penetration of aqueous solutions into models for coating layers, in Proceedings from TAPPI Advance Coating Fundamentals Symposium, Dallas, 17-25, 1995.

Elton, N.J., Optical measurement of microroughness of pigment coatings on rough substrates, Measurement Science and Technology, 20, 025303, 2009.

Elton, N.J., Preston, J.S., Polarised light reflectometry for studies of paper coating structure II: Application to coating structure, gloss and porosity, TAPPI Journal, 8, 10-16, 2006.

Enomae, T., LePoutre, P., Gloss relaxation processes: surface roughening by water Journal of Pulp and Paper Science, 23, 34-39, 1997.

Ferderer, M., Paper re-moisturizing goes servo, Control Solutions, (K) GL: North America, USA, 75, 2, 52, 55-56, 2002.

Frank, E., Offset inks: trends and technical demands, 12th PTS CTP Deinking Symposium 2006, Leipzig, Germany, 25-27, Paper 2, 17, 2006.

Fröberg, J., Sundin, M., Tiberg, F., Voltaire, J., Effect of ink-fountain balance on ink tack development, 2000 International Printing and Graphic Arts Conference, Savannah, GA, USA, 1-4, 133-138, 2000.

Gane, P.A.C., Kettle, J.P., Matthews, G.P., Ridgway, C.J., Void space structure of compressible polymer spheres and consolidated calcium carbonate paper-coating formulations, Industrial Engineering and Chemistry Research, 35, 5, 1753-1764, 1996.

Gane, P.A.C., Schoelkopf, J., Spielmann, D.C., Matthews, G.P., Ridgway, C.J., Fluid transport into porous coating structures: Some novel findings, Tappi Journal, 83, 5, 77-78, 2000.

Gane, P.A.C., Mineral pigments for paper: Structure, function and development potential (Part I), Wochenblatt für Papierfabrikation, 129, 3, 110-116, 2001.

Gane, P.A.C., Ridgway, C.J., Schoelkopf, J., Absorption rate and volume dependency on the complexity of porous network structures, Transport in Porous Media, 54, 1, 79-106, 2004.

Gane, P.A.C., Ridgway, C.J., Burri, P., Arnold, M., Kagerer, K.-H., Madden, B., Ristolainen, M., Purontaus, J., Aquapiling: Coated substrate-related influences on reverse piling from a one-side single colour image in multicolour offset printing, Advances in Printing and Media Technology, Proceedings of the 34th IARIGAI International Research Conference, Grenoble, 2007.

Gane, P.A.C., Silfsten, P., Tåg, C.-M., Pääkkönen, P., Hiltunen, J., Kuivalainen, K., Oksman, A., Peiponen, K.-E., Isolating contributions to gloss from mechanical and optical roughness, thin layer refractive index and wavelength filtering as a function of illumination and geometry of incidence, Journal of Print and Media Technology Research, 2, 81-95, 2012.

Gate, L.F., Leaity, K., New aspects on the gloss of coated paper, TAPPI Coating Conference Proceedings, 473-478, 1991.

Gerson, D., Lewis, V., Fountain solutions: basic principles and trends, PaperCon '08.Sustainability: profits and performance for the pulp, paper and board industries, Dallas, TX, USA, 14, 2008.

Gerstner, P., Grönblom, T., Gane, P.A.C., Quality and efficiency enhancement in heatset web-offset drying by adopting thermally designed paper coatings, Advances in Printing Media Technology Vol. XXXVII, edited by Nils Enlund and Mladen Lovrecek, 135-145, 2010.

Gerstner, P., Ronkainen, P., Gane, P.A.C., The effect of latex binders on the vaporisation of ink solvents, International Paper Physics Conference & 8th International Paper and Coating Chemistry Symposium, Stockholm, Sweden, 2012.

Gojo, M., Dragcevic, K., Hincak, I., Dependence of the contact angle on the fountain solution concentration, Conference Proceedings, 15, Intergrafika, Zagreb: Grafički Fakultet, Acta Graphica 117-123, 1998.

Granberg, H., Paper optics and perception: Spectral light absorption and gloss of cyan & magenta inks, Acreo Tryckteknisk Forsning, Report No: acr009805, Kista, Sweden, 2002.

Hartmann, T., The interactions between paper, fountain solution and printing ink as seen by the printing machine supplier, 23rd PTS Coating Symposium, Baden-Baden, Germany, Papiertechnische Stiftung, 738, 2007.

Hiorns, A.G., Elton, E.J., Coggon, L., Parsons, D.J., Analysis of differences in coating structure induced through variable calendaring conditions. In: TAPPI, 1998 Coating Conference Proceedings, New Orleans, LA, USA, Atlanta, GA: Tappi Press, 2, 583-602, 1998.

Hirabayashi, T., Fujiwara, S., Fukui, T., Factors of the fluting of coated paper in web offset printing, Proceedings of 1998 Pan- Pacific and International Printing and Graphic Arts Conference, Pulp and Paper Technical Association of Canada, Montreal, 65-70, 1998.

Howland, R., Benatar, L., Rev. Ed., A practical guide to scanning probe microscopy, Veeco Instruments Inc., New York, 2005.

Hoyland, R.W., Field, R., A review of the transudation of water into paper - Part 5: The mechanism of penetration, and conclusions, Paper Technology and Industry, 18, 7-9, 1977.

Jacquemoud, S., Ustin, S.L., Application of radiative transfer models to moisture content estimation and burned land mapping, Joint European Association of Remote Sensing Laboratories (EARSeL) and GOFC/GOLD-Fire Program, 4th Workshop on Forest Fires, University Gent, Belgium, 2003.

Kamal Alm, H., Ström, G., Karlström, K., Schoelkopf, J., Gane, P.A.C., Effect of excess dispersant on surface properties and liquid interactions on calcium carbonate containing coatings, Nordic Pulp and Paper Research Journal, 25, 1, 82-92, 2010a.

Kamal Alm, H., Ström, G., Schoelkopf, J., Gane, P.A.C., Characterization of ink-paper coating adhesion failure: effect of predampening of carbonate containing coatings, Journal of Adhesion Science and Technology, 24, 3, 449-469, 2010b.

Kananen, J., Water transfer and dimensional changes of paper in a wet nip, Licentiate thesis, Helsinki University of Technology, Department of Forest Products, Espoo, Finland, 2003.

Keränen, J., Paaso, J., Timofeev, O., Kiiskinen, H., Moisture and temperature measurement of paper in thickness direction (Supported by simulations), Progress in Paper Physics Seminar PPPS 2008, Helsinki University of Technology, Espoo, 207-210, 2008.

Kipphan, H., Handbook of print media, Springer, Heidelberg, 2001.

Kiuru, J., Koivumäki, K., Kenttä, E., Sneck, A., Peltosaari, A., Passoja, S., Effects of ink - Fountain solution interactions on piling in heatset printing, Proceedings of the Technical Association of the Graphic Arts, TAGA, 55-69, 2010.

Kirmeier, M., The effect of process parameters in offset printing on the development of tack in inks applied to paper surfaces in the printing process, Druckfarbe und Papier (Printing ink and paper), Munich, Germany, 3, 2007.

Koivula, H., Toivakka, M., Gane, P., Short time spreading and wetting of offset printing liquids on model carbonate coating structures, Journal of Colloid and Interface Science, 369, 1, 426-434, 2012.

Krishnan, R., Klein, D., Ink/plate interactions in waterless lithography, TAGA Proceedings, Rochester, 478-489, 1991.

Kubelka, P., Munk, F., Ein Beitrag zur Optik der Farbanstriche, Zeitschrift für Technische Physik, Leipzig, 12, 593-601, 1931.

Kulachenko A., Mechanics of paper webs in printing press applications, Doctoral Thesis, Stockholm, Sweden, Royal Institute of Technology, 2006.

Land C., Laboratory method for the study of moisture-induced waviness in paper, Licentiate Thesis, Karlstad, Sweden, University of Karlstad, 2004.

Larrondo, L., St-Amour, S., Monasterios, C., The porous structure of paper coatings - A comparison of mercury porosimetry and stain-imbibition methods of measurement, 1995 TAPPI Coating Conference Proceedings, TAPPI Press, Atlanta, 79, 1995.

Lee, F.J., Acetylenic glycol based surfactants for use in fountain solutions, American Ink Maker, 9, 28-53, 1998.

Lehtonen, P., Paperin syvyyskosteusjakauman mittaaminen lähi-infrapunaspektroskopian ja kiiltomittauksen avulla, Oulun yliopisto, sähkö- ja tietotekniikan osasto, Masters thesis work, University of Oulu, 2005.

Lepoutre, P., The structure of paper coatings: An update, Progress in Organic Coatings, 17, 2, 89-106, 1989.

Lie, C., Kihl, L., Control of ink/water balance with help of an online densitometer, TAGA Proceedings, 443, 1992.

Lim, P.Y.W., Daniels, C.J., Sandholzer, R.E., Determination of the fountain solution picked up by the paper and ink in offset printing, TAPPI International Printing and Graphic Arts Conference, Minneapolis, USA 83-87, 1996.

Lindquist, U., Karttunen, S., Virtanen, J., New models for offset lithography, Advances in Printing Science and Technology, 16, 67-96, 1981.

Lipponen, J., Lappalainen, T., Astola, J., Grön, J., Novel method for quantitative starch penetration analysis through iodine staining and image analysis of cross-sections of uncoated fine paper, Nordic Pulp and Paper Research Journal, 19, 3, 300-308, 2004.

Liu, F., Mao, Y., Shen, W., Parker, I., The penetration of offset ink emulsion in fine paper: confocal microscopic evidence relevant to vessel picking and show through, 60th Appita annual conference and exhibition, Melbourne, Australia, Paper 2B23, 207-214, 2006.

Lyne, M.B., Huang, Y.C., Measuring acid-base and dispersive interactions with paper surfaces under dynamic conditions, Nordic Pulp and Paper Research Journal, 8, 1, 120–122, 1993.

Ma, D., Carter, R.D., Laine, J., Stenius, P., Gibbs energy analysis of ink oil imbibition during ink setting. Nordic Pulp and Paper Research Journal, 22, 4, 523-528, 2007.

MacPhee, J., Thompson, T.H., Change in moisture content of paper during lithographic printing, TAPPI Journal, 82, 6, 12-13, 1999.

MacPhee, J., Further insight into the lithographic process-with special emphasis on where the water goes, TAGA Journal, 269-297, 1985.

MacPhee, J., Bellini, V., Blom, B.E., Cieri, A.D., Pinzone, V., Potter, R.S., The effect of certain variables on fluting in heatset web offset printing, Web offset association, Affiliate of Printing Industries of America Inc., 2000.

McCormick-Goodhart, M.H., The allowable temperature and relative humidity range for the safe use and storage of photographic materials, Journal of the Society of Archivists, 17, 1, 7-21, 1996.

Massolt, P., Hohtari, H., Old problem new approach: the development and practical application of new methods for the investigation of several aspects related to laboratory scale printing of emulsified inks, 56th Appita annual conference, Rotorua, New Zealand, 18-20 Mar., 465-468, 2002.

Medina, S., Acetylenic-based surfactants, Problem solvers in complaint coating applications, Paint & Coatings Industry, 3, 66-72, 1997.

Meeten, G.H., Refraction and extinction of polymers in Meeten, G.H. (Ed) Optical Properties of Polymers, Elsevier, London, 1986.

Meggs, Philip B., A History of Graphic Design. John Wiley & Sons, Inc., 58–69, 1998.

Mirschel, G., Heymann, K., Savchuk, O., Genest, B., Scherzera, T., In-line monitoring of the thickness of printed layers by near-infrared (NIR) spectroscopy at a printing press, Applied Spectroscopy, 66, 7, 765-772, 2012.

Mochizuki, S., Aoyama, J., Effects of fast ink drying conditions on multi-colored moving web, TAGA Proceedings, 43-55, 1981.

Musselman, S.W., Chander, S., Wetting and adsorption of acetylenic diol based non-ionic surfactants on heterogeneous surfaces, Colloids and Surfaces A, 206, 1-3, 497-513, 2002.

Niemi, H., Paulapuro, H., Mahlberg, R., Review: application of scanning probe miscroscopy to wood, fibre and paper research, Paperi ja puu (eng.: Paper and Timber) 84, 6, 389-406, 2002.

Niskanen, K.J., Paper physics, Papermaking Science and Technology, Finland, 1998.

Niskanen, I., Räty, J., Peiponen, K.E., Complex refractive index of turbid liquids, Optics Letters, 32, 7, 862-864, 2007.

Nordström, J.-E.P., Studies on waterless offset, Doctoral Thesis, Åbo Akademi University, Åbo, Finland, 2002.

Oittinen, P., Fundamental rheological properties and tack of printing inks and their influence on ink behaviour in a printing nip, Helsinki University of Technology, Helsinki, Finland, Doctoral thesis, 1976.

Oittinen, P., Saarelma, H., Print media – principles, processes and quality, papermaking science and technology, Fapet Oy, 2009.

Olejniczak, C., Vanlaer, B., van Duuren, M., Paper, ink and press chemistry, exploring key print variables, Sappi Technical Brochure 2004, 1-23, 2004.

Oliver, J.F., Mason, S.G., Scanning electron microscope studies of spreading of liquids on paper, in The Fundamental Properties of Paper Related to its Uses, Technical Division, BPBIF, London, V. 2, 428, 1976.

Paaso, J., Lehtonen, P., Suopajärvi, P., Tenhunen, J., Pajari, H., Koskela, H., Forsström U., Measurement System for Monitoring the Paper Coating Process, Wochenblatt für Papierfabrikation, Professional Papermaking, 1, 39-43 2006.

Paaso, J., Moisture depth profiling in paper using near-infrared spectroscopy, Doctoral thesis, University of Oulu, 2007.

Paltakari, J., Internal and external factors affecting the paper drying process, Doctoral thesis, Helsinki University of Technology, Series A12, Espoo, Finland, 2000.

Passoja, S., Mattila, U., Sneck, A., Mechanisms of non-image area accumulation in heatset web offset, in Proceedings of 34th International Research Conference of IARIGAI, Grenoble, France 2007., 1–8, 2007.

Paulapuro, H., (editor). Papermaking science and technology: Papermaking part 1, stock preparation and wet end, Fapet Oy, Helsinki, 1999.

Pauler, N., Opacity and reflectivity of multilayered structures, Structure and Properties, 10, 203-224, 1986.

Pauler, N., Wågberg, J., Eidenvall, L., Simulation of optical properties of prints with Kubelka-Munk theory, FSCN Report R-01-18, Mid Sweden University, Fiber Science and Communication Network, Sweden, 1-23, 2001.

Peltonen, J., Järn, M., Areva, S., Lindén, M., Rosenholm, J.B., Topographical parameters for specifying a three-dimensional surface, Langmuir, 20, 22, 9428-9431, 2004.

Pineaux, B., Gandini, A., Has, M., The effect of water hardness of fountain solutions on printing quality in offset lithography. TAGA proceedings 1997 – 49th Annual Technical Conference, Quebec City, Canada, 844-860, 1997.

Preston, J.S., Elton, N.J., Legrix, A., Nutbeem, C., Husband, J.C., The role of pore density in the setting of offset printing ink on coated paper. TAPPI Journal, 1, 3, 3-5, 2002.

Preston, J.S., Parsons, D.J., Jones, M., Gate, L.F., Husband, J.C., Legrix, A., Ink gloss development mechanisms after printing- Part 1 - The influence of ink film thickness, International Printing and Graphic Arts, Bordeaux, France, 2002.

Preston, J.S., Parsons, D.J., Husband, J.C., Nutbeem, C., Ink gloss development mechanisms after printing, Spring TAPPI Advanced Coating Fundamentals Symposium, 2003.

Preston, J.S., Husband, J.C., Norouzi, N., Blair, D., Heard, P.J., The measurement and analysis of the distribution of fountain solution in kaolin and calcium carbonate containing coatings, TAPPI/PIMA PaperCon ´08 Conference, St Louis, USA, 1-14, 2008.

Pugh, J.F., The infrared measurement of surface moisture in paper, TAPPI Journal, 63, 10, 131-134, 1980.

Quéré, D., Inertial capillarity, Europhysics Letters, 39, 5, 533-538, 1997.

Rautiainen, P., (editor) Papermaking part 3, Finishing, Volume 10, 2010 Fapet Oy, Helsinki.

Reinius, H., Pajari, H., Tahkola, K., Mikkilä, J., Pöhler, T., Nieminen, S., Hermansson, E., Schulze, U., Knowledge of the interaction between fountain solution and coating provides ways to improve printed paper quality, Proc. PTS Streicherei Symposium, 2003.

Rennes, S., Eklund, D., The influence of binders on the structure and water sorption of coated paper, Paper and Timber, 71, 698, 1989.

Ridgway C.J., Gane P.A.C., Dynamic absorption into simulated porous structures, Colloids and Surfaces A, 206, 1-3, 217-239, 2002.

Ridgway, C.J., Gane, P.A.C., Schoelkopf, J., Effect of capillary element aspect ratio on the dynamic imbibition with porous networks, Journal of Colloid and Interface Science, 252, 2, 373-382, 2002.

Ridgway, C.J., Gane, P.A.C., Bulk density measurement and coating porosity calculation for coated paper samples, Nordic Pulp and Paper Research Journal, 18, 1, 24-31, 2003.

Ridgway, C.J., Schoelkopf, J., Gane, P.A.C., A new method for measuring the liquid permeability of coated and uncoated papers and boards, Nordic Pulp and Paper Research Journal, 18, 4, 377-381, 2003.

Ridgway, C.J., Gane, P.A.C., Schoelkopf, J., Modified calcium carbonate coatings with rapid absorption and extensive liquid uptake capacity, Colloids and Surfaces A, 236, 1-3, 91-102, 2004.

Ridgway C J, Gane P.A.C., Schoelkopf, J., Achieving rapid absorption and extensive liquid uptake capacity in porous structures by decoupling capillarity and permeability: Nanoporous modified calcium carbonate, Transport in Porous Media, 63, 2, 239-259, 2006.

Rosenberg, A., What part play surface water and emulsified water in the lithographic process, TAGA Proceedings, 264-282, 1985.

Rosenholm, J.B., Wetting of surfaces and interfaces. A conceptual equilibrium thermodynamic approach, in: Th. Tadros, Ed., Colloid Stability-The Role of Surface Forces, Wiley, 1-83, 2007.

Rousu, S., Gane, P.A.C., Spielmann, D., Eklund, D., Separation of off-set ink components during absorption into pigment coating structures, Nordic Pulp and Paper Research Journal, 15, 5, 527–535, 2000.

Rousu, S., Gane P., Eklund, D., Print quality and the distribution of offset ink constituents in paper coatings, TAPPI Journal, 4, 7, 9-15, 2005.

Salminen, P.J., Water transport into paper-the effect of some liquid and paper variables, TAPPI Journal, 71, 9, 195-200, 1988.

Salminen, P., Studies of water transport in paper during short contact times, Doctoral thesis, Laboratory of Paper Chemistry, Department of Chemical Engineering, Åbo Akademi University, 1988.

Sandås, P.E., Salminen, P.J., Water penetration in coated papers, Tappi Coating Conference, Houston, TX., 1987. TAPPI Press, Atlanta, 97-101, 1987.

Shibuichi, S., Onda, T., Satoh, N., Tsujii, K., Super water-repellent surfaces resulting from fractal structure, Journal of Physical Chemistry, 100, 19512-19517, 1996.

Schiebener, P., Straub, J., Levelt Sengers, J.M.H., Gallagher, J.S., Refractive index of water and steam as a function of wavelength, temperature and density, Journal of Physical Chemistry, 19, 677-717, 1990.

Schoelkopf, J., Ridgway, C.J., Gane, P.A.C., Matthews, G.P., Spielmann, D.C., Measurement and network modelling of liquid permeation into compacted mineral blocks, Journal of Colloid and Interface Science, 227, 1, 119-131, 2000.

Schoelkopf, J., Gane, P.A.C., Ridgway, C.J., Matthews, G.P., Influence of inertia on liquid absorption into paper coating structures, Nordic Pulp and Paper Research Journal, 15, 5, 422-430, 2000.

Schoelkopf, J., Gane, P.A.C., Ridgway, C.J., Matthews, G.P., Practical observation of deviation from Lucas-Washburn scaling in porous media, Colloids and Surfaces A, 206, 445-454, 2002.

Sederholm, R., Nieminen, S., The influence of coating layer on heatset roughening, IARIGAI 25th international research conference, Advances in offset printing, Sewickley, PA, USA, GATF, 1998.

Simmons, S., Blom, B., Dreher, C., Dewildt, D., Coffin, D., Parametric evaluation of web offset fluting, In Proceedings TAGA´s 53rd Annual Technical Conference, San Diego, CA, USA, 162-165, 2001.

Skowronski, J., Lepoutre, P., Water-paper interaction during paper coating, Tappi Journal, 68, 11, 98-102, 1985.

Smyth, S., The future of global printing – Market forecasts to 2014, Leatherhead, Surrey, UK, Pira International, 2009.

Songok, J., Bousfield, D., Gane, P.A.C., Toivakka, M., Heat and mass transfer models to understand the drying mechanisms of a porous substrate, International Paper Physics Conference & 8th International Paper and Coating Chemistry Symposium, Stockholm, Sweden, 2012.

Stephens, J.A., Water, pH and conductivity for printers, Anchor International Paper Imaging Products Division, 1, 14, 1993.

Strong, W., A study of fluting in coated papers printed by blanket-to-blanket offset presses. In: Proc. GATF Technical forum, Chicago, USA, 20.21-20.32, 1984.

Ström, G., The importance of surface energetics and dynamic wetting in offset printing, Journal of Pulp and Paper Science, 19, 2, J79-J85, 1993.

Ström, G., Englund, A., Karathanasis, M., Effect of coating structure on print gloss after sheet-fed offset printing. Nordic Pulp and Paper Research Journal, 18, 1, 108-115, 2003.

Ström, G., Interaction between offset ink and coated paper—a review of the present understanding, in 13th Fundamental Research Symposium, Advances in Paper Science and Technology, Cambridge, United Kingdom, 2005.

Ström, G., Karathanasis, M., Relationship between ink film topography and print gloss in offset printson coated surfaces, Nordic Pulp and Paper Research Journal, 23, 2, 156-163, 2008.

Ström, G., Borg, J., Svanholm, E., Short-time water absorption by model coatings, TAPPI Advanced Coating Fundamentals Symposium, Montreal, Canada, 204-216, 2008.

Swerin, A., König, A., Andersson, K., Lindgren, E., The use of silica pigments in coated media for inkjet printing: Effects of absorption and porosity on printing performance, In Proceedings from 23rd PTS Coating Symposium, 2007.

Szekely, J., Neumann, A.W., Chuang, Y.K., The temperature dependence of contact angles. Polytetrafluoroethylene/n-Alkanes, Journal of Colloid and Interface Science, 35, 273-278, 1971.

Säynevirta, T., Karttunen, S., New fountain solution for offset newspapers, Graphic Arts in Finland 2, 1-12, 1973.

Tamura, T., Cesium sorption reactions as indicator of clay mineral structures, 10th National Conf. On Clays & Clay minerals, 10, 1, 389-398, 1961.

Taniguchi, M., Belfort, G., Correcting for surface roughness: Advancing and receding contact angles, Langmuir, 18, 6465-6467, 2002.

Thormählen, I., Testing the lithographic behaviour of printing ink in printing presses and in the laboratory, TAGA Proc., 220-226, 1988.

Tian, J., Liu, F., Shen, W., Ink transfer and refusal mechanisms in litho-graphic offset printing and the measurement of the splitting force of fountain solution film, Australian and New Zealand Pulp and Paper Industry Journal, 62, 3, 188-193, 2009.

Timofeev, O., Keränen, J., Kiiskinen, H., Paper curl induced by drying, Pulp and Paper Canada, 103, 8, 25-28, 2002.

Trollsås, P.E., Eriksson, E., Determination of time dependence of dimensional changes of newsprint, International Printing and Graphic arts conference 1992, CPPA, TAPPI Press, Atlanta, 341-349, 1992.

Trollsås, P.E., Water uptake in newsprint during offset printing, TAPPI Journal, 78, 155-160, 1995.

Tuominen, S., Passoja, S., Renius, H., Nieminen, S., Fountain solution transfer in offset: Role of paper, Advances in Printing Science and Technology, 32, 2003.

Tåg, C.-M., Pykönen, M., Rosenholm, J.B., Backfolk, K., Wettability of model fountain solutions: The influence on topo-chemical and -physical properties of offset paper, Journal of Colloid and Interface Science, 330, 2, 428-436, 2009.

Voltaire, J., Bachelor, W., Fogden, A., Sudarno, A., Banham, P., New technique for monitoring ink-water balance on an offset press, Australian and New Zealand Pulp and Paper Industry Journal, 60, 2, 120-128, 2007.

Vyörykkä, J., Fogden, A., Andrew, D., Daicic, J., Ernstson, M., Jääskeläinen, A.-S., Characterization of paper coatings – review and future possibilities, TAPPI Advanced Coating Fundamentals Symposium, Turku, 41-66, 2006.

Washburn, E.W., The dynamics of capillary flow, Physical Review, 17, 3, 273–283, 1921.

Wenzel, R.N., Resistance of solid surfaces to wetting by water, Industrial Engineering and Chemistry Research, 28, 8, 988-994, 1936.

Wessman, D., Harding, S., Stenström, S., Moisture profiles measured by NMR imaging during the convective drying of cardboard, In Proceedings, IDS 2000, 12th International Drying Symposium, Netherlands, 2000.

Whalem-Shaw, M., Eby, T., An investigation of factors related to back trap mottle in coated papers using electron probe micro analysis, In TAPPI Coating Conference Proceedings, TAPPI Press, Atlanta, GA, 401–409, 1991.

Wieliczka, D.M., Weng, S., Querry, M.R., Wedge shaped cell for highly absorbent liquids: infrared optical constants of water, Applied Optics, 28, 9, 1714-1719, 1989.

Workman, J.J. Jr., Review of process and non-invasive near-infrared and infrared spectroscopy: 1993-1999, Applied Spectroscopy Reviews, 34, 1-89, 1999.

Wygant, R.W., Pruett, R.J., Chen, C.Y., A review of techniques for characterizing paper coating surfaces, structures and printability, TAPPI Coating Fundamentals Symposium Proceedings, 1995.

Xiang, Y., Bousfield, D.W., Effect of ink emulsification on ink gloss dynamics, Nordic Pulp and Paper Research Journal, 17, 1, 61-65, 2002.

Yan, N., Aspler, J.S., Surface texture controlling speckle-type print defects in a hard printing nip, Journal of Pulp and Paper Science, 29, 11, 357-362, 2003.

Zang, Y.H., Aspler, J.S., The influence of SB latex on the ink receptivity and print gloss development of model clay coatings. TAPPI Journal, 78, 1, 147-154, 1995.

Zou, X., Main factors affecting roughening of paper in coating and printing: a review of recent literature, Nordic Pulp and Paper Research Journal, 22, 3, 2007, 314-324, 2007.

Åbo Akademi University Press | ISBN 978-952-12-2830-8